Role of Lipid Nanodomains and F-actin in CD36 Signal Transduction

By

Swai Mon Khaing

A thesis submitted in partial fulfillment of the requirements for the degree of

Master of Science

Department of Biochemistry

University of Alberta

1. Abstract

CD36, a multi-ligand plasma membrane receptor, has been implicated in immunity, metabolism and angiogenesis. We have recently demonstrated that CD36 nanoclustering at the plasma membrane is key to the initiation of CD36 signaling. In endothelial cells (ECs), the binding of thrombospondin-1 (TSP-1, an endogenous extracellular matrix anti-angiogenic factor) to CD36 nanoclusters activates an associated Src family kinase, Fyn, leading to ECs apoptosis, hence, inhibiting angiogenesis. Our project centralized in elucidating the mechanisms of CD36-Fyn enrichment on the lipid nanodomains and actin cytoskeleton during TSP-1 induced signaling in ECs.

We hypothesized that lipid nanodomains play a role in bringing together CD36-Fyn to F-actin regions through adaptor molecules which forms a signaling platform. Using microscopy methods to visualize Fyn, various fluorescent lipid biosensors and F-actin (Phalloidin-AF647), we determined that Fyn is enriched on F-actin area at sites of phosphatidylinositol 4,5-bisphosphate enrichment (PIP2). During TSP-1 stimulation on Human Microvascular Endothelial Cells (HMEC), the CD36-Fyn-F-actin enrichment shift to domains containing PI(3,4,5)P3, suggesting a role for the phosphoinositide 3-kinase in signaling. To test the role of PI3K in Fyn activation and in CD36 nanocluster enhancements, we employed pharmacological inhibition of PI3K (LY294002) to arrest the production of PIP3 on the plasma membrane and depletion of membrane PI(4,5)P2, a precursor for PI(3,4,5)P3 using ionomycin which activates the PLC pathway. Using Immunoblotting and super-resolution fluorescence microscopy (TIRF-PALM), we determined that PI3K is important for Fyn activation and in CD36 nanocluster enhancements in CD36-Fyn signaling upon stimulation with TSP-1. Additionally, we employed a unique optogenetic tool (LARIAT) to facilitate in understanding the role of lipid nanodomains in CD36-Fyn signaling. Upon clustering of CD36 molecules using LARIAT, Fyn activation enhanced within these clusters and this activation is reduced by treatment with LY294002 which further supported our hypothesis that

engagement with PI3K (lipid nanodomains PI(4,5)P2 and PI(3,4,5)P3) play a significant role in Fyn activation and CD36 nanoclustering. With this, we proposed a model in which CD36 nanoclusters are located within PI(4,5)P2 domains and upon TSP-1 stimulation, PI3K is engaged, producing PI(3,4,5)P3 within the CD36 nanoclusters and enhances the nanoclusters and downstream Fyn activation. Furthermore, we characterized the potential adaptor proteins involved in connecting F-actin to lipid nanodomains and/or CD36 nanoclusters using BioID proximity dependent biotinylation, fractionation of cortical F actin and G actin and mass spectrometry (MS). The MS screen has narrowed down proteins that are biotinylated, adjacent to CD36 and enriched in F actin. There were nine potential candidate proteins identified and they are as follows; Alpha-actinin-4, RasGTPase-activating protein binding protein 1, E3 ubiquitin-protein ligase UBR4, PDZ and LIM domain protein 7, Erythrocyte band 7 integral membrane protein, Filamin-A, Plectin, RasGTPase-activating-like protein IQGAP1 and Talin-1. Altogether, our investigation provided novel insights into understanding the activity of CD36 signaling and organization of CD36 on the plasma membrane supported by the cortical F-actin.

2. Preface

The thesis entitled “Role of lipid nanodomains and F-actin in CD36 Signal Transduction” is written to fulfill the requirement of Master of Science Degree in Biochemistry at the University of Alberta. The experiments conducted as part of my research investigation along with the results presented here are a complete and an independent work of the author, Swai Khaing unless otherwise indicated. I joined Dr. Touret’s lab in January 2015 after completing my B.Sc. (Hons) Co-op from University of Manitoba. Dr. Touret has warmly welcomed me into his lab and carefully taught me the techniques in the lab. Coming from a background with very little knowledge of Biophysics, Dr. Touret has exposed me to the wonders of Biophysics and amazing discoveries achieved by super-resolution microscopy.

Dr. Touret’s lab focuses on elucidating the plasma membrane organizations of membrane receptors such as innate immune receptor, Dectin-1 and a multi-ligand plasma membrane receptor, CD36, using specialized microscopy techniques such as confocal, Total Internal Reflection Fluorescence (TIRF) and super-resolution microscopy. The uniqueness and versatility of these microscopy techniques particularly attracted me to Touret’s lab among many wonderful things it offers. Upon being accepted into the program, I began my journey to investigate the mechanism of the plasma membrane receptor, CD36 signal transduction controlled by lipid nanodomains and F-actin cytoskeleton in endothelial cells (ECs). Previous work done by former PhD student, Dr. John Githaka in Dr. Touret’s lab has provided me with preliminary data to pursue my research. Dr. Githaka has shown that CD36 signaling upon binding of thrombospondin 1 (TSP-1) was initiated by the formation of CD36 nanoclusters which in turns activate the downstream effector, Fyn, a member of the Src Family Kinases. Furthermore, Dr. Githaka has shown that plasma membrane organization of CD36 and activation of Fyn required is regulated by lipid domains sometime referred to as “lipid raft” and the association with cortical F-actin. With these preliminary findings, I sought to identify whether any specific inner leaflet lipids of the plasma

membrane and their role in signaling as well as defining the function of cortical F-actin in CD36 nanoclusters enhancement and activation of Fyn.

The implication of this research is diverse due to the multi-ligand binding capacity of CD36. CD36 has been discovered to be involved in many diseases such as atherosclerosis, malaria, anti-angiogenesis in cancer. Understanding the signaling mechanism of this receptor provides a basis for better comprehending the complex nature of these diseases. Moreover, TSP-1 is a major anti-angiogenic factor. Since our research primarily focuses on TSP-1 and CD36 signaling events in anti-angiogenesis in endothelial cells, my project will improve our understanding of the molecular mechanisms leading to anti-angiogenesis and apoptosis in endothelial cells. The findings could also be used to improve the designs and effectiveness of TSP-1 in targeting cancer.

Our research goals were achieved by utilizing biochemical methods and advanced microscopy techniques such as TIRF, confocal and super-resolution followed by quantitative analysis. This thesis consists of five chapters. ***Chapter 1*** presents the organization of CD36 on the plasma membrane and highlights the importance of plasma membrane lipid environment and the F-actin cytoskeleton. ***Chapter 2*** illustrates the materials and methods used to achieve the research goals in this thesis. ***Chapter 3*** recounts the role and significance of inner leaflet lipids in CD36-Fyn signal transduction. ***Chapter 4*** outlines the data that delivers insights into the connection of CD36 with cortical F-actin. Finally, ***Chapter 5*** provides the overall summary of the projects and depict a model demonstrating the interplay of membrane lipids and cortical F-actin cytoskeleton on CD36 nanocluster formation and activation of Fyn as well as remarks for future research.

3. Dedication

To my partner, Aung for your unwavering support and to my family for your unconditional love and encouragement.

4. Acknowledgment

I would like to offer my sincere appreciation to my supervisor, Dr. Nicolas Touret for his support and his guidance through my master research. Dr. Touret was incredibly patient with me in teaching the techniques of microscopy. He is a great mentor and thank you, Dr. Touret for your kindness over the years and thank you for taking me in as a master student exposing me to many wonderful opportunities in the field of biophysics. I would also like to thank my committee members, who are also part of my examining committee, Dr. Richard Fahlman and Dr. Gary Eitzen for their support and insights into my research throughout the years. I would also like to thank my examiner, Dr. Marek Michalak.

I would like to express my sincere thanks to Dr. John Githaka, my former lab mate in the Touret's lab for all his help and guidance, without whom I would not have been able to progress in my research. I would also like to thank Alberta Proteomics and Mass Spectrometry Laboratory and Dr. Fahlman's lab for all the help in proteomics. Thank you Sandra in the Touret's lab for all her wonderful technical support and all my friends, Luana, Sara, Mohamed, Alaaa, Maria and many bright colleagues I met over the years. Thank you, Dr. Barbara Niemeyer and her lab for hosting me in Germany.

I wish to thank the funding agencies; International Research Training Group in Membrane Biology from NSERC-CREATE, Canadian Institutes of Health Research and Natural Sciences and Engineering Research Council (NSERC).

I thank my family, mom, dad and my sisters for all the encouragement and strength. Last but not least, my partner and my best friend, Aung for being with me through thick and thin, for driving me back and forth to the lab every day, even at unreasonable hours, for never saying no to my requests, for making my life bearable during tough times and for all the emotional, mental and financial support. I am forever grateful.

5. Table of Contents

6. List of Figures

7. List of Tables

8. List of Abbreviation

CD36 – Cluster of Differentiation 36

EC – Endothelial Cell

TSP-1 – Thrombospondin 1

PIP2 / PI(4,5)P2 - Phosphatidylinositol 4,5-bisphosphate

PIP3 / PI(3,4,5)P3 – Phosphatidylinositol 3,4,5- triphosphate

HMEC - Human Microvascular Endothelial Cells

PI3K - Phosphoinositide 3-kinase

TIRF-M – Total Internal Reflection Fluorescence Microscopy

PALM – Photoactivatable Localization Microscopy

LARIAT – Light-Activated Reversible Inhibition by Assembly Trap

BioID – Proximity Dependent Biotin Identification

oxPL - Oxidized Phospholipids

oxLDL - Oxidized Low-density Lipoprotein

CLESH-1 - CD36 LIMP II Emp Structural Homology-1

TSR - Thrombospondins Type 1 repeat

MAPKs – Mitogen Activated Protein Kinases

TNFα – Tumor Necrosis Factor Alpha

Pyk 2 – Protein Tyrosine Kinase 2

FAK – Focal Adhesion Kinase

GEFs – Guanine Nucleotide Exchange Factors

SFK – Src Family Kinase

SH1 – Src Homology Domain 1

SH2 – Src Homology Domain 2

SH3 – Src Homology Domain 3

SH4 – Src Homology Domain 4

RPTPs - Receptor Protein Tyrosine Phosphatase

CD45 – Cluster of Differentiation 45

RPTPα – Receptor Protein Tyrosine Phosphatase alpha

RPTPε – Receptor Protein Tyrosine Phosphatase epsilon

LAR (PTPRF) - Receptor-type tyrosine-protein phosphatase F

PTP1B – Protein Tyrosine Phosphatase 1B

SHP1 - Src homology region 2 domain-containing phosphatase-1

SHP2 – Src homology region 2 domain-containing phosphatase-2

PA – Phosphatidate

PC – Phosphatidylcholine

PE – Phosphatidylethanolamine

PS – Phosphatidylserine

PI – Phosphatidylinositol

PI(3)P – Phosphatidylinositol 3-phosphate

PI(4)P - Phosphatidylinositol 4-phosphate

PI(5)P – Phosphatidylinositol 5-phosphate

PI(3,4)P2 – Phosphatidylinositol 3,4-bisphosphate

PI(3,5)P2 - Phosphatidylinositol 3,5-bisphosphate

PIP5K - Phosphatidylinositol 4-Phosphate-5 kinase

PTEN - Phosphatase and tensin homolog

OCRL - Inositol polyphosphate 5-phosphatase

Inpp5B - Type II inositol 1,4,5-trisphosphate 5-phosphatase

PH – Pleckstrin Homology

ENTH - The epsin N-terminal homology

FERM – F for 4.1 protein, E for ezrin, R for radixin and M for moesin

PX – Phox Homology

Akt (PKB) – Protein Kinase B

PDK - 3-phosphoinositide-dependent protein kinase

Arp2/3 – Actin-related protein 2/3

Eps8 - Epidermal growth factor receptor kinase substrate 8

Ena/VASP – Ena/ Vasodilator stimulated phosphoprotein

RhoA – Ras Homology Family Member A

Rac1 – Ras-related C3 botulinum toxin substrate 1

Cdc42 – Cell division control protein 42

Rif – Rho in filopodia

WAVE/WASP – WASP-family verprolin-homologous protein /Wiskott-Aldrich syndrome protein

IgM – Immunoglobulin M

SPA – Spatial Pattern Analysis

MβCD – Methyl β Cyclodextrin

MS – Mass Spectrometry

p38MAPK – p38 Mitogen Activated Protein Kinase

p130Cas – p130 Crk Associated Substrate

TIME - hTERT immortalized dermal microvascular endothelial cells

hTERT - Telomerase reverse transcriptase

FBS – Fetal Bovine Serum

PBS - Phosphate Buffered Saline

BSA - Bovine serum albumin

SPH – Sphingomyelin

GM1 – Monosialotetrahexosylganglioside

PLC – Phospholipase C

DAG – Diacylglycerol

IP3 - Inositol triphosphate

IP3R - Inositol triphosphate receptor

MP – Multimeric Protein

CIB1 - Cytochrome Interacting Basic helix-loop-helix protein

CRY2 - Cryptochrome 2

GEF – Guanine Nucleotide Exchange Factor

GAP – GTPase Activating Protein

Arf – ADP ribosylation factor

ADP – Adenosine diphosphate

LatB – Latrunculin B

Jas – Jasplakinolide

UBR4 - E3 ubiquitin-protein ligase UBR4

PDZ domain – Post synaptic density protein (PSD95), Drosophila disc large tumor suppressor (Dlg1), zonula occludens-1 protein (zo-1)

LIM domain - Lin11, Isl-1 & Mec-3

IQGAP - Ras GTPase activating like protein 1

FAS – Fatty Acid Synthase

Chapter 1 - **IntroductionCD36**

1. CD36 Domain Organization and background information

CD36 is a glycoprotein membrane receptor with a molecular weight of 88 kDa found on the surface of many mammalian cells including platelets, mononuclear phagocytes, adipocytes, hepatocytes, myocytes, some epithelia cells and endothelial cells (Silverstein and Febbraio, 2009). CD36 belongs to the class B scavenger receptor family which consists of scavenger receptor B1 and lysosomal integral membrane protein 2 (Park, 2014). The various expression pattern of CD36 in many cells is suggestive of its multicellular functions (Silverstein and Febbraio, 2009). Due to CD36's ability to bind to various ligands, CD36 has been implicated in many physiological processes (e.g. angiogenesis, fatty acid and cholesterol metabolism), and hence it is implicated in pathological conditions such as cancer, atherosclerosis, malaria and Alzheimer (Febbraio et al., 2001) .

CD36 is encoded by the human *Cd36 gene*, which is located on the chromosome 7 (7q11.2) and consists of 15 exons (Hoosdally et al., 2009). In humans, CD36 is made up of a single peptide

chain consists of 472 amino acids with a predicted molecular weight of approximately 53,000 Da without the glycosylation (Hoosdally et al., 2009). CD36 possesses two transmembrane domains, short intracytoplasmic domains of five to seven and eleven to thirteen amino acids and a large extracellular domain with three disulfide bridges (Park, 2014). CD36 is proposed to have “hairpin like” with α-helices and an anti-parallel β barrel core which serves as a hydrophobic tunnel (Gruarin et al., 2000). However, it was later determined that the ectodomain of human CD36 have an antiparallel β-barrel core which is not entirely hydrophobic with many short α-helical segments (Neculai et al., 2013). The β-barrel core consists of a solvent-exposed cavity with an opening of 5A x 5A connected to the cavity of an approximately 22A x 11A x 8A opening in the middle of the core with charged side chains and can transport cholesterol (esters) (Neculai et al., 2013). A helical bundle found at the apex regions of human CD36 ectodomain is thought to be contributed to the association of CD36 receptor the polyanionic ligands (Neculai et al., 2013).

Moreover, CD36 is heavily glycosylated and post translationally modified with disulfide bridges on the extracellular loop (Hoosdally et al., 2009). Crystal structure of CD36 ectodomain revealed nine out of ten predicted glycosylation sites and are showed to be N-linked glycosylated (Hoosdally et al., 2009). They are evenly distributed around the midsection of the protein (Neculai et al., 2013). These glycosylations and disulfide linkages in the extracellular loop are required for intracellular trafficking onto the plasma membrane (Gruarin et al., 1997). In addition, CD36 is palmitoylated on four cysteine residues, at position 3, 7, 464 and 466 on each side of the cytoplasmic tails (Tao et al., 1996). The presence of these lipid modifications has been reported to promote the association of CD36 with the membrane lipid nanodomains which is implicated in many CD36 functions such as signaling and endocytosis (Zeng et al., 2003) (Figure 1.1). Phosphorylation of Thr92 on extracellular domain of CD36 regulates its ligand binding activity, for instance, phosphorylated CD36 does not bind thrombospondin-1 and has significantly lower affinity for Plasmodium falciparum-infected erythrocytes (Asch et al., 1993; M. Ho et al., 2005).

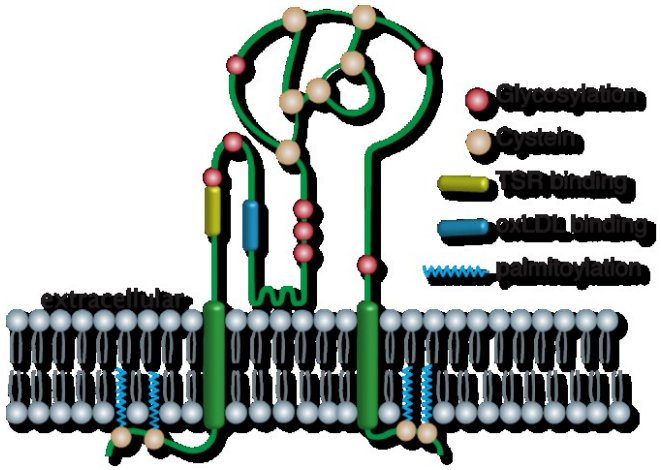

Figure 1.1 – Schematic of CD36.
CD36 has two transmembrane segments with two short cytosolic domains at the N- and C-termini with palmitoylation on four amino acid residues. It has a large extracellular domain with glycosylation and three disulfide bonds (adapted from Nicolas Touret's schematics)

2. Ligands of CD36

CD36 is known as a Scavenger Receptor and hence binds to many various ligands. The mechanisms by which CD36 binds to scavenger ligands leads to multiple outcomes in different cells. Some of the well-known ligands of CD36 are thrombospondin-1, oxidized phospholipids (oxPL), oxidized low-density lipoprotein (oxLDL), hexarelin, fibrillar Ab amyloid peptides, long-chain fatty acids, *Plasmodium falciparum*-infected erythrocytes, bacterial cell wall components of Staphylococcus and Mycobacterium, cell-derived microparticles and apoptotic cells (Park, 2014). However, binding of these ligands to CD36 occurs at different regions of CD36. For example, thrombospondin-1 binds to the CLESH-1 domain (CD36 LIMP II Emp Structural Homology-1) which is located between amino acid residues 93 to 155. The binding site for oxPL is located in amino acids 157–171, and the binding site for oxLDL is adjacent to the 155–183 sequence (Navazo et al., 1996). CD36 serves as a fatty acid translocase on adipocytes which binds to long-chain free fatty acids and enables their transport into cells. This function of CD36 provides an energy source for beta-oxidation to myocytes and lipid storage to adipocytes (Abumrad et al., 1993).

CD36 binding to TSP-1 in nascent microvascular ECs leads to anti-angiogenic effects through inhibiting their migration and triggering apoptosis (Dawson et al., 1997). My thesis research is centered around this signaling pathway in endothelial cells. In the section below (Chapter 1 - 3), I will introduce and discuss the TSP-1 mediated CD36 signaling.

2.1. Thrombospondin-1 (TSP-1)

The thrombospondin-1 (TSP-1) protein is a multi-domain glycoprotein that belong to the thrombospondin family (Simantov and Silverstein, 2003). It is a disulfide-linked homotrimeric protein complex with a molecular weight of 450 kDa (Baenziger et al., 1971). It has been identified as a natural and potent inhibitor of neovascularization and tumorigenesis in healthy tissue (Lawler and Lawler, 2012). It negatively modulates endothelial cell proliferations and migration and promotes apoptosis by inhibiting pro-angiogenic signals (Dawson et al., 1997). During dermal wound healing, TSP-1 is released from platelet alpha granules into thrombi and the extracellular matrix and hence interrupting the vascular remodeling (Esemuede et al., 2004). There are five members of the thrombospondin family from TSP-1 to TSP-5, however only TSP-1 and TSP-2 have been reported to have anti-angiogenic activity (Klenotic et al., 2013).

One of the unique features of TSP-1 and TSP-2 is the three highly homologous thrombospondins type 1 repeat (TSR) domains which are absent in the other members of the thrombospondin family (Klenotic et al., 2013). TSP-1 monomer (Figure 1.2) consists of the N-terminal domain which mediates heparin binding and disulfide bond dependent trimerization of TSP-1 monomers, cysteine- rich region (homologous to procollagen), three copies of the type 1 repeat (TSR), three copies of type 2 repeats and seven type 3 repeats that share homology to calcium binding sites in many other proteins followed by a globular C-terminal domain (Simantov and Silverstein, 2003). The presence of TSR domains underscores the importance of anti-angiogenic function (Tolsma et al., 1993). In endothelial cells, TSR domains of TSP-1 bind and activate transforming growth factor – β (Murphy-Ullrich and Poczatek, 2000), heparan sulfate

proteoglycans and fibronectin (Jimenez et al., 2000) assisting in apoptosis via the cell surface receptor CD36 (Ren et al., 2006). According to the two crystal structures of TSP-1-TSR regions, a positively charged surface ridge exists within each TSR regions (Klenotic et al., 2011; Tan and Lawler, 2009). These ridges on TSP-1 and TSP-2 have been reported to recognize the CLESH (CD36, LIMP-2, Emp sequence homology) domain with approximately 30 residues within CD36 (Pearce et al., 1995; Tan et al., 2002). The interaction between positively charged ridge on TSP-1 and negatively charged CLESH domain is regulated by the phosphorylation of threonine (T92) adjacent to the CLESH domain on CD36 (Chu and Silverstein, 2012). However, potential CD36 phosphorylation at threonine 92 residue by protein kinase C (PKCα) intracellularly before translocating to the plasma membrane suppresses TSP-1 binding and abrogate anti-angiogenic effect (Asch et al., 1993)

Upon TSP-1 binding to CD36 in endothelial cells, Fyn is reported to be activated and this activation is required for the ability of TSP-1 to induce anti-angiogenic response (Jimenez et al., 2000). Angiogenesis is the formation of new blood vessels important for tumor proliferation and metastatic spread. Growth and proliferation of cancer cells depends on an adequate supply of oxygen and nutrients and the removal of waste products. Regulation of angiogenesis is carried about balance between activator and inhibitor molecules. Over a dozen different proteins have been recognized as potential angiogenic activator and inhibitors (Nishida et al., 2006). The discovery of angiogenic inhibitors is critical in reducing the morbidity rate of cancers. For therapeutics, TSR-derived peptides have been tested in phase II clinical trials, however, the results are varied (Markovic et al., 2007). More recently, A peptide mimicking TSR (ATB-510) was tested unsuccessfully in clinical trials for the treatment of several cancers (Russell et al., 2015). To design future therapies against angiogenesis, more detailed understanding of TSR domains is needed. Our work stems from the need to advance our knowledge on this signaling pathway to support the development of better anti-angiogenic treatments.

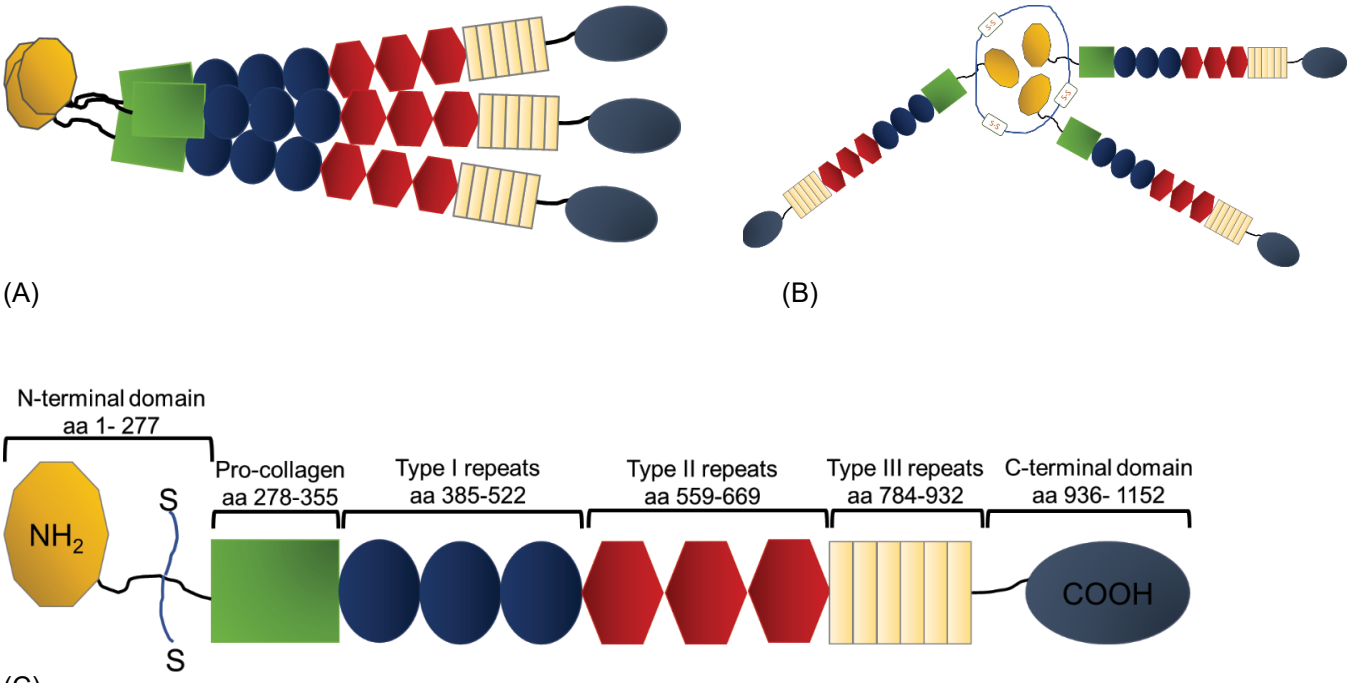

Figure 1.2 – Schematic of TSP-1 Domain Organization

(A) TSP-1 exists in homotrimer (B) Three TSP-1 monomers are joined together by intermolecular disulfide bridges (Top view). (C) Schematic representation of TSP-1 monomer containing different domains. The anti-angiogenetic activity of TSP-1 is restricted to the thrombospondin structural repeats (TSRs). The schematics are adapted from (Simantov and Silverstein, 2003).

3. CD36-TSP-1 Signaling and Anti-Angiogenic Pathway

Thrombospondin-1 binding to CD36 on endothelial cells inhibits angiogenesis by inducing apoptosis. On microvascular endothelial cells, CD36 serves as an endogenous negative regulator of angiogenesis (Dawson et al., 1997). CD36 inhibits the vascular endothelial growth factor induced pro-angiogenic signals involved in endothelial cell proliferation, migration and tube formation and produces anti-angiogenic response in cell as an alternative eventually leading to endothelial cell death (Dawson et al., 1997; Jimenez et al., 2000). The intracellular signaling of CD36 upon TSP-1 stimulation includes the activation of Src family non-receptor tyrosine protein kinases Fyn, mitogen activated protein kinases (MAPKs) p38, c-JUN N terminal kinase and caspase 3 (Jimenez et al., 2001). Jimenez et al., has identified that in endothelial cells, Fyn, Caspase 3-like proteases and the stress-activated p38 mitogen-activated protein kinases are

required for inhibition of neovascularization by TSP-1. Mice treated systemically with TSP-1 showed an increase in the number of apoptotic endothelial cells in areas of neovascularization (Jimenez et al., 2001). Expression of additional proapoptotic effectors such as Fas ligand and tumor necrosis factor-α, TNFα have been reported (Rege et al., 2009; Volpert et al., 2002). Signaling events downstream of Fyn are not fully understood in TSP-1-CD36 signaling in endothelial cells, however, the role of focal adhesion components such as tyrosine kinases Pyk 2 and FAK (Focal adhesion kinase) and the adaptor proteins such as pCas130 and paxillin have been implicated (Park et al., 2009). The Vav family of proteins associate with CD36 in macrophages, microglial cells and platelets for downstream signaling events (Wilkinson et al., 2006). The Vav family of proteins are activated by Fyn and Lyn and act as guanine nucleotide exchange factors (GEFs) for Rho and Rac guanosine triphosphatases (GTPases) (Welch et al., 2003) .

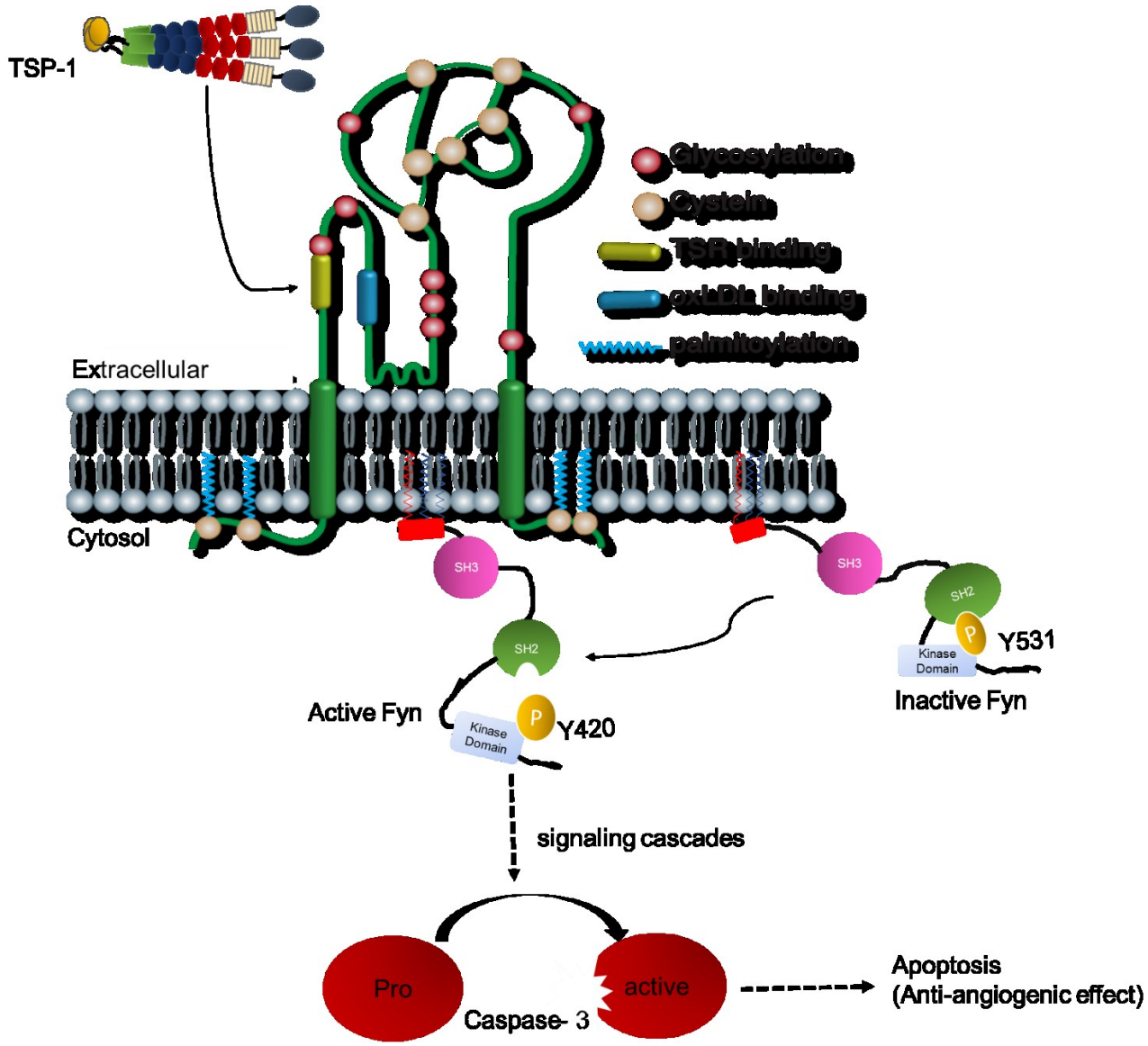

Figure 1.3 – TSP-1 stimulation of CD36 activates Fyn and initiate anti-angiogenic response in endothelial cells.

TSP-1, a homotrimer binds to CD36 via CLESH domain resulting in activation of Fyn through autophosphorylation of tyrosine 420. Fyn activation leads to a signaling cascade which ultimately results in apoptosis of endothelial cells through caspase-3 activation.

3.1. Fyn

Fyn, a member of the Src Family Kinase (SFK) is 59 kDa non-receptor tyrosine kinase which is implicated in many biological processes including regulation of cell growth and survival, cell adhesion, integrin-mediated signaling, cytoskeletal remodeling, cell motility, immune response

and axon guidance (Wolf et al., 2001). Fyn is associated with several cell surface receptors such as B and T cell receptor, integrins, ion channels and CD36 (Hisatsune et al., 2004) and this association is observed on the cytoplasmic surface (Sen and Johnson, 2011). Fyn localization to the cytoplasmic leaflet of the plasma membrane is dependent on the palmitoylation state of SH4 domain in Fyn (Sato et al., 2009). Upon receptor activation, Fyn phosphorylates tyrosine residues on other molecules involved in variety of signaling pathways (Posadas et al., 2009). Tyrosine phosphorylation by Fyn regulates protein activity or create a signaling platform which allows the recruitment of other signaling molecules.

Fyn shares a conserved domain structure with other nine members of the SFKs. It is composed of consecutive SH3, SH2 and tyrosine kinase (SH1) domains, SH4 membrane-targeting region at the N-terminus with lipid modifications such as myristoylations and palmitoylations and finally a short C-terminal tail containing a tyrosine residue with an auto-inhibitory phosphorylation (Figure 1.4) (Okada, 2012). Fyn activation is regulated by intramolecular interactions between phosphorylation and de-phosphorylation of key tyrosine residues. Fyn is inactive when the SH2 domain is blocked by a phosphorylated C terminal tyrosine at position 531 (Tyr^{531}). Upon stimulation of the cell surface receptors, the interaction between SH2 domain and phosphorylated Tyr^{531} become disrupted enabling the SH2 and SH3 domains to be exposed for interactions with other molecules. Catalytic activity of Fyn is achieved by de-phosphorylation of Tyr^{531} and autophosphorylation of a conserved tyrosine in the activation loop, Tyr^{420} (Vacaresse et al., 2008). Many receptor and non-receptor phosphatases have been implicated in controlling the de-phosphorylation of Tyr^{531} (Roskoski, 2005). Activated Fyn maybe de-activated by re-phosphorylation of Tyr^{531} by Csk (C-terminal Src kinase) (Amata et al., 2014). Some of the known protein tyrosine phosphatases involved in SFK activation include receptor protein tyrosine phosphatase (RPTPs) such as CD45, RPTPα, RPTPε and LAR and non-receptor protein tyrosine phosphatase such as PTP1B, SHP1 and SHP2 (Yang et al., 2006). In

hemopoietic cells, cytoplasmic domain of CD45 dephosphorylates Tyr531 of Fyn and activates it (Huntington and Tarlinton, 2004). Although not much is known about the dephosphorylation of Tyr531 in endothelial cells, RPTPα is reported to localize in lipid rafts and activate c-Src and Fyn by reducing phosphorylation of Tyr531 in growth factor mediated response (Zheng et al., 2000).

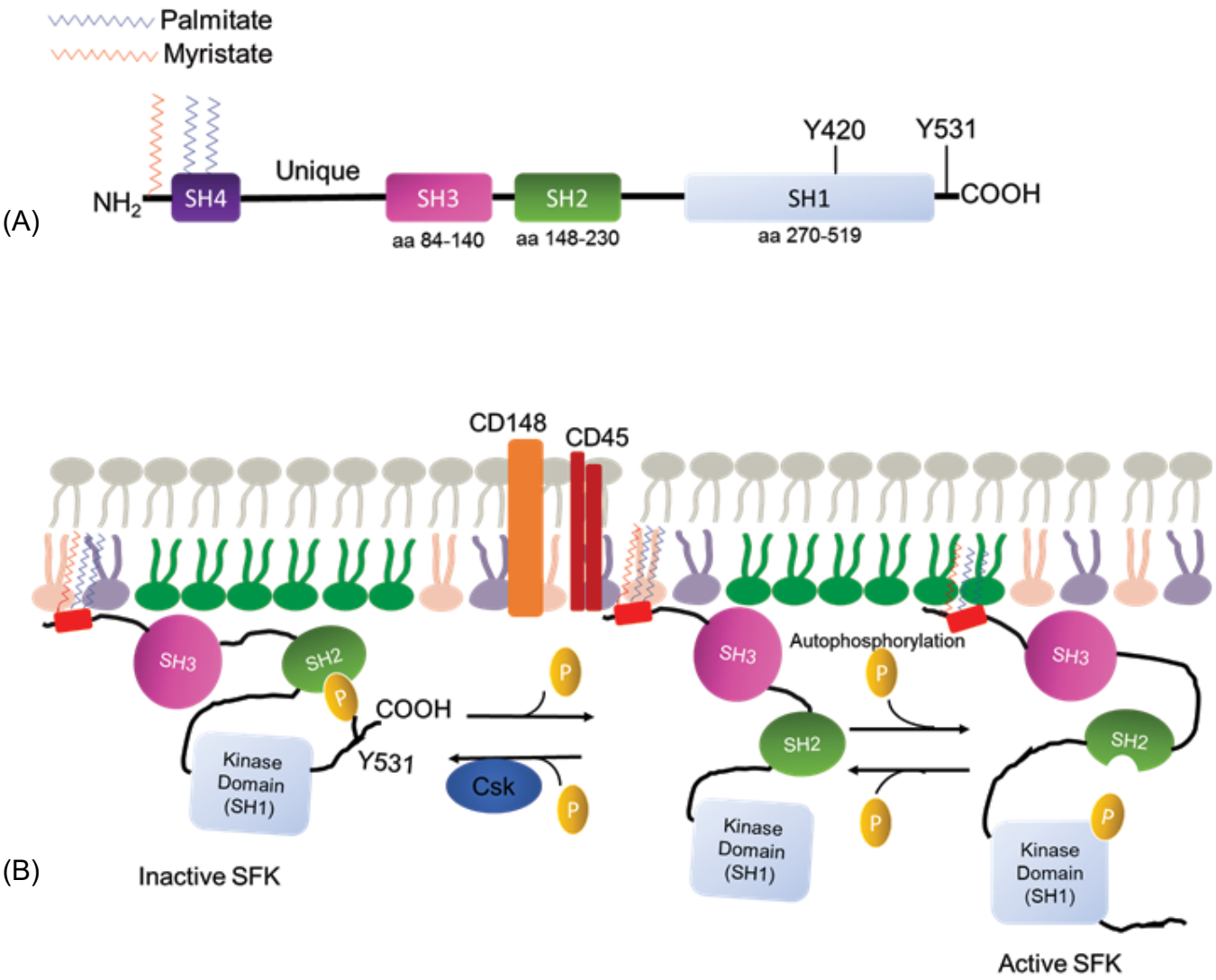

Figure 1.4 – Domain Organization of Fyn and Schematic representation of Fyn activation. (A) Fyn kinase domain organization including SH3, SH2 and catalytic domain for tyrosine phosphorylation. (Adapted from Okada, 2012) (B) Mechanism of Fyn activation. Fyn remains inactive due to phosphorylation at Y531 and becomes active after intermolecular rearrangement exposing SH2 and SH3 domains leading to autophosphorylation of Y420. Adapted from (Goodridge et al., 2012).

4. Plasma Membrane Organization

Eukaryotic plasma membrane is composed of different biological molecules namely proteins, lipids and carbohydrates (Lodish et al., 2000b). However, the composition of these molecules varies in different cell types and are continuously adapting for fluidity and changes in the environment (Van Meer et al., 2008). Singer and Nicolson proposed a membrane model (fluid mosaic model) in 1972 stating that plasma membrane is a two-dimensional discontinuous fluid bilayer with integral proteins arranged in amphipathic structure (Singer and Nicolson, 1972). However, newer models of plasma membrane organization have been emerging which are loosely based on the fluid mosaic model but differs in many aspects. In the next section, I will briefly discuss the important features that provide a new look on the plasma membrane organization.

There are three classes of lipids which make up the plasma membrane; glycerophospholipids, sphingolipids and sterols, with cholesterol being the only sterols present in the mammalian cell membrane (Simons and Sampaio, 2011). Among these lipids, glycerophospholipids are the most abundant, contributing for over 50% of all lipids in plasma membranes (Noutsi et al., 2016). Phospholipids generally consist of two hydrophobic fatty acid tails and a hydrophilic head comprising of a phosphate group (Zachowski, 1993). The head and tails are connected by a glycerol molecule. The phosphate head group can be hydrolyzed to produce phosphatidate (PA) or modified with choline, ethanolamine, serine and inositol creating phosphatidylcholine (PC), phosphatidylethanolamine (PE), phosphatidylserine (PS) and phosphatidylinositol (PI) which is one of the crucial players in lipid signaling and discuss in detailed in the section below (Koldsø and Sansom, 2015).

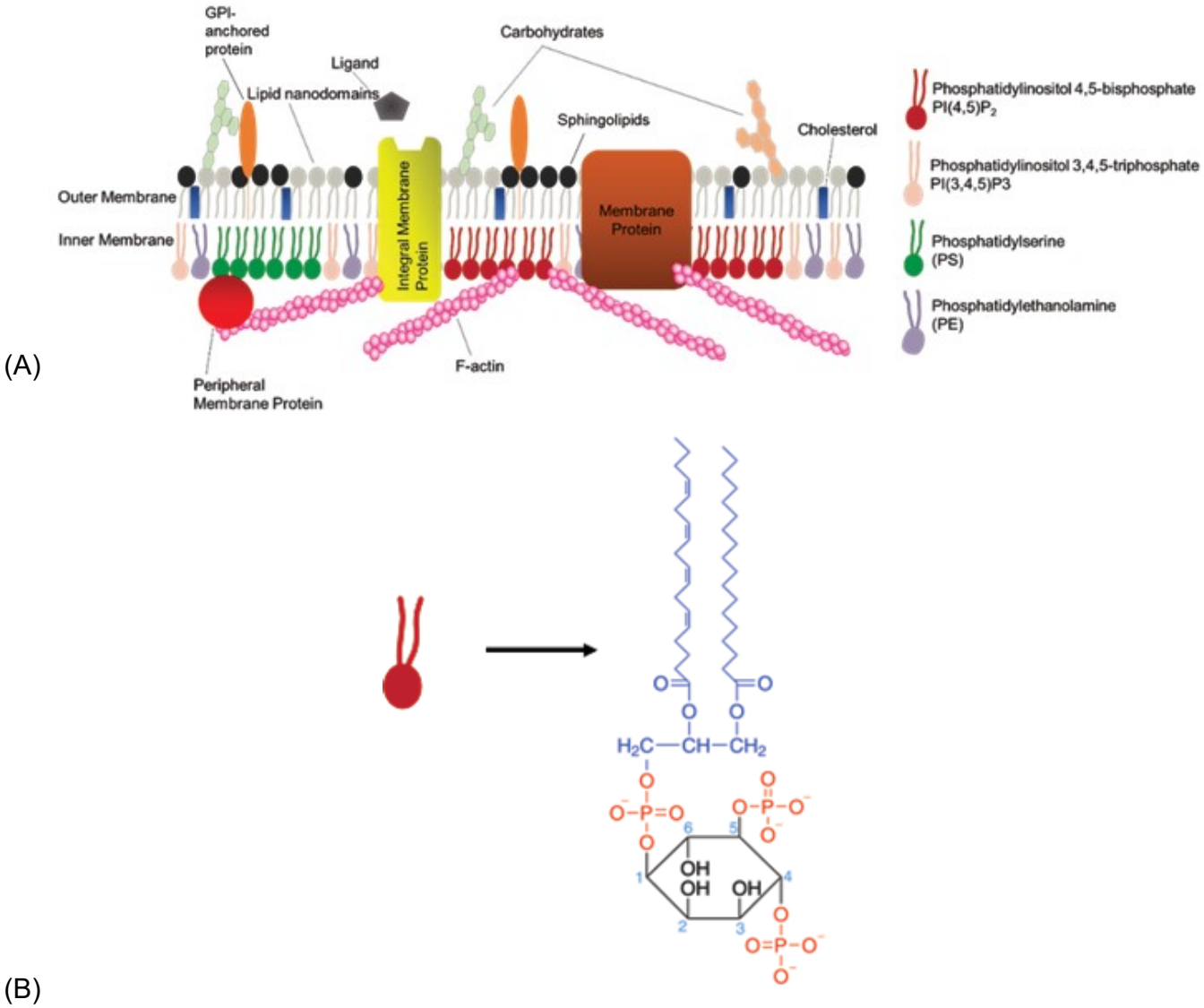

Figure 1.5 – Plasma Membrane Organization.

(A) Schematic representation of plasma membrane organization (adapted from Nicolas Touret's schematics) describing various membrane proteins in the lipid bilayer. Plasma membrane is surrounded by carbohydrates, cholesterol and enriched in cortical F-actin. Lipid composition between outer and inner membrane is not homogenous. Lipid nanodomains are reported to provide signaling platform and cortical F-actin is involved in organization of plasma membrane components. Inner leaflet of plasmid membrane is enriched with different types of phospholipids namely, PS, PE and PIs. (B) Chemical structure of phosphoinositides represented by PI(4,5)P2 present in the inner leaflet.

4.1. Features of Phosphoinositides

Phosphatidylinositol and its phosphorylated derivatives, phosphoinositides (PIs) are versatile due to their diverse roles in regulating many cellular events such as membrane trafficking, intracellular signaling, cytoskeleton organization and apoptosis (Di Paolo and De Camilli, 2006; Niggli, 2005). PIs are also involved in many human diseases acting as signaling lipids during inflammation, cancer and metabolic diseases (Saarikangas et al., 2010). They are concentrated on the cytosolic side of the membrane. PI and its derivatives make up about 10% of the total cellular lipids in most cells (Hagelberg and Allan, 1990). Phosphatidylinositol can undergo reversible phosphorylation at the D-3, D-4 or D-5 positions of the inositol ring producing seven distinct phosphoinositide species [PI(3)P, PI(4)P, PI(5)P, PI(3,4)P2, PI(3,5)P2, PI(4,5)P2, and PI(3,4,5)P3] (Czech, 2003). Each cellular compartment can be marked by these specific phosphoinositide species. In this thesis, we will mainly discuss the roles of PI(4,5)P2 and PI(3,4,5)P3, however, I will also provide properties of these phosphoinositide species very briefly and their presence on different cellular compartments.

(A)

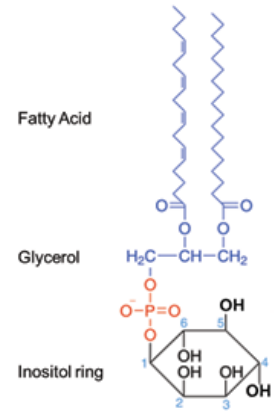

(B)

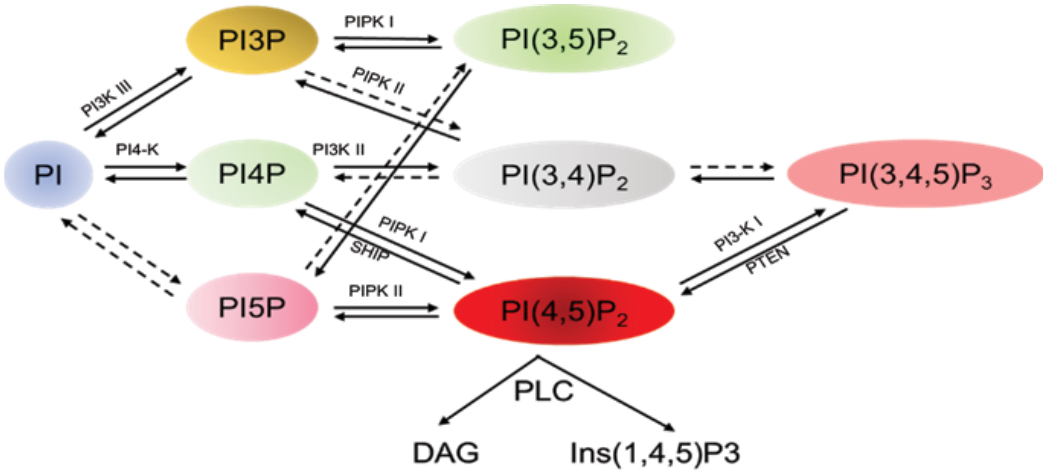

Figure 1.6 – Illustration of phosphoinositide (PI) and pathway of PI metabolism.
(A) Chemical structure of Phosphoinositide (PI). It is made up of two fatty acid chains which serves as phospholipid tail, a glycerol backbone and an inositol head group. Inositol head group can be replaced with different head groups such as serine, choline and ethanolamine. (B) Brief metabolic pathways of PIs. Seven different PI species can be produced by different kinases and phosphatases (Czech, 2003). Metabolic pathways shown by dotted lines represent the ambiguity of physiological relevance *in vivo*.

PI3P is primarily found in the cytoplasmic leaflet of the membrane of early endosomes. It was also observed on internal vesicles of multivesicular bodies. Proteins containing FYVE (Fab 1/YOTB/Vac1/EEA1) and certain types of PX domains have been shown to bind PI3P (Lemmon, 2008). PI4P is mainly present in the Golgi apparatus and serves as a marker for this organelle. It is also present in low quantity on endosomes, the plasma membrane and the ER (D'Angelo et al., 2008). PI5P is not as well characterized as the other members of the phosphoinositides family. It

is found in very low quantity and the detection of this specie has been challenging (Coronas et al., 2007). PI(3,4)P2 similar to PI(3,4,5)P3 is present in low concentration on the plasma membrane and it serves as a secondary messenger involved in survival signaling (Karathanassis et al., 2002). Last, PI(3,5)P2 is enriched on the late endosomal compartment (Dove et al., 2009; C. Y. Ho et al., 2012)and involves in regulation of endosomal trafficking (Ikonomov et al., 2001).

4.2. PI(4,5)P2

PI(4,5)2 predominantly resides at the inner leaflet of the plasma membrane and constitutes about 1-2 mol % of the phospholipids (McLaughlin et al., 2002). PI(4,5)P2 is produced when phosphorylation of PI(4)P by type I PIP5K or dephosphorylation of PI(3,4,5)P3 by PTEN occurs (Doughman et al., 2003). PI(4,5)P2 itself can be dephosphorylated by a number of 5 phosphatases such as synaptojanin, OCRL and Inpp5B (T. Sasaki et al., 2009). Phosphorylation of PI(4,5)P2 by type I PI3K produces PI(3,4,5)P3 which is an important secondary messenger for signaling. PI(4,5)P2 is recognized by variety of proteins containing PH (pleckstrin homology), ENTH (epsin NH2-terminal homology), FERM (band 4.1/ezrin/radixin/moesin), and other domains. Consequently, PI(4,5)P2 interacts with a myriad of proteins involved in cytoskeletal dynamics, endocytosis and exocytosis, assembly of distinct multimolecular complexes that control protein activity, receptor signaling and regulation of potassium ion channel activity.

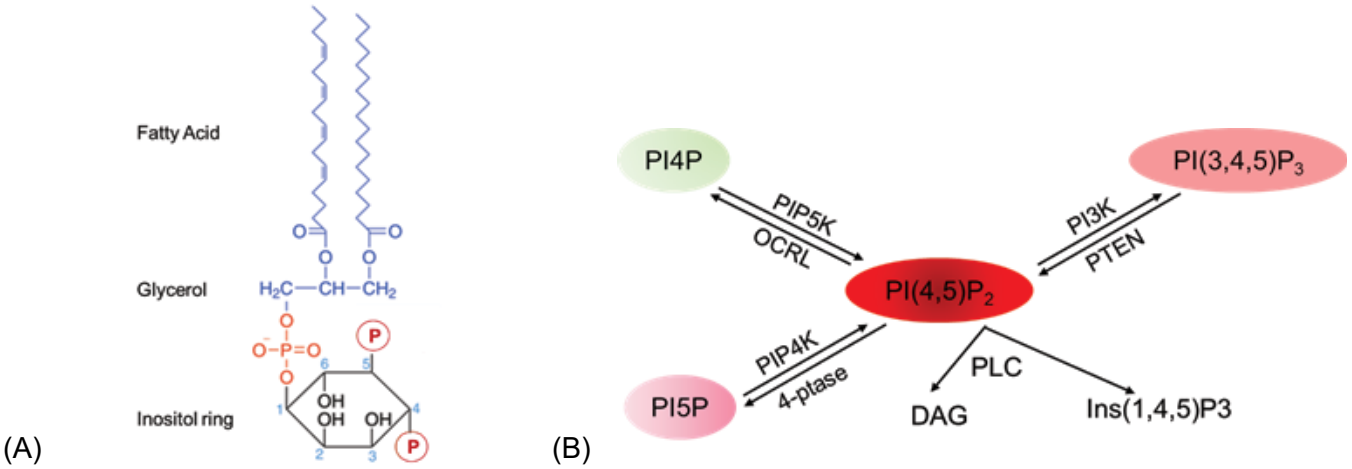

Figure 1.7 – Chemical structure of phosphatidylinositol 4,5- bisphosphate PI(4,5)P2.
(A) PI(4,5)P2 is generated by phosphorylation of D-4 and D-5 positions of the inositol ring which is usually carried out by distinct classes of phosphatidylinositol kinases that are differentially localized within the cells. (B) Pathways of generating PI(4,5)P2 from PI4P, PI5P and PI(3,4,5)P3. The major pathway of production of PI(4,5)P2 is from PI(3,4,5)P3 via class I PI3K.

4.3. PI(3,4,5)P3

PI(3,4,5)P3 is a critical signaling molecule and a survival signal. PI(3,4,5)P3 is nearly undetectable in resting cells and even after stimulation by growth promoters, the cellular concentration of PI(3,4,5)P3 is less than 1% of the total lipids and at least 25 times lower than the concentration of PI(4,5)P2 (Falkenburger et al., 2010). PI(3,4,5)P2 can be dephosphorylated by 3-phosphatases such as PTEN and type II inositol 5-phosphatastes such as SHIP, producing PI(4,5)P2 and PI(3,4)P2 respectively. Alternatively, PI(3,4,5)P3 can be produced from phosphorylation of PI(4,5)P2 by class I PI3K. Class I PI3K is made up of two subunits; a catalytic or p110 and a regulatory subunit (Liu et al., 2009). Mutations in the catalytic subunit of class I PI3K and inhibitory mutations in PTEN are associated with many human cancers. It is reported that the simultaneous manifestation of these mutations is sufficient to induce tumorigenesis in mice (Vanhaesebroeck et al., 2012). PI(3,4,5)P3 is recognized by proteins with a specific type of PH or PX (phagocyte oxidase homology) domain and a number of important signaling proteins

such as Akt, Vav and PDK isoforms (Lindmo and Stenmark, 2006). These signaling proteins get recruited to the membrane and become activated which in turn leads to cell proliferation, survival, cytoskeleton motility transformation and growth translation (Bohdanowicz and Grinstein, 2013).

(A)

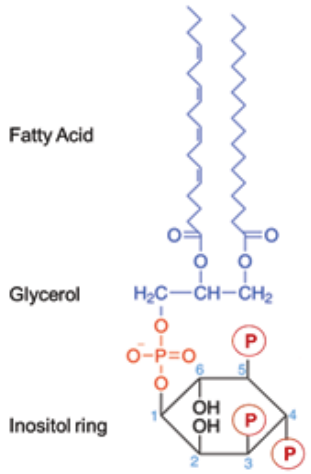

(B)

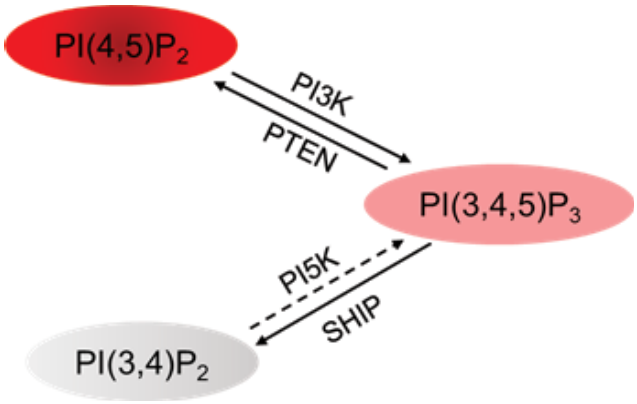

Figure 1.8 – Chemical structure of phosphatidylinositol 3,4,5- triphosphate PI(3,4,5)P3.
(A) PI(3,4,5)P3 is generated by phosphorylation of D-3, D-4 and D-5 positions of the inositol ring which is usually carried out by family of class I phosphatidylinositol 3-kinases that are largely plasma membrane associated. (B) Pathways of generating PI(3,4,5)P3 from PI(4,5)P2, PI(3,4)P2. PI(3,4,5)P3 represent less than 1 % of total lipids in the plasma membrane and known as a major signaling motif and a survival signal.

5. The Role of The Actin Cytoskeleton

The actin cytoskeleton plays a fundamental role in many processes in all eukaryotic cells. Actin is involved in important cellular processes such as muscle contraction, cell motility, cell division (Bruce et al., 2007), cytokinesis, cellular trafficking, cell signaling (Geli and Riezman, 1998) and maintaining cell shape. These actin dependent cellular processes are typically mediated by interactions with the plasma membrane. Actin filaments are most abundant in a narrow zone beneath the plasma membrane called the cortex (Lodish et al., 2000a). The cortex usually consists of F-actin filaments, myosin motors and actin binding proteins and connects to the cell membrane via diverse membrane-anchoring proteins (Gunning et al., 2015). Mutations in

genes that regulate production of actin or its associated proteins has been shown to cause various skeletal and cardiac myopathies (Alberts et al., 2002).

5.1. Types of Actin and Polymerization

Cellular actin exists in two forms namely, G-actin and F-actin. G-actin is a globular monomer and F-actin is a filamentous polymer which is made up of G-actin subunits. Each actin molecule possesses two lobes separated by a cleft comprising a Mg^{2+} ion complexed with either ATP or ADP (Lodish et al., 2000). Under physiological conditions, G-actin polymerize into polar helical filaments (F-actin) which generate two distinct ends that are called “barbed end” and “pointed end”. During steady-state conditions, G-actin subunits are added to the F- actin filaments at the barbed end while G-actin subunits dissociate at the pointed end due to the destabilization of F-actin filaments by hydrolysis of bound ATP. This phenomenon is known as “filament treadmilling” which is a major player actin based motile processes in cells (Marcora et al., 2008).

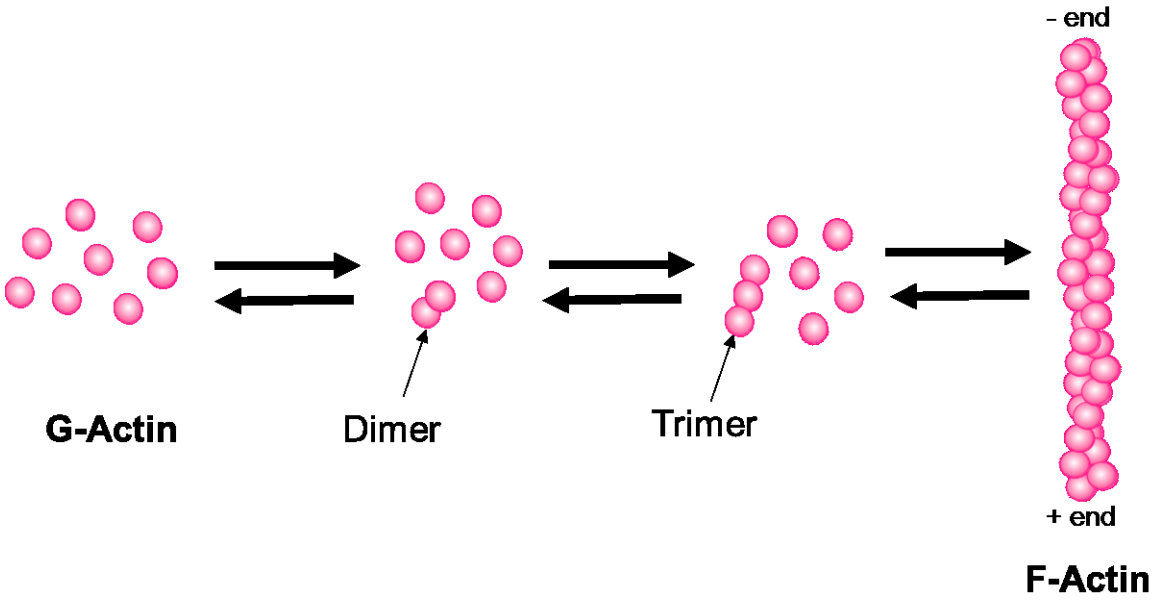

Figure 1.9

Figure 1.9 – Types of actin.
Actin exist in monomeric form called G-actin which undergo nucleation to become a trimer which is a more stable form of actin and begins polymerization with the help of Arp2/3 complex, profilin

and ADF/cofilin to become filamentous form called F-actin.

5.2. Actin Binding Proteins and Membrane Phosphoinositdies

The many functions of the actin cytoskeleton in cells are regulated by different types actin binding proteins that promote new actin filaments nucleation (Arp2/3 complexes, formins, Cobl, Spire, leiomodin) and proteins that increase actin filament depolymerization (ADF/cofilins, gelsolin) (Saarikangas et al., 2010). Moreover, proteins that interact with actin monomers (G-actin) are profilin, twinfilin, β-thymosins and proteins that interact with filament barbed ends (F-actin) are capping proteins, Eps8, Ena/VASP, altogether they work to control actin filament polymerization (Saarikangas et al., 2010). The activities of actin binding proteins are regulated by various signaling pathways to ensure proper regulation of actin dynamics in cells. One of the best characterized players in actin binding proteins regulation are the Rho-family small GTPases (Jaffe and Hall, 2005). These proteins include RhoA, Rac1, Cdc42 and Rif which regulate the formation of contractile stress fibers, promote lamellipodial actin filament network formation at the leading edge of motile cells and induce thin actin rich filopodial protrusions formation at cell periphery, respectively. Additionally, membrane phosphoinositides (PIs) play a central role in regulating the dynamics of the actin cytoskeleton (Hilpelä et al., 2004). They not only contribute in regulating the activities of Rho GTPases but also directly interact with actin binding proteins (Sechi and Wehland, 2000). Among different PIs, PI(4,5)P2 is the best categorized regulator of the actin cytoskeleton. It interacts directly with numerous actin-binding proteins such as ERM proteins, Talin, WAVE/WASP complex, Gelsolin, ADF/cofilin and Profilin/Twinfilin (Yamaguchi et al., 2009). Increase in concentration of PI(4,5)P2 at the plasma membrane has been associated with improvement in membrane-actin interaction, increase cell adhesion and F-actin assembly (Yamamoto et al., 2001). However, PI(4,5)P2 inhibit filament barbed end capping by gelsolin, filament depolymerization and actin monomer sequestration. As a result, PI(4,5)P2 promotes the

formation of actin filament structures beneath the plasma membrane and other phosphoinositide rich membrane organelles (Saarikangas et al., 2010) (Saarikangas, Zhao & Lappalainen, 2010).

Linear and branched actin networks coexist in cells but are not necessarily distributed equally. A prime example is presented by cells performing chemotaxis, where branching occurs predominantly at the leading edge, while myosin-based contractility of linear actin bundles occurs at the rear. The asymmetric distribution of plasmalemmal phosphoinositides supports the polarization of the distinct actin networks: at the back, PtdIns(4,5)P2 recruits ERM and cofilin, fostering anchorage and stabilization of linear filaments. At the front, PtdIns(3,4,5)P3 recruits guanine nucleotide exchange factors (GEFs) that activate Rac to nucleate branched actin via Arp2/3. This dichotomy relies on the maintenance of front-to-back gradients of the phosphoinositides.

5.3. Cortical cytoskeleton organization on the plasma membrane

The classical model (Fluid Mosaic Model) of the plasma membrane by Nicolson and Singer developed in 1972 postulated that the plasma membrane is a homogenous environment with random distribution of lipids and proteins embedded in the lipid bilayer (Singer and Nicolson, 1972). Subsequently, findings such as “clusters of lipids” caused from thermal effects on the membrane were developed to augment the fluid mosaic model (Lee et al., 1974; Wunderlich et al., 1975). Over the past 40 years, many scientific observations have arisen that contributed to the better understanding of plasma membrane organization proposing complex interactions of lipid-lipid, lipid-protein and protein-protein (Simons and Gerl, 2010). Additionally, more recent membrane models have proposed the presence of specialized membrane domains such as lipid rafts and protein/glycoprotein complexes as well as the roles of membrane-associated cytoskeletal fences and extracellular matrix structures in plasma membrane organization (Nicolson, 2014). These updated models are based from the classical model to enhance the

knowledge of the plasma membrane regarding the limitation of lateral diffusion and range of motion of membrane components (Nicolson, 2014).

The regulation of cortical cytoskeleton on plasma membrane first materialized from studies investigating the movement of many membrane proteins using single-particle tracking (SPT) (Kusumi et al., 1993; Kusumi and Sako, 1996). These studies suggested that many plasma membrane proteins do not diffuse freely and possess lower diffusion coefficients than in pure lipid bilayers (Kusumi and Sako, 1996; Kusumi et al., 2005) which led Kusumi et al. to propose a model called “fence and picket” model in which the presence of diffusion barriers and corrals created by transmembrane proteins or “pickets” anchored to cortical actin cytoskeleton “fences” control the movement of plasmalemma proteins (Kalay et al., 2014; Kusumi et al., 2012). Observations such as the restricted lateral diffusion caused by the cortical actin cytoskeleton of GPI anchor protein, which is mainly present in the outer leaflet of the plasma membrane (Saha et al., 2015) provided a compelling evidence for the concept of “fence and picket” model.

The consequence of this model is that the transmembrane proteins “pickets” create compartments (30-700 nm) (Ritchie et al., 2005) that allow the free diffusion of proteins and lipids within the same compartment but limits diffusion of these proteins and lipids to another compartment. However, this can be overcome by an occasional inter-compartmental hop which may perhaps be caused by 1) thermal fluctuations of the plasma membrane which creates spaces between the membrane and cytoskeleton 2) temporary breakage of actin cytoskeleton and 3) fluctuations in the kinetic energy of the membrane molecules (Ritchie et al., 2005). Although the “picket and fence” model serves as one of the explanations for the regulation of cortical cytoskeleton on plasma membrane organization, it is still unclear how these picket proteins are attached to the cortical actin cytoskeleton. Some membrane receptors have capacity to adhere to the actin cytoskeleton either directly or indirectly through adaptor molecules namely actin binding proteins.

Membrane proteins identified as directly binding to actin are mostly ion channels, for instance, CFTR (Cystic Fibrosis Transmembrane Conductance Regulator), Enac (Epithelia Sodium Channel), Maxi-K (potassium channel), TRPV 4 (Transient Receptor Potential Cation Channel Subfamily V member 4) and VDAC (Voltage Dependent Anion Channel) (S. Sasaki et al., 2014). These proteins were shown to interact with actin directly using co-sedimentation, co-immunoprecipitation, gel overlay, surface plasmon resonance, fluorescence cross-correlation spectroscopy, FRET, and atomic force microscopy (Sasaki et al., 2014). Indirect binding of membrane receptors to cortical actin cytoskeleton is carried out via adaptor molecules called actin binding proteins (mentioned above). Receptors such as CD44 (Freeman et al., 2018) , CD9 and CD81 (Tetraspanins) are known to possess a binding site for actin linking molecule, ezrin-radixin-moesin (ERM) (Sala-Valdés et al., 2006).

Recently, advance in biophysical and biochemical techniques have shed more light on understanding the role of cortical cytoskeleton in plasma membrane dynamics and organization and it has become apparent that the role of cortical cytoskeleton cannot be sufficiently define as the mechanism of cell locomotion. Hence, we are interested in elucidating the other roles of cortical cytoskeleton especially in regulating transmembrane signaling, particularly in organization of CD36. CD36 serves as a unique example to study this as it has been shown previously to be controlled by cell cortical cytoskeleton at the plasma membrane of macrophages (Jaqaman et al., 2011). Connection of CD36 with cortical F-actin in controlling CD36 signaling has been established in our lab previously, however, additional investigation is necessary (Githaka et al., 2016). An apparent lack of evidence in direct binding of CD36 and cortical actin cytoskeleton has directed us to hypothesize the presence of adaptor molecules linking CD36 and cortical cytoskeleton and thus we sought to characterize these molecules.

6. Super-resolution microscopy

In the past, detailed study of structural organization of proteins, lipids, other biological molecules and their association to the surrounding environment has been difficult. However, advances in the biophysical methods have opened a wide and exciting field for many scientists. The development of super-resolution microscopy (SRM) has expanded the field of investigations for nanoscale biological structure. Super-resolution microscopy permits the experimenter to overcome the diffraction limit of light and allow discoveries of cellular structures at the nanometer scale from individual proteins to entire organelles. The SRM technique we employ commonly in the lab is called Photo-Activated Localization Microscopy (PALM) and Stochastic Optical Reconstruction Microscopy (STORM). It utilizes photoswitchable fluorescent proteins (PALM) and photoswitchable organic dyes (STORM). These techniques apply the principles of stochastically activating a subgroup of photoswitchable probes at a time and then determines the center of the position of each point spread function (Sydor et al., 2015). This application can be combined with either wide-field or TIRF microscopy explained in Chapter-2 Material and Methods and can have the resolution of up to 10-30 nm.

In our project, we employed the technique of PALM imaging with TIRF which allows us to focus clustering of CD36 particularly on the plasma membrane of endothelial cells. The data generated by PALM-TIRF imaging (Jaqaman et al., 2008) is then analyzed using Spatial Pattern Analysis (SPA) developed by Jaqaman an Touret group (Githaka et al, 2016).

7. Previous Findings, Hypothesis and Rationale

CD36 signaling in endothelial cells begins with the binding of TSP-1 to the receptor which activates the downstream Src family kinase member, Fyn. Some of the downstream effectors of this signaling pathway includes mitogen activated kinases (MAPK) p38 and c-Jun N-terminal kinase (JNK) and caspase 3, eventually leading to endothelial cell death by apoptosis. The capacity of CD36 to undergo signaling after binding TSP-1 had been poorly understood, mainly

due to the lack of intrinsic signaling capabilities of CD36. To understand more about CD36-TSP-1 signaling, researchers began to consider the ligands of CD36 themselves. TSP-1 which exists as trimer with multiple binding sites for CD36 was one of the first evidence to suggest that CD36 signaling may be clustering dependent. The hypothesis was that CD36 clustering by multivalent ligands is important for Fyn activation and downstream signaling. Moreover, decavalent anti-CD36 IgM (clone SMφ) and not bivalent IgG (clone FA6-152) activates Fyn and induces endothelial cell apoptosis (Jimenez et al., 2000).In macrophages, CD36 activation is dependent on the actin cytoskeleton. Our lab investigated the mechanism of CD36 signaling in endothelial cells. The previous work done in our lab has shown that CD36-TSP-1 signaling begins by clustering of CD36 molecules. Using photoactivated localization microscopy (PALM) combined with total internal reflection microscopy (TIRF) and Spatial Pattern Analysis (SPA) (Owen et al., 2010), CD36 nanoclusters properties were studied with or without TSP-1 stimulation. These methods allowed the determination of CD36 nanoclusters properties. CD36 nanoclusters exist in 70 nm size and 4000 molecules/μm^2 before TSP-1 treatment and nanoclusters size and density increases to 90 nm and approximately 4800 molecules/μm^2 after TSP-1 treatment (Githaka et al., 2016). This increase in size and density of CD36 nanoclusters promote activation of Fyn and eventually lead to the activation of downstream effectors such as p38MAPK and p130Cas. Our lab proposed a model that CD36 is organized into nanoclusters at basal state enriched with the downstream effector Fyn. Upon TSP-1 ligation, Fyn gets activated due to ligand-induced enhancement of CD36 nanoclusters. In addition, CD36 nanoclusters are associated with GM1 on the outer leaflet of the plasma membrane and F-actin cortical cytoskeleton. Disruption of plasma membrane lipid compositions using methyl beta cyclodextrin (MβCD) and actin cytoskeleton using Latrunculin B diminished the CD36 nanoclusters enhancement and activation of Fyn. These data suggested that CD36 nanoclusters enhancement and Fyn activation depends not only on the ligand but also on F-actin and cholesterol (lipid environment) of the plasma membrane. CD36-TSP-1 signaling is promoted by F-actin and specific plasma membrane organization.

With these findings, our lab sought to understand the role of plasma membrane phospholipids focusing on membrane phosphoinositides (PI(4,5)P2 and PI(3,4,5)P3) and actin cytoskeleton in Fyn activation and CD36 nanoclusters enrichment. The two main goals of our research study are to characterize the role of lipids nanodomains in Fyn activation and CD36 nanoclusters enrichment and to identify potential adaptor proteins connecting F-actin and CD36 nanoclusters. By using pharmacological inhibition of PI3K to stop production of PI(3,4,5)P3 and ionomycin to deplete PI(4,5)P2 from the membrane upon TSP-1 activation, we sought to investigate the CD36 nanoclusters enhancement and Fyn activation. As for the second part of my project, we screened for potential adaptor proteins between CD36 and cortical F-actin using Proximity Dependent Biotin Identification combined with Mass Spectrometry.

8. References

Abumrad, N.A., El-Maghrabi, M.R., Amri, E.Z., Lopez, E., and Grimaldi, P.A. (1993). Cloning of a rat adipocyte membrane protein implicated in binding or transport of long-chain fatty acids that is induced during preadipocyte differentiation. Homology with human CD36. J. Biol. Chem. *268,* 17665-17668.

Alberts, B., Johnson, A., Lewis, J., Raff, M., Roberts, K., and Walter, P. (2002). Molecular Biology of the Cell, (Garland Science, New York, 2008). Google Scholar 652.

Amata, I., Maffei, M., and Pons, M. (2014). Phosphorylation of unique domains of Src family kinases. Frontiers in Genetics *5,* 181.

Asch, A.S., Liu, I., Briccetti, F.M., Barnwell, J.W., Kwakye-Berko, F., Dokun, A., Goldberger, J., and Pernambuco, M. (1993). Analysis of CD36 binding domains: ligand specificity controlled by dephosphorylation of an ectodomain. Science *262,* 1436-1440.

Baenziger, N.L., Brodie, G.N., and Majerus, P.W. (1971). A thrombin-sensitive protein of human platelet membranes. Proceedings of the National Academy of Sciences *68,* 240-243.

Bohdanowicz, M., and Grinstein, S. (2013). Role of phospholipids in endocytosis, phagocytosis, and macropinocytosis. Physiol. Rev. *93,* 69-106.

Bruce, A., Johnson, A., Lewis, J., Raff, M., Roberts, K., and Walter, P. (2007). Molecular Biology of the Cell 5th edn (New York: Garland Science).

Chu, L., and Silverstein, R.L. (2012). CD36 ectodomain phosphorylation blocks thrombospondin-1 binding: structure-function relationships and regulation by protein kinase C. Arterioscler. Thromb. Vasc. Biol. *32,* 760-767.

Coronas, S., Ramel, D., Pendaries, C., Gaits-Iacovoni, F., Tronchere, H., and Payrastre, B. Paper presented at Biochemical Society Symposia.

Czech, M.P. (2003). Dynamics of phosphoinositides in membrane retrieval and insertion. Annu. Rev. Physiol. *65,* 791-815.

D'Angelo, G., Vicinanza, M., Di Campli, A., and De Matteis, M.A. (2008). The multiple roles of PtdIns (4) P–not just the precursor of PtdIns (4, 5) P2. J. Cell. Sci. *121,* 1955-1963.

Dawson, D.W., Pearce, S.F.A., Zhong, R., Silverstein, R.L., Frazier, W.A., and Bouck, N.P. (1997). CD36 mediates the in vitro inhibitory effects of thrombospondin-1 on endothelial cells. J. Cell Biol. *138,* 707-717.

Di Paolo, G., and De Camilli, P. (2006). Phosphoinositides in cell regulation and membrane dynamics. Nature *443,* 651.

Doughman, R.L., Firestone, A.J., and Anderson, R.A. (2003). Phosphatidylinositol phosphate kinases put PI4, 5P 2 in its place. J. Membr. Biol. *194,* 77-89.

Dove, S.K., Dong, K., Kobayashi, T., Williams, F.K., and Michell, R.H. (2009). Phosphatidylinositol 3, 5-bisphosphate and Fab1p/PIKfyve underPPIn endo-lysosome function. Biochem. J. *419,* 1-13.

Esemuede, N., Lee, T., Pierre-Paul, D., Sumpio, B.E., and Gahtan, V. (2004). The role of thrombospondin-1 in human disease1. J. Surg. Res. *122,* 135-142.

Falkenburger, B.H., Jensen, J.B., Dickson, E.J., Suh, B., and Hille, B. (2010). Symposium Review: Phosphoinositides: lipid regulators of membrane proteins. J. Physiol. (Lond.) *588,* 3179-3185.

Febbraio, M., Hajjar, D.P., and Silverstein, R.L. (2001). CD36: a class B scavenger receptor involved in angiogenesis, atherosclerosis, inflammation, and lipid metabolism. J. Clin. Invest. *108,* 785-791.

Freeman, S.A., Vega, A., Riedl, M., Collins, R.F., Ostrowski, P.P., Woods, E.C., Bertozzi, C.R., Tammi, M.I., Lidke, D.S., and Johnson, P. (2018). Transmembrane Pickets Connect Cyto-and Pericellular Skeletons Forming Barriers to Receptor Engagement. Cell *172,* 317. e10.

Geli, M.I., and Riezman, H. (1998). Endocytic internalization in yeast and animal cells: similar and different. J. Cell. Sci. *111,* 1031-1037.

Githaka, J.M., Vega, A.R., Baird, M.A., Davidson, M.W., Jaqaman, K., and Touret, N. (2016). Ligand-induced growth and compaction of CD36 nanoclusters enriched in Fyn induces Fyn signaling. J. Cell. Sci. *129,* 4175-4189.

Goodridge, H.S., Underhill, D.M., and Touret, N. (2012). Mechanisms of Fc Receptor and Dectin-1 Activation for Phagocytosis. Traffic *13,* 1062-1071.

Gruarin, P., Sitia, R., and Alessio, M. (1997). Formation of one or more intrachain disulphide bonds is required for the intracellular processing and transport of CD36. Biochem. J. *328,* 635.

Gruarin, P., Thorne, R.F., Dorahy, D.J., Burns, G.F., Sitia, R., and Alessio, M. (2000). CD36 is a ditopic glycoprotein with the N-terminal domain implicated in intracellular transport. Biochem. Biophys. Res. Commun. *275,* 446-454.

Gunning, P.W., Ghoshdastider, U., Whitaker, S., Popp, D., and Robinson, R.C. (2015). The evolution of compositionally and functionally distinct actin filaments. J. Cell. Sci. *128,* 2009-2019.

Hagelberg, C., and Allan, D. (1990). Restricted diffusion of integral membrane proteins and polyphosphoinositides leads to their depletion in microvesicles released from human erythrocytes. Biochem. J. *271,* 831.

Hilpelä, P., Vartiainen, M.K., and Lappalainen, P. (2004). Regulation of the actin cytoskeleton by PI (4, 5) P 2 and PI (3, 4, 5) P 3. In Phosphoinositides in Subcellular Targeting and Enzyme Activation, Springer) pp. 117-163.

Hisatsune, C., Kuroda, Y., Nakamura, K., Inoue, T., Nakamura, T., Michikawa, T., Mizutani, A., and Mikoshiba, K. (2004). Regulation of TRPC6 channel activity by tyrosine phosphorylation. J. Biol. Chem. *279,* 18887-18894.

Ho, C.Y., Alghamdi, T.A., and Botelho, R.J. (2012). Phosphatidylinositol-3, 5-Bisphosphate: No Longer the Poor PIP2. Traffic *13,* 1-8.

Ho, M., Hoang, H.L., Lee, K.M., Liu, N., MacRae, T., Montes, L., Flatt, C.L., Yipp, B.G., Berger, B.J., and Looareesuwan, S. (2005). Ectophosphorylation of CD36 regulates cytoadherence of Plasmodium falciparum to microvascular endothelium under flow conditions. Infect. Immun. *73,* 8179-8187.

Hoosdally, S.J., Andress, E.J., Wooding, C., Martin, C.A., and Linton, K.J. (2009). The human scavenger receptor CD36 glycosylation status and its role in trafficking and function. J. Biol. Chem. *284,* 16277-16288.

Huntington, N.D., and Tarlinton, D.M. (2004). CD45: direct and indirect government of immune regulation. Immunol. Lett. *94,* 167-174.

Ikonomov, O.C., Sbrissa, D., and Shisheva, A. (2001). Mammalian cell morphology and endocytic membrane homeostasis require enzymatically active phosphoinositide 5-kinase PIKfyve. J. Biol. Chem. *276,* 26141-26147.

Jaffe, A.B., and Hall, A. (2005). Rho GTPases: biochemistry and biology. Annu.Rev.Cell Dev.Biol. *21,* 247-269.

Jaqaman, K., Kuwata, H., Touret, N., Collins, R., Trimble, W.S., Danuser, G., and Grinstein, S. (2011). Cytoskeletal control of CD36 diffusion promotes its receptor and signaling function. Cell *146,* 593-606.

Jaqaman, K., Loerke, D., Mettlen, M., Kuwata, H., Grinstein, S., Schmid, S.L., and Danuser, G. (2008). Robust single-particle tracking in live-cell time-lapse sequences. Nature Methods *5,* 695.

Jimenez, B., Volpert, O.V., Crawford, S.E., Febbraio, M., Silverstein, R.L., and Bouck, N. (2000). Signals leading to apoptosis-dependent inhibition of neovascularization by thrombospondin-1. Nat. Med. *6,* 41.

Jimenez, B., Volpert, O.V., Reiher, F., Chang, L., Munoz, A., Karin, M., and Bouck, N. (2001). c-Jun N-terminal kinase activation is required for the inhibition of neovascularization by thrombospondin-1. Oncogene *20,* 3443.

Kalay, Z., Fujiwara, T.K., Otaka, A., and Kusumi, A. (2014). Lateral diffusion in a discrete fluid membrane with immobile particles. Physical Review E *89,* 022724.

Karathanassis, D., Stahelin, R.V., Bravo, J., Perisic, O., Pacold, C.M., Cho, W., and Williams, R.L. (2002). Binding of the PX domain of p47phox to phosphatidylinositol 3, 4-bisphosphate and phosphatidic acid is masked by an intramolecular interaction. Embo J. *21,* 5057-5068.

Klenotic, P.A., Page, R.C., Li, W., Amick, J., Misra, S., and Silverstein, R.L. (2013). Molecular Basis of Antiangiogenic Thrombospondin-1 Type 1 Repeat Domain Interactions With CD36Significance. Arterioscler. Thromb. Vasc. Biol. *33,* 1655-1662.

Klenotic, P.A., Page, R.C., Misra, S., and Silverstein, R.L. (2011). Expression, purification and structural characterization of functionally replete thrombospondin-1 type 1 repeats in a bacterial expression system. Protein Expr. Purif. *80,* 253-259.

Koldsø, H., and Sansom, M.S. (2015). Organization and dynamics of receptor proteins in a plasma membrane. J. Am. Chem. Soc. *137,* 14694-14704.

Kusumi, A., Fujiwara, T.K., Chadda, R., Xie, M., Tsunoyama, T.A., Kalay, Z., Kasai, R.S., and Suzuki, K.G. (2012). Dynamic organizing principles of the plasma membrane that regulate signal transduction: commemorating the fortieth anniversary of Singer and Nicolson's fluid-mosaic model. Annu. Rev. Cell Dev. Biol. *28,* 215-250.

Kusumi, A., Nakada, C., Ritchie, K., Murase, K., Suzuki, K., Murakoshi, H., Kasai, R.S., Kondo, J., and Fujiwara, T. (2005). Paradigm shift of the plasma membrane concept from the two-dimensional continuum fluid to the partitioned fluid: high-speed single-molecule tracking of membrane molecules. Annu.Rev.Biophys.Biomol.Struct. *34,* 351-378.

Kusumi, A., and Sako, Y. (1996). Cell surface organization by the membrane skeleton. Curr. Opin. Cell Biol. *8,* 566-574.

Kusumi, A., Sako, Y., and Yamamoto, M. (1993). Confined lateral diffusion of membrane receptors as studied by single particle tracking (nanovid microscopy). Effects of calcium-induced differentiation in cultured epithelial cells. Biophys. J. *65,* 2021-2040.

Lawler, P.R., and Lawler, J. (2012). Molecular basis for the regulation of angiogenesis by thrombospondin-1 and-2. Cold Spring Harbor Perspectives in Medicine *2,* a006627.

Lee, A.G., Birdsall, N., Metcalfe, J.C., Toon, P.A., and Warren, G.B. (1974). Clusters in lipid bilayers and the interpretation of thermal effects in biological membranes. Biochemistry (N. Y.) *13,* 3699-3705.

Lemmon, M.A. (2008). Membrane recognition by phospholipid-binding domains. Nature Reviews Molecular Cell Biology *9,* 99.

Lindmo, K., and Stenmark, H. (2006). Regulation of membrane traffic by phosphoinositide 3-kinases. J. Cell. Sci. *119,* 605-614.

Liu, P., Cheng, H., Roberts, T.M., and Zhao, J.J. (2009). Targeting the phosphoinositide 3-kinase pathway in cancer. Nature Reviews Drug Discovery *8,* 627.

Lodish, H., Berk, A., Zipursky, S.L., Matsudaira, P., Baltimore, D., and Darnell, J. (2000a). The actin cytoskeleton.

Lodish, H., Berk, A., Zipursky, S.L., Matsudaira, P., Baltimore, D., and Darnell, J. (2000b). Biomembranes: Structural organization and basic functions.

Marcora, E., Carlisle, H.J., and Kennedy, M.B. (2008). The Role of the Postsynaptic Density and the Spine Cytoskeleton in Synaptic Plasticity.

Markovic, S.N., Suman, V.J., Rao, R.A., Ingle, J.N., Kaur, J.S., Erickson, L.A., Pitot, H.C., Croghan, G.A., McWilliams, R.R., and Merchan, J. (2007). A phase II study of ABT-510 (thrombospondin-1 analog) for the treatment of metastatic melanoma. American Journal of Clinical Oncology *30,* 303-309.

McLaughlin, S., Wang, J., Gambhir, A., and Murray, D. (2002). PIP2 and proteins: interactions, organization, and information flow. Annu. Rev. Biophys. Biomol. Struct. *31,* 151-175.

Murphy-Ullrich, J.E., and Poczatek, M. (2000). Activation of latent TGF-β by thrombospondin-1: mechanisms and physiology. Cytokine Growth Factor Rev. *11,* 59-69.

Navazo, M.D.P., Daviet, L., Ninio, E., and McGregor, J.L. (1996). Identification on human CD36 of a domain (155-183) implicated in binding oxidized low-density lipoproteins (Ox-LDL). Arterioscler. Thromb. Vasc. Biol. *16,* 1033-1039.

Neculai, D., Schwake, M., Ravichandran, M., Zunke, F., Collins, R.F., Peters, J., Neculai, M., Plumb, J., Loppnau, P., and Pizarro, J.C. (2013). Structure of LIMP-2 provides functional insights with implications for SR-BI and CD36. Nature *504,* 172.

Nicolson, G.L. (2014). The Fluid—Mosaic Model of Membrane Structure: Still relevant to understanding the structure, function and dynamics of biological membranes after more than 40years. Biochimica Et Biophysica Acta (BBA)-Biomembranes *1838,* 1451-1466.

Niggli, V. (2005). Regulation of protein activities by phosphoinositide phosphates. Annu.Rev.Cell Dev.Biol. *21,* 57-79.

Nishida, N., Yano, H., Nishida, T., Kamura, T., and Kojiro, M. (2006). Angiogenesis in cancer. Vascular Health and Risk Management *2,* 213.

Noutsi, P., Gratton, E., and Chaieb, S. (2016). Assessment of Membrane Fluidity Fluctuations during Cellular Development Reveals Time and Cell Type Specificity. PloS One *11,* e0158313.

Okada, M. (2012). Regulation of the SRC family kinases by Csk. International Journal of Biological Sciences *8,* 1385.

Owen, D.M., Rentero, C., Rossy, J., Magenau, A., Williamson, D., Rodriguez, M., and Gaus, K. (2010). PALM imaging and cluster analysis of protein heterogeneity at the cell surface. Journal of Biophotonics *3,* 446-454.

Park, Y.M. (2014). CD36, a scavenger receptor implicated in atherosclerosis. Exp. Mol. Med. *46,* e99.

Park, Y.M., Febbraio, M., and Silverstein, R.L. (2009). CD36 modulates migration of mouse and human macrophages in response to oxidized LDL and may contribute to macrophage trapping in the arterial intima. J. Clin. Invest. *119,* 136-145.

Pearce, S.F.A., Wu, J., and Silverstein, R.L. (1995). Recombinant GST/CD36 Fusion Proteins Define a Thrombospondin Binding Domain EVIDENCE FOR A SINGLE CALCIUM-DEPENDENT BINDING SITE ON CD36. J. Biol. Chem. *270,* 2981-2986.

Posadas, E.M., Al-Ahmadie, H., Robinson, V.L., Jagadeeswaran, R., Otto, K., Kasza, K.E., Tretiakov, M., Siddiqui, J., Pienta, K.J., and Stadler, W.M. (2009). FYN is overexpressed in human prostate cancer. BJU Int. *103,* 171-177.

Rege, T.A., Stewart, J., Dranka, B., Benveniste, E.N., Silverstein, R.L., and Gladson, C.L. (2009). Thrombospondin-1-induced apoptosis of brain microvascular endothelial cells can be mediated by TNF-R1. J. Cell. Physiol. *218,* 94-103.

Ren, B., Yee, K.O., Lawler, J., and Khosravi-Far, R. (2006). Regulation of tumor angiogenesis by thrombospondin-1. Biochimica Et Biophysica Acta (BBA)-Reviews on Cancer *1765,* 178-188.

Ritchie, K., Shan, X., Kondo, J., Iwasawa, K., Fujiwara, T., and Kusumi, A. (2005). Detection of non-Brownian diffusion in the cell membrane in single molecule tracking. Biophys. J. *88,* 2266-2277.

Roskoski, R. (2005). Src kinase regulation by phosphorylation and dephosphorylation. Biochem. Biophys. Res. Commun. *331,* 1-14.

Russell, S., Duquette, M., Liu, J., Drapkin, R., Lawler, J., and Petrik, J. (2015). Combined therapy with thrombospondin-1 type I repeats (3TSR) and chemotherapy induces regression and significantly improves survival in a preclinical model of advanced stage epithelial ovarian cancer. The FASEB Journal *29,* 576-588.

Saarikangas, J., Zhao, H., and Lappalainen, P. (2010). Regulation of the actin cytoskeleton-plasma membrane interplay by phosphoinositides. Physiol. Rev. *90,* 259-289.

Saha, S., Lee, I., Polley, A., Groves, J.T., Rao, M., and Mayor, S. (2015). Diffusion of GPI-anchored proteins is influenced by the activity of dynamic cortical actin. Mol. Biol. Cell *26,* 4033-4045.

Sala-Valdés, M., Ursa, A, Charrin, S., Rubinstein, E., Hemler, M.E., Sánchez-Madrid, F., and Yáñez-Mó, M. (2006). EWI-2 and EWI-F link the tetraspanin web to the actin cytoskeleton through their direct association with ezrin-radixin-moesin proteins. J. Biol. Chem. *281,* 19665-19675.

Sasaki, S., Yui, N., and Noda, Y. (2014). Actin directly interacts with different membrane channel proteins and influences channel activities: AQP2 as a model. Biochimica Et Biophysica Acta (BBA)-Biomembranes *1838,* 514-520.

Sasaki, T., Takasuga, S., Sasaki, J., Kofuji, S., Eguchi, S., Yamazaki, M., and Suzuki, A. (2009). Mammalian phosphoinositide kinases and phosphatases. Prog. Lipid Res. *48,* 307-343.

Sato, I., Obata, Y., Kasahara, K., Nakayama, Y., Fukumoto, Y., Yamasaki, T., Yokoyama, K.K., Saito, T., and Yamaguchi, N. (2009). Differential trafficking of Src, Lyn, Yes and Fyn is specified by the state of palmitoylation in the SH4 domain. J. Cell. Sci. *122,* 965-975.

Sechi, A.S., and Wehland, J. (2000). The actin cytoskeleton and plasma membrane connection: PtdIns (4, 5) P (2) influences cytoskeletal protein activity at the plasma membrane. J. Cell. Sci. *113,* 3685-3695.

Sen, B., and Johnson, F.M. (2011). Regulation of SRC family kinases in human cancers. Journal of Signal Transduction *2011,*

Silverstein, R.L., and Febbraio, M. (2009). CD36, a scavenger receptor involved in immunity, metabolism, angiogenesis, and behavior. Sci.Signal. *2,* re3.

Simantov, R., and Silverstein, R.L. (2003). CD36: a critical anti-angiogenic receptor. Front. Biosci. *8,* 874.

Simons, K., and Gerl, M.J. (2010). Revitalizing membrane rafts: new tools and insights. Nature Reviews Molecular Cell Biology *11,* nrm2977.

Simons, K., and Sampaio, J.L. (2011). Membrane organization and lipid rafts. Cold Spring Harbor Perspectives in Biology *3,* a004697.

Singer, S.J., and Nicolson, G.L. (1972). The fluid mosaic model of the structure of cell membranes. Science *175,* 720-731.

Sydor, A.M., Czymmek, K.J., Puchner, E.M., and Mennella, V. (2015). Super-resolution microscopy: from single molecules to supramolecular assemblies. Trends Cell Biol. *25,* 730-748.

Tan, K., Duquette, M., Liu, J., Dong, Y., Zhang, R., Joachimiak, A., Lawler, J., and Wang, J. (2002). Crystal structure of the TSP-1 type 1 repeats: a novel layered fold and its biological implication. J. Cell Biol. *159,* 373-382.

Tan, K., and Lawler, J. (2009). The interaction of Thrombospondins with extracellular matrix proteins. Journal of Cell Communication and Signaling *3,* 177-187.

Tao, N., Wagner, S.J., and Lublin, D.M. (1996). CD36 is palmitoylated on both N-and C-terminal cytoplasmic tails. J. Biol. Chem. *271,* 22315-22320.

Tolsma, S.S., Volpert, O.V., Good, D.J., Frazier, W.A., Polverini, P.J., and Bouck, N. (1993). Peptides derived from two separate domains of the matrix protein thrombospondin-1 have anti-angiogenic activity. J. Cell Biol. *122,* 497-511.

Vacaresse, N., Møller, B., Danielsen, E.M., Okada, M., and Sap, J. (2008). Activation of c-Src and Fyn kinases by protein-tyrosine phosphatase RPTPα is substrate-specific and compatible with lipid raft localization. J. Biol. Chem. *283,* 35815-35824.

Van Meer, G., Voelker, D.R., and Feigenson, G.W. (2008). Membrane lipids: where they are and how they behave. Nature Reviews Molecular Cell Biology *9,* 112.

Vanhaesebroeck, B., Stephens, L., and Hawkins, P. (2012). PI3K signalling: the path to discovery and understanding. Nature Reviews Molecular Cell Biology *13,* 195.

Volpert, O.V., Zaichuk, T., Zhou, W., Reiher, F., Ferguson, T.A., Stuart, P.M., Amin, M., and Bouck, N.P. (2002). Inducer-stimulated Fas targets activated endothelium for destruction by anti-angiogenic thrombospondin-1 and pigment epithelium–derived factor. Nat. Med. *8,* 349.

Welch, H.C., Coadwell, W.J., Stephens, L.R., and Hawkins, P.T. (2003). Phosphoinositide 3-kinase-dependent activation of Rac. FEBS Lett. *546,* 93-97.

Wilkinson, B., Koenigsknecht-Talboo, J., Grommes, C., Lee, C.D., and Landreth, G. (2006). Fibrillar β-amyloid-stimulated intracellular signaling cascades require Vav for induction of respiratory burst and phagocytosis in monocytes and microglia. J. Biol. Chem. *281,* 20842-20850.

Wolf, R.M., Wilkes, J.J., Chao, M.V., and Resh, M.D. (2001). Tyrosine phosphorylation of p190 RhoGAP by Fyn regulates oligodendrocyte differentiation. Developmental Neurobiology *49,* 62-78.

Wunderlich, F., Ronai, A., Speth, V., Seelig, J., and Blume, A. (1975). Thermotropic lipid clustering in Tetrahymena membranes. Biochemistry (N. Y.) *14,* 3730-3735.

Yamaguchi, H., Shiraishi, M., Fukami, K., Tanabe, A., Ikeda-Matsuo, Y., Naito, Y., and Sasaki, Y. (2009). MARCKS regulates lamellipodia formation induced by IGF-I via association with PIP2 and β-actin at membrane microdomains. J. Cell. Physiol. *220,* 748-755.

Yamamoto, M., Hilgemann, D.H., Feng, S., Bito, H., Ishihara, H., Shibasaki, Y., and Yin, H.L. (2001). Phosphatidylinositol 4, 5-bisphosphate induces actin stress-fiber formation and inhibits membrane ruffling in CV1 cells. J. Cell Biol. *152,* 867-876.

Yang, T., Massa, S.M., and Longo, F.M. (2006). LAR protein tyrosine phosphatase receptor associates with TrkB and modulates neurotrophic signaling pathways. Developmental Neurobiology *66,* 1420-1436.

Zachowski, A. (1993). Phospholipids in animal eukaryotic membranes: transverse asymmetry and movement. Biochem. J. *294,* 1.

Zeng, Y., Tao, N., Chung, K., Heuser, J.E., and Lublin, D.M. (2003). Endocytosis of oxidized low density lipoprotein through scavenger receptor CD36 utilizes a lipid raft pathway that does not require caveolin-1. J. Biol. Chem. *278,* 45931-45936.

Zheng, X., Resnick, R.J., and Shalloway, D. (2000). A phosphotyrosine displacement mechanism for activation of Src by PTPα. Embo J. *19,* 964-978.

Chapter 2 - **Materials and Methods**

1. Materials

1.1. Cell Culture

In our experiments, we used three cell lines, human microvascular endothelial cell line (HMEC-1) (Centre for Disease Control and Prevention, Atlanta, GA, USA), immortalized human foreskin dermal microvascular endothelium (TIME (ATCC® CRL-4025™)) and human cervical adenocarcinoma epithelial cells (HeLa (ATCC® CCL-2™)). HMEC-1 cells were cultured in MCDB-131 media (Gibco, Life Technologies, Burlington, ON, Canada) supplemented with 20% FBS (Wisent Bioproducts, St-Bruno, Quebec, Canada), 10 mM L-Glutamate (Gibco), 10 ng/mL Epidermal Growth Factor (BD Biosciences, Mississagua, ON, Canada),1 µg/mL hydrocortisone (Sigma-Aldrich, St. Louis, MO, USA), 1 mg/mL G418 (Life Technology, Paisley, UK) and 1 mg/mL Pen Strep (Life Technology, Paisley, UK). HeLa cells were maintained in Dulbecco's Modified Eagle's medium (DMEM) (ATCC®-30-2002™) supplemented with 10% FBS and 1 mg/mL Penicilin / Streptomycin. TIME cells expressing CD36-mEmerald were maintained in Vascular Cell Basal

Medium (ATCC® PCS-100-030), supplemented with Microvascular Endothelial Cell Growth Kit-VEGF (ATCC® PCS-110-041) and 12.5 µg/mL blasticidine.

1.2. DNA plasmids and Stable Expression of Constructs

Stable expression of CD36-mApple, CD36-PAmcherry and CD36-myc in HMEC-1 cells were generated as described in Githaka, J et al, 2016. However, TIME cells stably expressing CD36-mEmerald and HeLa cells stably expressing CD36-BirA-Flag, implemented in Tetracycline Inducible System were generated in our lab by first cloning the CD36-mEmerald and CD36-BirA-Flag into pLVX-TREG containing tetracycline response element prepared previously in our lab.

The plasmids, pLVX-TREG-BirA-Flag-CD36 and pLVX-TREG-CD36-mEmerald were extracted and purified using QIAGEN Plasmid Maxi Kit (Qiagen, Hilden, Germany). These plasmids were transfected in HEK 293T cells for production of viral particles using SingleShot kit (Clonetech, Mountainview, California, USA). 3 days post transfection, the lentivirus containing supernatants were collected, concentrated and infected into respective cell types grown to 70% confluency. After 48 h of infection, 1 mg/mL of G418 (Sigma-Aldrich) and 1 mg/mL of Puromycin was added into the culture media for selection of stable cell lines. The selection with G418 was continued for 14 days to obtain HeLa-TREG-BirA-Flag-CD36 and TIME-TREG-CD36-mEmerald.

2. Methods | Cell Handling

2.1. Transfection

Stable transfections were performed on HMEC-1 with CD36-mApple and CD36-PAmcherry, CD36-myc, on TIME cells with CD36-mEmerald and on HeLa cells with CD36-BioID-Flag using viral transections as described in Githaka, J et al, 2016. Transient transfections were performed using FugeneHD (Promega, Fitchburg, WI, USA) according to manufacturer's instructions for HMEC cells. TIME cells were transiently transfected with Cytofect HUVECs Transfection Kit (Cell Applications, San Diego, CA, USA) according to manufacturer's instructions.

HMEC cells expressing CD36-mApple were grown on coverslips or Lab-Tek chambers (Fisher Scientific) and maintained in MCDB-131 complete medium (10% FBS, 10 mM L-Glutamate,10 ng/mL Epidermal Growth Factor, 1 µg/mL hydrocortisone, 1 mg/mL Pen Strep and 1 mg/mL G418) in 37°C at 5% CO_2. Lab-Tek chambers was treated with 1µg/cm^2 human Fibronectin (BD Biosciences). When the cells reached 80% confluency, they were transiently transfected with lipid probes pcDNA3-AKT-PH-GFP (Addgene plasmid # 18836) targeting PI(3,4,5)P3, GFP-C1-PLCdelta-PH (Addgene plasmid # 21179) targeting PI(4,5)P2 and GPI-GFP (Addgene plasmid # 32601). The cells were transfected for 5 to 6 h. Once the transfection was done, the cells were washed and incubated with MCDB-131 complete medium overnight and serum starved for 3 h the next day.

TIME cells expressing CD36-mEmerald were grown on coverslips or Lab-Tek chambers (Fisher Scientific) and maintained in Vascular Cell Basal Medium (ATCC® PCS-100-030), supplemented with Microvascular Endothelial Cell Growth Kit-VEGF (ATCC® PCS-110-041) and 12.5 µg/mL blasticidine. When the cells reached 80% confluency, they were transiently transfected with light inducible probes pCMV-SNAP-CRY2-VHH(GFP) (Addgene plasmid # 58370) targeting CD36-mEmerald, pCMV-CIB1-mRFP1-MP (Addgene plasmid # 58367) targeting CRY2 fragment and pCMV-CIB1-mCherry (Addgene plasmid # 58369). The cells were transfected for 1h using Cytofect. Once the transfection was done, the cells were washed and incubated with Vascular Cell Complete Medium and 0.5 µg Doxycycline for 24 h and serum starved for 3 h the next day. The cells were processed for light induced heterodimerization as written in 2.5.

2.2. Drug Treatments

Serum Starved HMEC cells expressing CD36-mApple and CD36-PAmcherry were treated with 100 µM of LY294002 (Cayman Chemical Company, Ann Arbor, MI, USA) for 30 min. Cells

were then administered with or without 10 nM TSP-1 (Athens Research and Technology, Athens, GA, USA) for 15 min at 37°C.

HeLa cells expressing CD36-BirA-Flag were treated with 1 µg doxycycline (Sigma Aldrich) for 24 h at 37°C to induce expression and treated with 100 µM biotin (Sigma Aldrich) for 18 h at 37°C to allow for proximity dependent biotinylation. Cells were treated 200 nM Latrunculin B (Sigma-Aldrich) and 1 µM of Jasplakinolide (Cayman Chemical Company, Ann Arbor, MI, USA) in basal MCDB-131 for 30 min at 37°C as a control experiment to study the effects of manipulating G and F actin.

2.3. Fixation

Once the activation with TSP-1 was completed, cells were washed with ice cold PBS (Phosphate Buffered Saline) twice and fixed on ice with 4% paraformaldehyde (Electron Microscopy Sciences, Hatfield, PA, USA) for 20 min. Fixative was removed from the cells by washing with PBS three times and imaged by Total Internal Reflection Fluorescence Microscopy (TIRF).

HMEC cells expressing CD36-PAmcherry (photoactivatable fluorescence protein) were subjected to similar methods without transfection and analyzed using Photoactivated Localization Microscopy (PALM).

2.4. Membrane depletion of PI(4,5)P2

HMEC cells stably expressing CD36-mApple were transfected with lipid probes as mentioned 2.2.1. The cells were rinsed once with Ca^{2+} free buffer (140 mM NaCl, 5 mM KCl, 1 mM $MgCl_2$, 10 mM glucose, 20 mM HEPES, and 100 µM EGTA at pH 7.4) and incubated in the same buffer at 37°C for 3 min. Once the incubation was complete, the cells were incubated again with Ca^{2+} buffer (140 mM NaCl, 5 mM KCl, 1 mM $MgCl_2$, 10 mM glucose, 20 mM HEPES, and 2.2

mM $CaCl_2$ at pH 7.4) and 1 µM ionomycin (Sigma Aldrich) for 5 mins at 37°C. The Lab-Tek chambers (Fisher Scientific) were fixed as described in 2.3.

2.5. Light induced heterodimerization

TIME cells stably expressing CD36-mEmerald were transiently transfected with light inducible plasmids as mentioned in 2.1. Half the coverslips are kept in dark for 1 min while the other half was taken onto a UV plate (Vilber Lourmat, Marne-la-Vallée cedex 3, France) illuminated with 115 V and 60 Hz UV light for 1 min. The samples were then fixed according to 2.3.

2.6. Immunofluorescence

Cells grown on coverslips were fixed using 4% paraformaldehyde (Electron Microscopy Sciences, Hatfield, PA, USA) at room temperature for 20 min. Cell were washed with PBS and permeabilized with 0.1% Triton X-100 (Sigma Aldrich) for 10 min at room temperature. After washing the cells 3 times, they were blocked with 3% bovine serum albumin (BSA) (Equitech-Bio Inc, Kerrville, Texas, USA) for 30 min at room temperature. To stain for phosphoFyn (P-Y420), the coverslips were incubated with 1:400 polyclonal rabbit anti P-Y420 (Invitrogen, Carlsbad, CA, USA) in blocking buffer for 1 h at room temperature and subsequently, stained with 1:1000 donkey anti-rabbit AlexaFluor 647 (Jackson ImmunoResearch Laboratories Inc., West Grove, PA, USA) for 30 min at room temperature in the dark. Coverslips were post fixed for 10 min at room temperature with 4% paraformaldehyde. Coverslips were imaged on Total Internal Reflection Fluorescence (TIRF-M) microscope.

3. Methods | Biochemistry

3.1. Western Blotting

Cells were grown on 6 well plates and exposed to serum starvation, drug treatments and TSP-1 activation. Cells were washed twice in ice cold PBS and lysed with phosphoprotein lysis buffer (140 mM NaCl, 20 mM MOPS at pH 7, 2 mM EGTA, 5 mM EDTA, 1% Triton X-100)

supplemented with 1:100 PhosSTOP (Phosphatase Inhibitor Cocktail, Roche Applied Science, Basel, Switzerland), 1 mM NaOrthovanadate and 1:100 protease inhibitor cocktail (Sigma Aldrich) for 20 min on ice. Cells were than scraped and centrifuged at maximum speed for 20 min at 4°C. The supernatant was recovered and used for western blotting.

The lysates were resolved on 10% SDS-PAGE gels for 1 h at 150 V. The proteins were transferred to nitrocellulose membrane for 1 h at 110 V and blocked for 1 h with 3% BSA in 1x Tris Buffered Saline Tween (TBST) at room temperature. The membrane was incubated with primary antibody, 1:2000 rabbit anti pSrc (Invitrogen, Frederick, MD, USA) overnight at 4°C or 1: 2000 mouse anti Flag (Sigma Aldrich). The membrane was washed 3 times with TBST for 10 min each at room temperature and incubated with donkey anti rabbit IRDye 680RD (Licor Biosciences, Lincoln, NE, USA) or rabbit anti Streptavidin IRDye 680 for 1 h at room temperature in the dark. The western blot image was taken using Li-Cor Odyssey (Li-Cor Biosciences, Lincoln, NE, USA) after exposing the blots for 2 min or 10 min.

3.2. F-actin and G-actin separation

F and G-actin separation was done on HeLa cells stably expressing CD36-BirA-Flag. Cells were grown on 10 cm dishes and induced with 1 µg of doxycycline for 24 h and 100 µM biotin for 18 h at 37°C. The cells were lysed using warm lysis and F-actin stabilization buffer (50 mM PIPES at pH 6.9, 50 mM NaCl, 5 mM $MgCl_2$, 5 mM EGTA, 5% (v/v) Glycerol, 0.1% Nonidet P40, 0.1%Triton X-100, 0.1% Tween 20, 0.1% 2-mercapto-ethanol) supplemented with 1 mM ATP solution and 1:100 protease inhibitor cocktail. After the harvest, cells were homogenized and incubated at 37°C for 10 min. Cells were later centrifuged at 2000 g at room temperature for 5 min. Supernatant was recovered and ultracentrifuged at 100,000 g at room temperature for 1 h leaving the F-actin in the pellet and G-actin in the supernatant. F-actin remained in the pellet was then depolymerized using F-actin depolymerizing buffer (140 mM NaCl, 20 mM Tris at pH 7.2, 2 mM EGTA, 10 µM Cytochalsin B) accompanied by 1:100 protease inhibitor and 1% Triton X-100

on ice for 1 h. G-actin and F-actin fractions were collected and ran on western blots as described above.

3.3. On-beads digestion and Mass Spectrometry

The F-actin and G-actin fractions collected were enriched by incubating with Pierce Streptavidin Plus UltraLink Resin (ThermoFisher, Waltham, MA, USA) overnight at 4°C to isolate the biotinylated proteins present in the samples. For western blotting, the samples were washed with lysis buffer (140 mM NaCl, 20 mM Tris at pH 7.2, 2 mM EGTA, 1:100 Protease Inhibitor Cocktail, 1% Triton X-100) and eluted by heating 5 min at 95°C with SDS sample buffer. For mass spectrometry, the resin was washed with binding buffer (PBS at pH 7.2) for 3 times and 50 mM ammonium bicarbonate (Sigma Aldrich) for 5 times.

The samples were submitted to Alberta Proteomics and Mass Spectrometry Facility for protein identification and analyzed using LC-MS (nanoLC – Thermo Fischer Scientific (nLC-II) and MS- Thermo Fischer Scientific (LTQ Obitrap XL)).

4. Methods | Microscopy

4.1. TIRF-M Imaging

Total Internal Reflection Fluorescence Microscopy (TIRFM) imaging was completed on an Olympus IX-81 motorized inverted base installed by Quorum Technologies (Guelph, ON, Canada). The images were acquired by 100x, 1.45 numerical aperture oil objective lens with Hamamatsu EM-CCD camera (ImageEM91013, Hamamatsu) using Volocity software (PerkinElmer, Waltham, MA, USA).

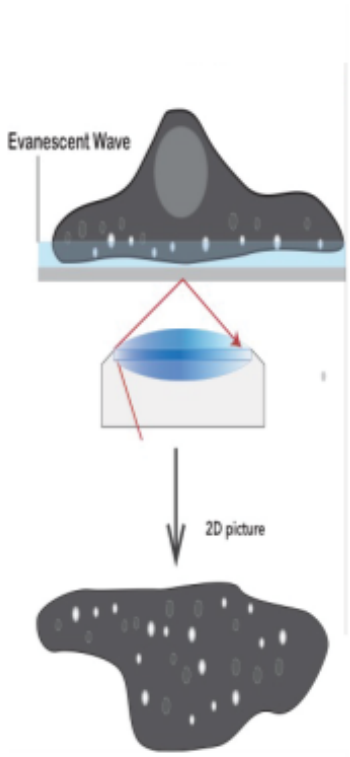

Figure 2.1 – Schematic of Total Internal Reflection Fluorescence Microscopy (TIRF-M).
A collimated laser is focused at the back aperture of the objective lens and the angle of illumination is set to the critical angle, resulting in its reflection at the interface between the oil and water interface. An evanescent wave (light blue) propagates within the aqueous medium for ~140 nm resulting in a restricted illumination to only the cell interface near the coverslip. The resulting image recorder on the EM-CCD camera has a higher signal to noise ratio because fluorescence molecules deeper in the cell are not excited.

4.2. PALM Imaging

Photoactivated Localization Microscopy (PALM) imaging of CD36 molecules was achieved by combination with TIRFM imaging. Cells grown on Lab-Tek chambers were illuminated with 20 µW of 405 nm laser (Spectral Applied Research, Richmond Hill, ON, Canada). Illumination with the 405 nm laser, photo-activated the PAmCherry-CD36 molecules that get excited with 1 mW of 561 nm and emitted fluorescence signals at 605 nm. The exposure time was set for 100 ms and captured 5000 frames until all the molecules are photo-bleached. Image analysis was performed using MatLab (MathWorks) as described in next section (Chapter 2 - 5.2).

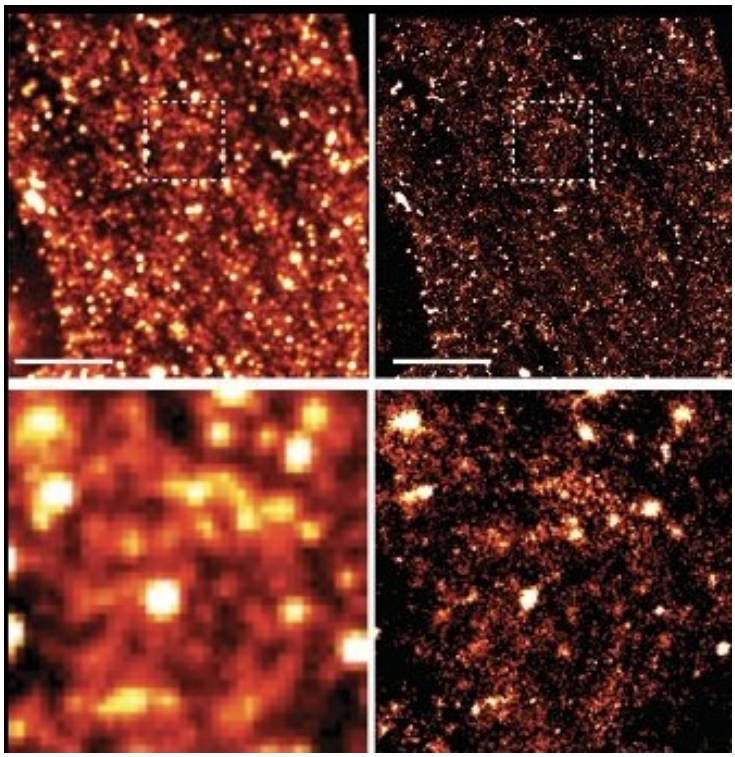

Figure 2.2 – Comparison of Diffraction limited image and super-resolution image acquired by PALM.

5. Methods | Image Analysis

All image analysis and quantifications were done on MATLAB2016b (MathWorks, Natick, MA, USA), Volocity 6.3 (Perkin Elmer) and ImageJ (Schneider, Rasband & Eliceiri 2012).

5.1. Colocalization of CD36 and lipid probes

The colocalization of CD36 with lipid probes PIP2 and PIP3 is identified by using a method called Punta-continuum colocalization analysis developed by Dr. John Githaka based on previous work by Jaqaman et al 2008. A user-friendly interface was developed by John using MatLab to analyze multiple images at the same time. This analysis relies on the pixel intensity of different lipid probes within CD36 spots. The TIRFM images were quantified as the average ratio of mean PIP2 and PIP3 pixel intensity within CD36 spots to mean PIP2 and PIP3 pixel intensity outside these spots.

This approach eliminates the limitation of other image analysis in quantifying images with both punctated and diffuse channels. CD36 channel which is more punctated compared to the lipid probes channel was taken to select the region of interest (ROI) for quantification. The circular area, CD36 spots were selected to measure of the intensity of PIP2 and PIP3 colocalizing with CD36 spots. The intensity of PIP2 and PIP3 were measured inside these CD36 spots and outside of these spots. The intensity of lipid probes was given as follow:

$$\boldsymbol{Intensity\ of\ lipid\ probes} = \frac{\boldsymbol{Intensity\ of\ lipid\ probes\ inside\ CD36\ spots}}{\boldsymbol{Intensity\ of\ lipid\ probes\ outside\ CD36\ spots}}$$

5.2. PALM Analysis

Photoactivated Localization Microscopy (PALM) imaging analysis was done by using Gaussian mixture-model fitting (Jaqaman et al., 2008). The analysis first provided the positions of the CD36 molecules and the standard deviations (20.24 nm) in each image of 5000 frames. Localizations with standard deviation above 50 nm (~0.0003% of localization) were eliminated from further analysis of the identified localizations. Over counting of molecules were avoided by using a tracking program previously developed by particle tracking algorithm (u-track; (Jaqaman et al., 2008)). For molecules with multiple appearances in more than one frame, the average position was calculated within each of their tracks and taken as a final position of that molecule providing a more accurate position in addition to avoid over-counting.

5.3. Spatial Pattern Analysis

To determine CD36 nanoclusters properties, we employed an analysis based on the work of Owen et al., (Owen et al., 2010; Williamson and Shmoys, 2011) described in Githaka, J et al (Githaka et al., 2016). Using this method, we were able to define the CD36 nanoclusters radii in

nanometers, ROI density in molecules/μm^2, number of molecules per CD36 nanoclusters and percent of CD36 clusters.

6. Methods | Data representation and statistical analysis

Bar graphs and boxplots (Tukey) were created using GraphPad prism (Graphpad Software, La Jolla, CA, USA). The error bars on the bar graphs are presented as mean ± standard deviation. The statistical analysis of bar graphs was done using two-tailed unpaired t-test at $\alpha<0.05$ on GraphPad prism. The images were presented with box plots exhibiting the minimum, 25^{th} percentile, median, 75^{th} percentile and maximum. The outliers were removed using ROUT method with a Q value set at 1%. The statistical analysis for box plots were carried out in GraphPad prism using two-tailed non-parametric Mann Whitney's test with $\alpha<0.05$. By using these statistical approaches, if significant, the actual p-value is give up to four decimal places and if not significant, written as ns.

7. References

Githaka, J.M., Vega, A.R., Baird, M.A., Davidson, M.W., Jaqaman, K., and Touret, N. (2016). Ligand-induced growth and compaction of CD36 nanoclusters enriched in Fyn induces Fyn signaling. J. Cell. Sci. 129, 4175-4189.

Jaqaman, K., Loerke, D., Mettlen, M., Kuwata, H., Grinstein, S., Schmid, S.L., and Danuser, G. (2008). Robust single-particle tracking in live-cell time-lapse sequences. Nature Methods 5, 695.

Owen, D.M., Rentero, C., Rossy, J., Magenau, A., Williamson, D., Rodriguez, M., and Gaus, K. (2010). PALM imaging and cluster analysis of protein heterogeneity at the cell surface. Journal of Biophotonics 3, 446-454.

Williamson, D.P., and Shmoys, D.B. (2011). The design of approximation algorithms Cambridge university press).

Chapter 3 - **Role of phosphoinositides in CD36 organization and Fyn activation**

1. Introduction

The plasma membrane of cells is a dynamic and heterogeneous structure whose role is to maintain cellular integrity but also allow exchange of ions and nutrients and signals. Membrane lipid compositions vary slightly between different cell types mainly in cholesterol content (Rastogi and Nordøy, 1980; Shevchenko and Simons, 2010). Usually human plasma membrane is comprised mainly of glycerolipids, sphingolipids and sterols and the distribution of lipids within outer and inner leaflet is asymmetric (Van Meer et al., 2008). The outer leaflet is made up of phosphatidylcholine (PC), sphingomyelin (SPH), glycosphingolipids such as

monosialodihexosylganglioside (GM3) and cholesterol. The inner leaflet consists of phosphatidylethanolamine (PE), phosphatidylserine (PS), phosphatidylinositols (PIs) such as phosphatidylinsotiol-4,5-bisphospate (PIP2) and cholesterol (Zachowski, 1993). The presence of anionic lipids such as PS and PIs in the inner leaflet explains the anionic nature of the plasma membrane (Zachowski, 1993). Recent advances in super-resolution microscopy have provided insights into the diverse functions of the plasma membrane. The current definition for the role of cell membrane simply as a barrier has become insufficient as the evidence for the role of cell membranes in regulation of membrane protein, in membrane trafficking and membrane compartmentalization via formation of lipid nanodomains became more distinct (Lingwood et al., 2009). As explained in Chapter 1, our research focus on the inner membrane lipids (PIs) in signaling and membrane organization of CD36 receptor in endothelial cells. Previous work in our lab has defined that Fyn is enriched in CD36 nanoclusters in cholesterol rich plasma membrane compartment containing the sphingolipid GM1 (detected using cholera toxin B subunit) on the outer leaflet and localized to region rich in cortical F-actin (Githaka et al., 2016). The goal of the current study is to investigate the organization of CD36 and Fyn in regards to inner leaflet lipids of the plasma membrane and determine if these lipids control nanocluster formation and/or Fyn activation In this chapter, we sought to investigate the role of phosphoinositides, PI(4,5)P2 and PI(3,4,5)P3 in CD36-Fyn signaling in endothelial cells.

2. Results

2.1. Identification of inner leaflet lipids in CD36-TSP-1 signaling

.To determine the nature of the inner lipids that are enriched with CD36 nanoclusters, we transfected human microvascular endothelial cells (HMEC) with lipid probes targeting PI, phosphatidylserine and anionic lipids and visualized with Total Internal Reflection Fluorescence Microscopy (TIRFM) (Figure 2.1) which focuses on the plasma membrane area apposed to the coverslip. We determined that phosphatidylserine and phosphoinositides are present with CD36

nanoclusters (Figure 3.1). We observed that CD36 nanoclusters are enriched in PI(4,5)P2 (PIP2) before activation with TSP-1 and more enriched in PI(3,4,5)P3 (PIP3) after TSP-1 activation. However, no change in the levels of PS is observed upon TSP-1 stimulation. Once we identified the lipids that are enriched with CD36, we presented the data showing the ratio of PIP3 to PIP2 (Figure 3.1C).

(A)

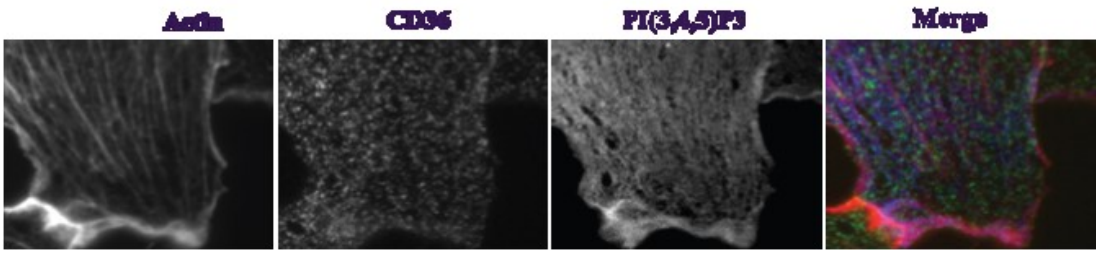
Actin
CD36
PI(3,4,5)P3
Merge

(B)

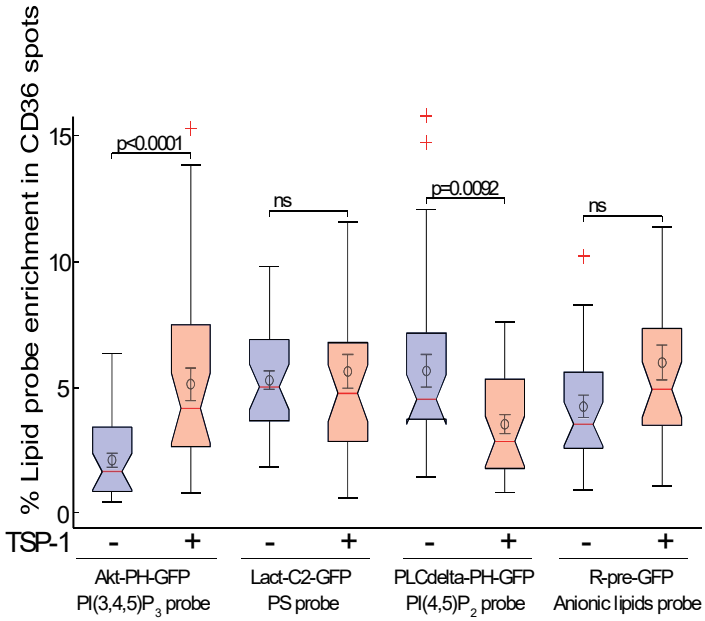
% Lipid probe enrichment in CD36 spots
15
10
5
0
p<0.0001
ns
p=0.0092
ns
TSP-1
- + - + - + - +
Akt-PH-GFP
PI(3,4,5)P3 probe
Lact-C2-GFP
PS probe
PLCdelta-PH-GFP
PI(4,5)P2 probe
R-pre-GFP
Anionic lipids probe

(C)

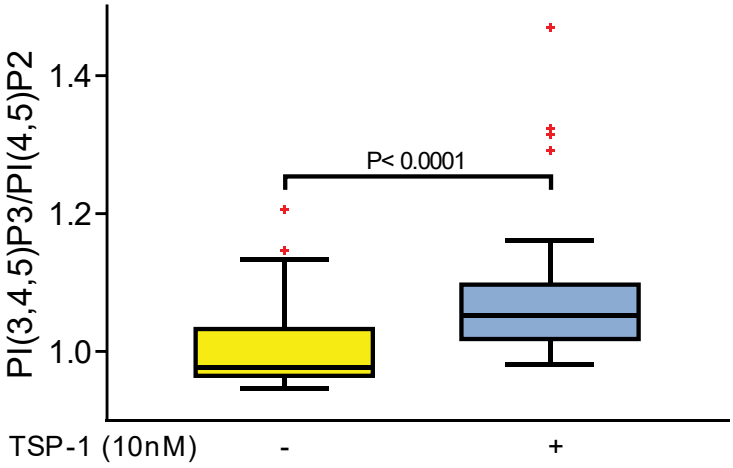
PI(3,4,5)P3/PI(4,5)P2
1.4
1.2
1.0
P< 0.0001
TSP-1 (10nM)
-
+

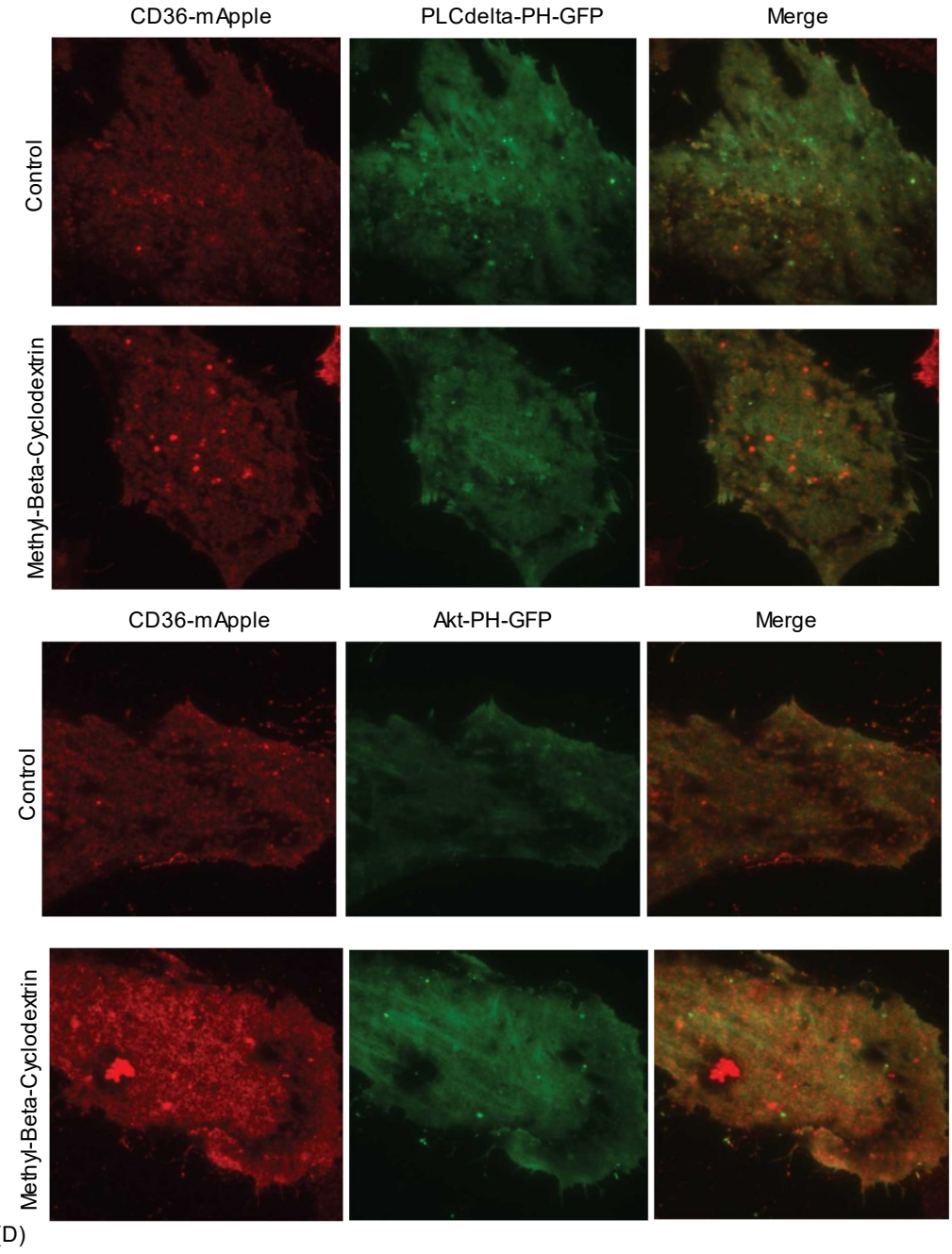
CD36-mApple
PLCdelta-PH-GFP
Merge
Control
Methyl-Beta-Cyclodextrin
CD36-mApple
Akt-PH-GFP
Merge
Control
Methyl-Beta-Cyclodextrin

(D)

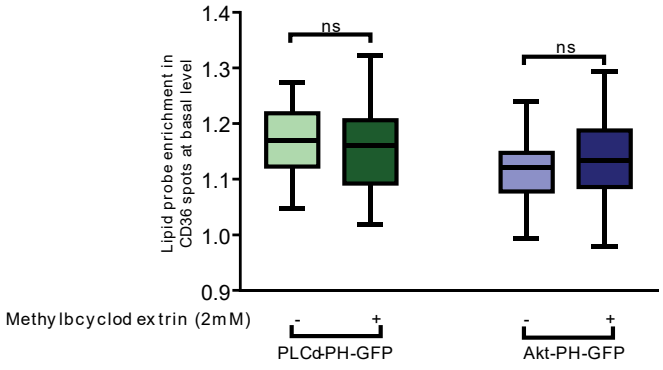
Lipid probe enrichment in CD36 spots at basal level
1.4
1.3
1.2
1.1
1.0
0.9
ns
ns
Methylbcyclodextrin (2mM)
-
+
-
+
PLCd-PH-GFP
Akt-PH-GFP

(E)

Figure 3.1 – CD36 is enriched in PI(4,5)P2 before activation and enriched with PI(3,4,5)P3 after activation with TSP-1.
(A) TIRF-M images of enrichment of CD36 with PI(3,4,5)P3 on cortical F-actin (Githaka's unpublished data) before or after stimulation (B) Percentage of different lipid probes enriched in CD36 spots (Githaka's unpublished data). (C) Levels of PIP3 to PIP2 enriched with CD36 spots (D) TIRF-M images enrichment of CD36 with PI(4,5)P2 and PI(3,4,5)P3 with or without treatment with methyl-β-cyclodextrin. (E) PI(4,5)P2 and PI(3,4,5)P3 enrichment in CD36 spots with or without treatment with methyl-β-cyclodextrin. ~33 to 40 data points from 2 independent experiments were analyzed for methyl-β-cyclodextrin treated condition for images. Boxplots and statistical analysis was performed as described in Chapter 2 - 6.

Using lipid binding probes in ECs, we were able to determine that PS and PIPs are present in the inner leaflet of the plasma membrane where CD36 nanoclusters are localized. We also investigated if the PI(4,5)P2 and PI(3,4,5)P3 are present with CD36 in the domains enriched with cholesterol by treating the cells with methyl-β-cyclodextrin (MβCD) which removes cholesterol and disrupt these domains and saw that there were no significant changes in the levels of PIPs enrichment in CD36 clusters with the MβCD (Figure 3.1E), suggesting the CD36 nanoclusters and PIPs enrichment on the plasma membrane is not organized in cholesterol rich domains. In addition, we identified that PIP2 likely converted to PIP3 during stimulation, since its increase enrichment is concomitant to a decreased enrichment in PIP2. This conversion suggests the involvement of a PI3-Kinase (Figure 3.2).

2.2. Role of PI3K in CD36-Fyn Signaling

To get a better understanding into the role of phosphoinositides in Fyn activation and CD36 nanoclustering, we performed pharmacological inhibition of the kinase responsible for phosphorylating PIP2 to PIP3. PIP2 can be phosphorylated at 3 position hydroxyl group of the inositol ring by PI3K to produce PIP3. PI3K plays an important role in regulating cellular functions including metabolism growth, proliferation, survival, transcription and protein synthesis (Vanhaesebroeck et al., 2012). Dysregulation of PI3K has been implicated in many diseases such

as cancer. Pharmacological inhibition of PI3K using LY294002 (100µM) was performed on HMEC cells stably expressing CD36-mApple transfected with PIP2 or PIP3 lipid probes (Figure 3.2). The intensity of PIP2 and PIP3 inside the CD36 spots were measured according to the methods in Chapter 2 - 5.1 - Colocalization of CD36 and lipid probes. The analysis shown that CD36 spots are enriched with PIP2 at steady state and lipid remodeling to PIP3 was seen after TSP-1 activation. The treatment with LY294200, an inhibitor of PI3K, blocked the phosphorylation of PIP2 to PIP3 as seen by the lack of increase in the PIP3/PIP2 ratio upon TSP-1 stimulation (Figure 3.2). These results confirmed the implication of PI3-Kinase in the PIP2 to PIP3 conversion in CD36 nanoclusters.

Next, we investigated whether the production of PIP3 had a role in signal transduction. Therefore, we studied the activation of Fyn using immunoblotting after inhibition of PI3K. After stimulation with TSP-1 for 15 min at 37°C, we detected the activation of Fyn using a rabbit polyclonal antibody targeted against phosphorylation of Tyrosine 418 in Src (this antibody also detects phosphorylation at Tyrosine 420 for Fyn since it was designed to detect the activation of SFK members). The western blots were then quantified by measuring the intensity of the corresponding band and normalized to the control condition (without TSP-1 and LY294002). From the western blots, we determined that inhibiting PI3K diminishes Fyn activation indicating that production of PIP3 from PIP2 is important for the activation of downstream Fyn in TSP-1-CD36 signaling in endothelial cells.

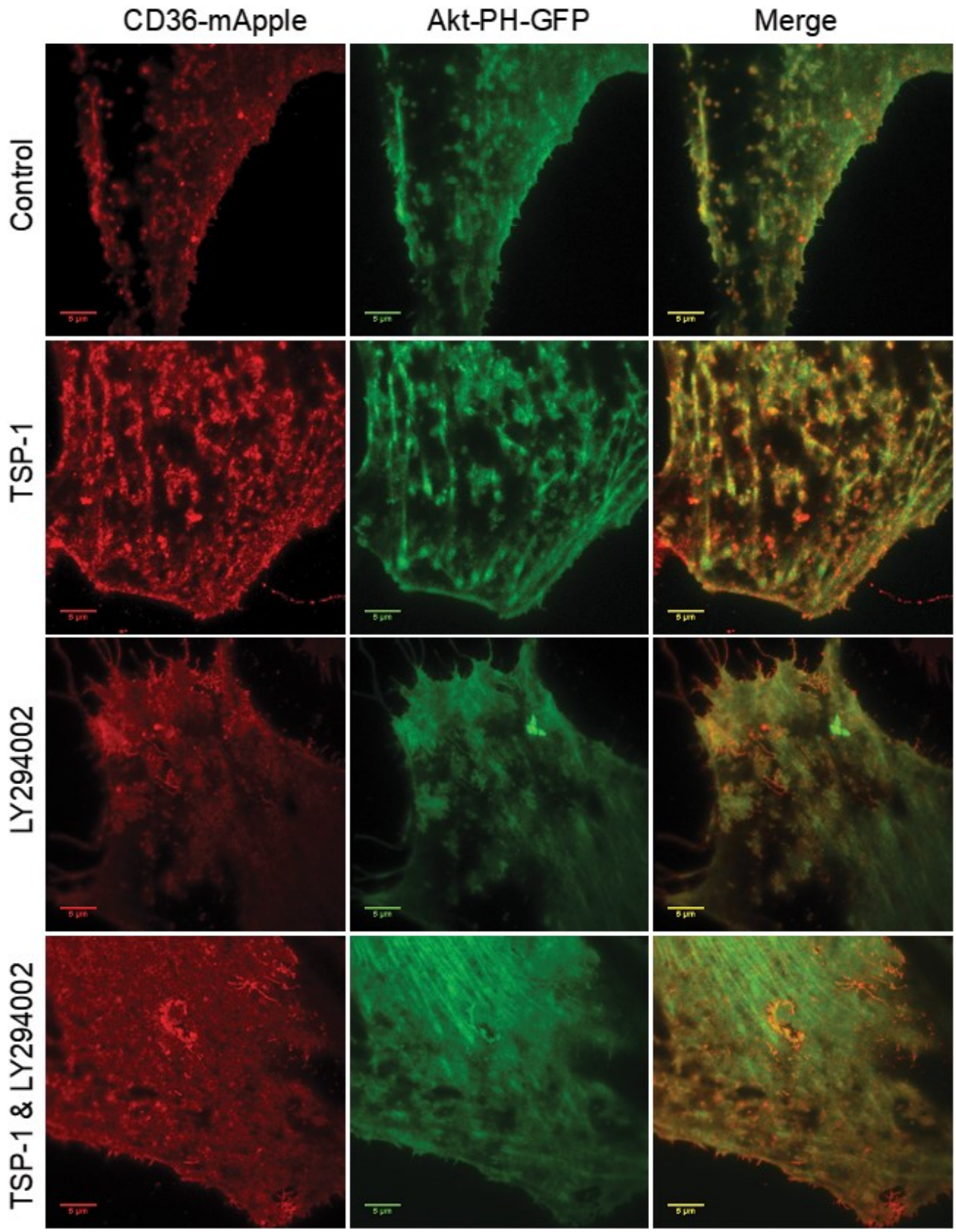
CD36-mApple
Akt-PH-GFP
Merge
Control
TSP-1
LY294002
TSP-1 & LY294002

(A)

(B)

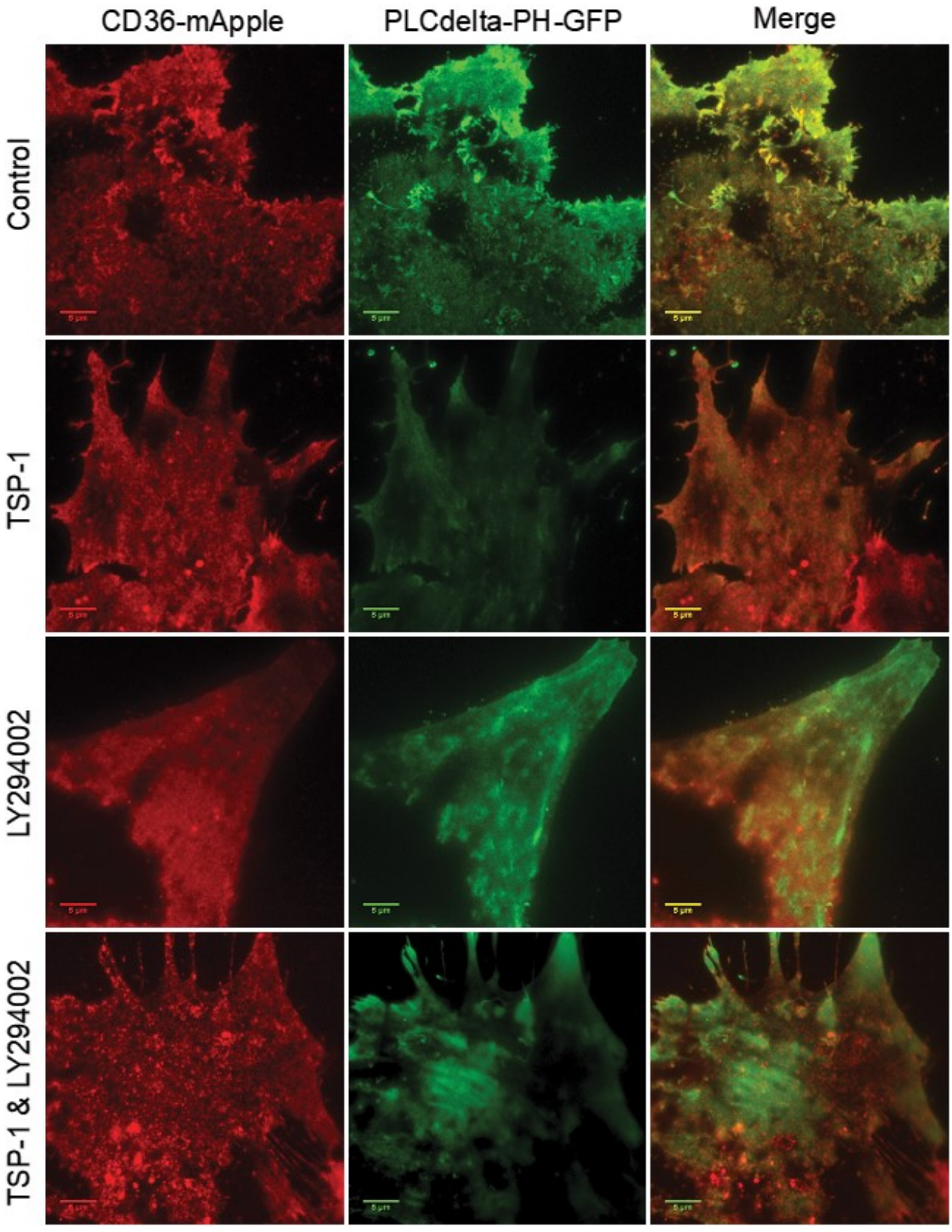
CD36-mApple
PLCdelta-PH-GFP
Merge
Control
TSP-1
LY294002
TSP-1 & LY294002

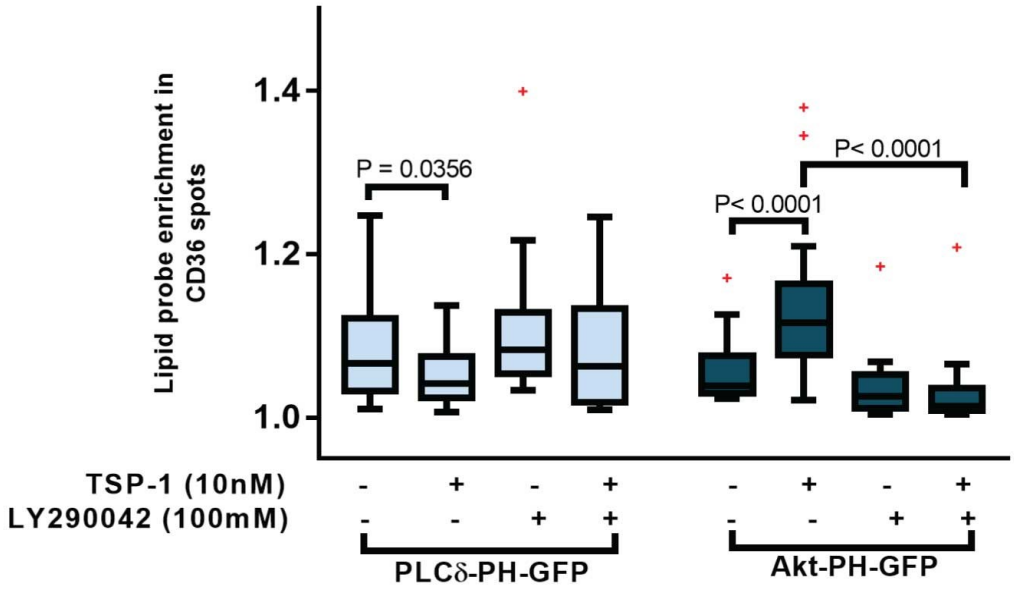
Lipid probe enrichment in CD36 spots
1.4
1.2
1.0
P = 0.0356
P< 0.0001
P< 0.0001
TSP-1 (10nM) - + - + - + - +
LY290042 (100mM) - - + + - - + +
PLCδ-PH-GFP
Akt-PH-GFP

(C)

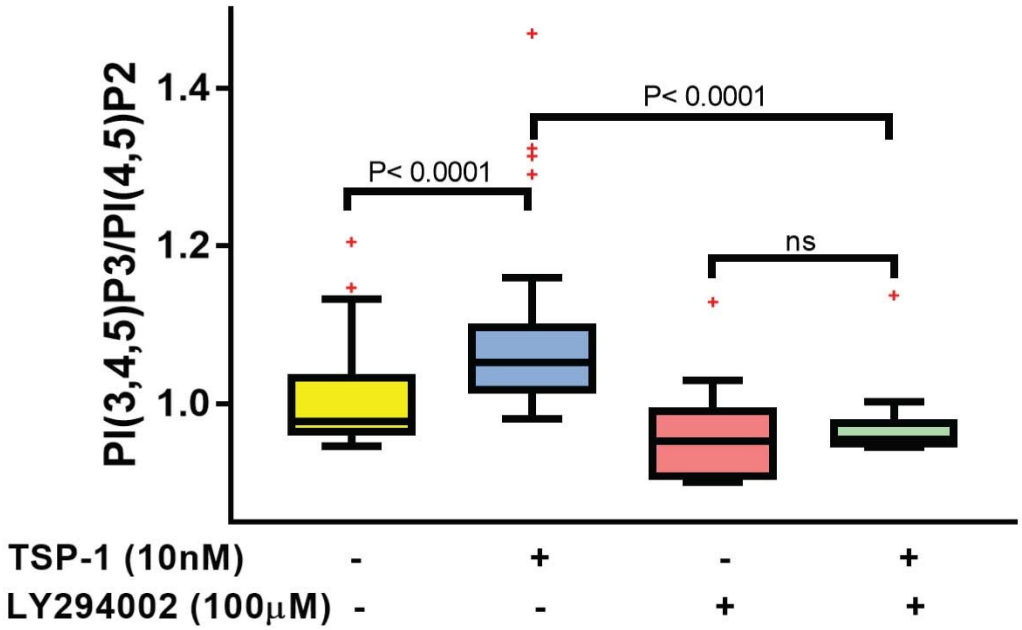
PI(3,4,5)P3/PI(4,5)P2
1.4
1.2
1.0
P< 0.0001
P< 0.0001
ns
TSP-1 (10nM) - + - +
LY294002 (100μM) - - + +

(D)

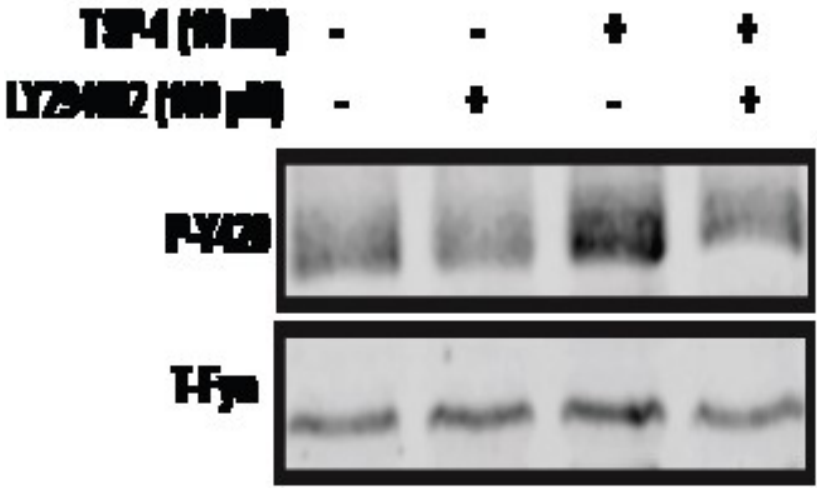

(E)

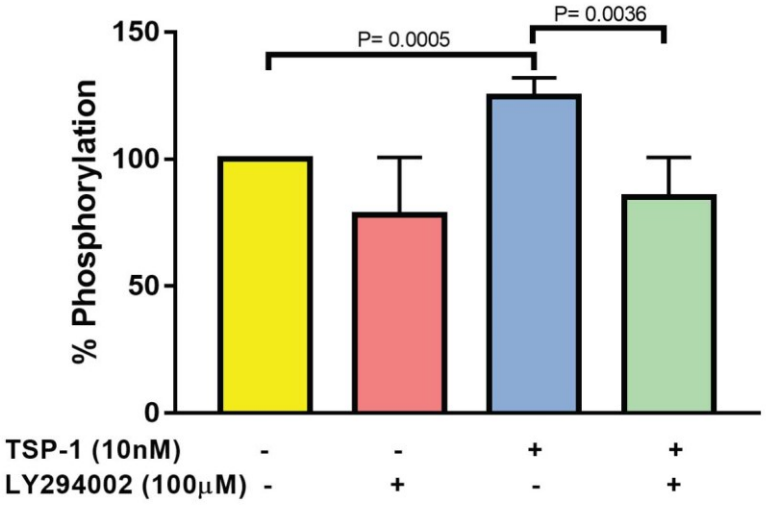

(F)

Figure 3.2 – PI(4,5)P2 and PI(3,4,5)P3 enrichment in CD36 spots after activation with 10 nM TSP-1 and treatment with 100 μM LY294002.

(A) TIRF-M images of enrichment of PI(3,4,5)P3 with CD36 spots (B) TIRF-M images of enrichment of PI(4,5)P2 with CD36 spots (C) Normalized levels of PIP2 and PIP3 intensity in un-ligated CD36 clusters after inhibiting PI3K using LY294002 (D) Ratio of PIP3 to PIP2 in CD36 clusters after 100 μM LY294002 (E) Activation of Fyn after treatment with 10 nM TSP-1 and 100 μM LY294002 (F) Normalized Fyn activation to total Fyn. 60 data points from 3 independent experiments were analyzed for all conditions for images and data from 4 independent experiments for western blots. Boxplots, bar graphs and statistical analysis was performed as described in Chapter 2 - 6.

The involvement of PI3K in CD36-TSP-1 signaling pathway has further led us to study the activation of known downstream target such as PKB (Akt) a well-known PI3K downstream effector. Since PI3K signaling pathway is well-characterized, we presumed the investigation into activation of other downstream effectors of PI3K is necessary. Using, HMEC-mApplec-CD36 cells stimulated with or without TSP-1 and incubated in the absence and presence of the PI3K inhibitor (100 μM LY294002) for 30 min, we prepared cell lysates and determined the level of Akt phosphorylation on Ser473 (a known target site in the PI3K pathway) by immunoblotting. We performed western blot using PI3K inhibitor to investigate the role of Akt in the CD36-TSP-1 pathway. As observe in (Figure 3.3), the phosphorylation of Akt on Serine 473 is completely abolished by treatment with LY294002 in unstimulated condition (Suggest that there is a basal level of Akt activation supported by PI3K). Following TSP-1 stimulation, the level of Akt activation remained like those of the basal state indicative of no further increase of Akt in response to TSP-1. This result suggest that Akt is not activated in CD36-TSP-1 signaling pathway. In conclusion, while we demonstrated the involvement of PI3K in the production of PIP3 in CD36 nanoclusters, this activation is not followed by the phosphorylation of Akt. The presence and activation of PI3K and production of PI(3,4,5) P3 in this pathway may be limited to either CD36 nanocluster formation or Fyn activation which is discussed in detail in discussion section.

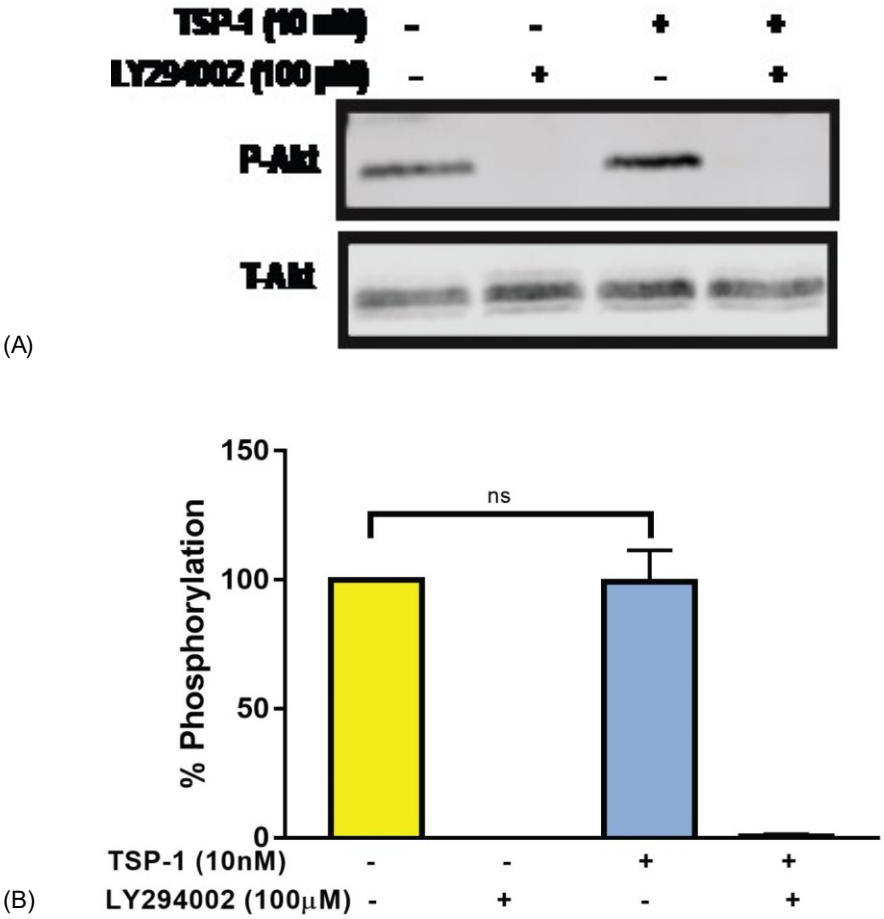

Figure 3.3 – Activation of Akt after stimulation with10 nM TSP-1 and treatment with 100 μM LY294002.

(A) Activation of Akt after treatment with 10 nM TSP-1 and 100 μM LY294002, normalized to total Akt (B) Normalized Akt activation to total Akt. 4 independent experiments were carried out for western blots. Bar graphs and statistical analysis was performed as described in Chapter 2 - 6.

2.3. Role of PI3K in CD36 nanocluster formation

To understand further the role of PI3K in CD36-Fyn signaling, we questioned the role of PI3K and production of PIP3 in CD36 nanocluster formation. CD36 molecules pre-exist in clusters on the plasma membrane of endothelia cells (Githaka et al., 2016) and in macrophages (Jaqaman et al., 2011). In TSP-1-CD36-Fyn signaling, TSP-1 enhances the radius and density of CD36 nanoclusters which in turn activates downstream kinase Fyn. Previously, we've shown that PI3K is important for Fyn activation upon stimulation with TSP-1, however, to establish further the role

of PIP3 production in TSP-1 induce CD36 signaling, we explored to study the effects of PI3K inhibition on CD36 nanocluster enhancement. We resorted to super-resolution imaging (SRI) using PhotoActivated Localization Microscopy (PALM) of HMEC-PAmCherry-CD36 by Total Internal Reflection Fluorescence microscopy (TIRF-M) followed by Spatial Pattern Analysis (SPA) to characterize CD36 nanocluster properties (Figure 3.4).

Human Microvascular Endothelia Cells (HMEC) stably expressing CD36-PAmCherry were treated with pharmacological inhibitor of PI3K, LY294002 for 1 h and stimulated with TSP-1 for 15 min. We then acquired super-resolution images using PALM (Chapter 2 - 4.2) and TIRF (Chapter 2 - 4.1) and analyzed the data using Spatial Pattern Analysis (Chapter 2 - 5.3) and plotted the cluster properties using boxplots.

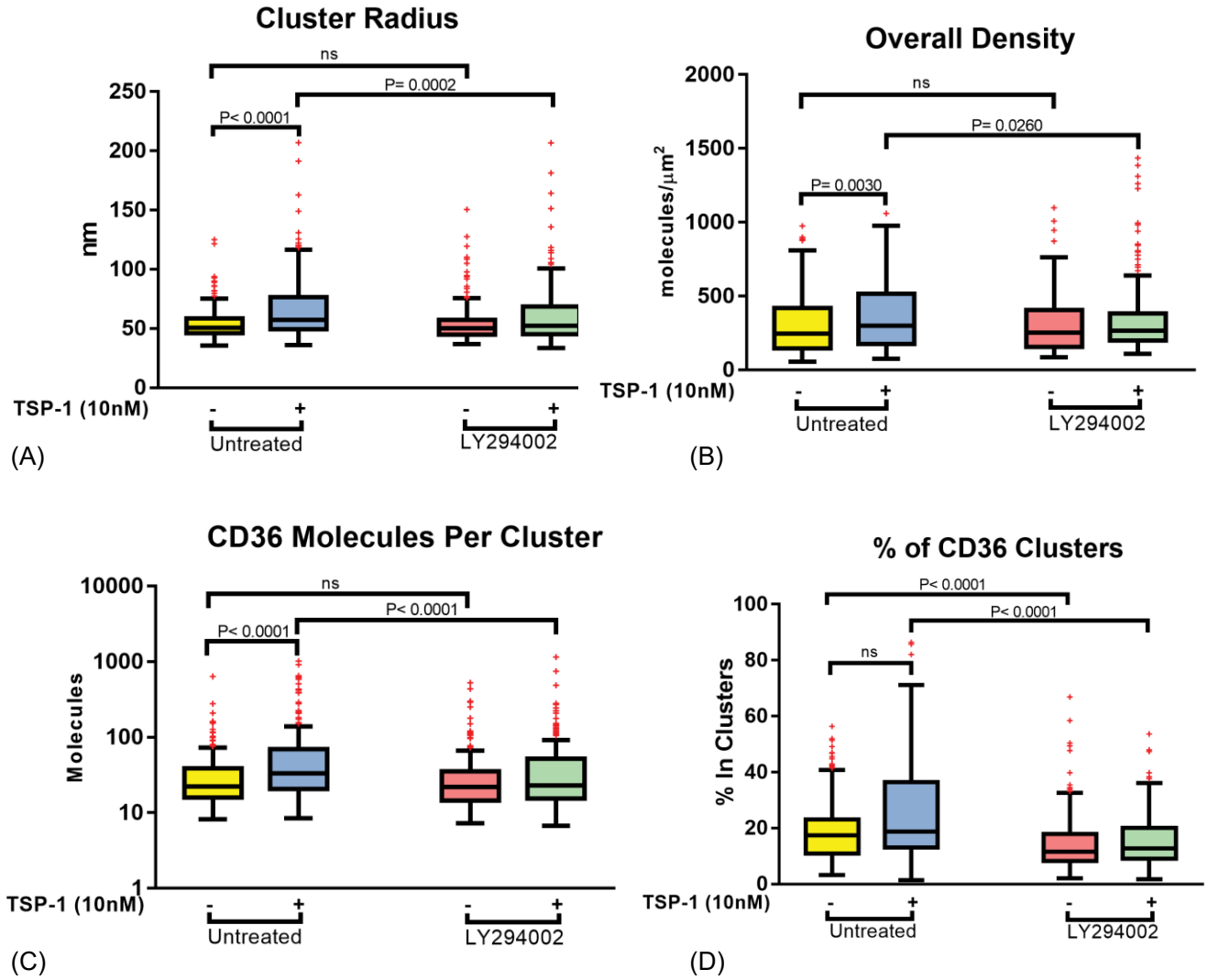

Figure 3.4 - Properties of CD36 nanoclusters after stimulation with 10 nM TSP-1 and treatment with 100 µM LY294002.

(A) CD36 nanoclusters radii in nm (B) Density of CD36 nanoclusters in molecules/µm^2 (C) CD36 molecules per cluster (D) Percent of CD36 molecules in clusters. 175 data points from 4 independent experiments were analyzed for all conditions for images. Boxplots and statistical analysis was performed as described in Chapter 2 - 6.

The clustering analysis suggests that there is a small enhancement of CD36 nanoclusters after stimulation with TSP-1. CD36 nanoclusters exhibited increase in radii, density as well as the number of molecules per cluster which is consistent with our previous findings. Interestingly, TSP-1 did not increase the percentage of CD36 molecules existing in clusters. The treatment with

LY294002 has significantly decreased the CD36 nanoclusters radii, density and number of molecules per cluster indicating that PIP3 production plays a role in CD36 nanocluster formation.

2.4. Depletion of PI(4,5)P2 from plasma membrane using ionomycin

To study the role of PI(4,5)P2 in Fyn activation and CD36 nanocluster formation in HMEC cells expressing CD36, we depleted PI(4,5)P2 from the membrane using ionomycin. Ionomycin is an ionophore for the transport Ca^{2+} across cell membrane in direction of the concentration gradient. Here we used ionomycin in presence of 2 mM extracellular calcium to raise intracellular concentration (Kosenko and Hoshi, 2013) and activate the phosphoinositide specific phospholipase C (PLC). Upon increase intracellular calcium, PLCdelta translocate to the plasma membrane and hydrolyze PI(4,5)P2 producing two intracellular messengers, diacylglycerol (DAG) and inositol triphosphate (IP_3) (Kosenko and Hoshi, 2013). As shown in Figure 3.5, the process of raising intracellular Ca^{2+} occurs in six steps. In step 1, ionomycin creates pores in the membrane to allow for the passage of extracellular Ca^{2+} into the cell. When intracellular Ca^{2+} rises, PLC is activated in step 2 and 3. PLC then translocate to the plasma membrane and hydrolyze membrane phosphoinositide PIP2 to IP_3 and DAG in step 4. IP_3 binds to the IP_3R on the endoplasmic reticulum (ER) in step 5 and allow the release of Ca^{2+} into the cytosol to further increase the level of intracellular Ca^{2+} in step 6. We employed this technique combined with TIRF-M to deplete the PI(4,5)P2 from the membrane and study its effect on the activation of Fyn and CD36 nanocluster formation.

In order to confirm this method in our cell system, we transfected HMEC cells expressing CD36-mApple with various lipid probes: PLCδ-PH-GFP and AKT-PH-GFP targeting PI(4,5)P2 and PI(3,4,5)P3 respectively, and as control GPI-GFP (glycosylphosphoatidylinositol anchored GFP localized to the extracellular leaflet)and PM-GFP (correspond to the 11 N-terminal residues of Lyn carrying 2 fatty acid modifications). As shown in (Figure 3.5B), there is a significant decrease in the intensity of PLCδ-PH-GFP compared to GPI-GFP and PM-GFP, and a slight

decrease in levels AKT-PH-GFP which indicates that after 5 min treatment with ionomycin, there was a significant depletion of PI(4,5)P2 from the plasma membrane, however, we were unable to observe the intensity changes in control lipid probes such as GPI-GFP and PM-GFP. These data indicate that using ionomycin in presence of Ca^{2+} allows depletion of PIP2 in ECs.

(A)

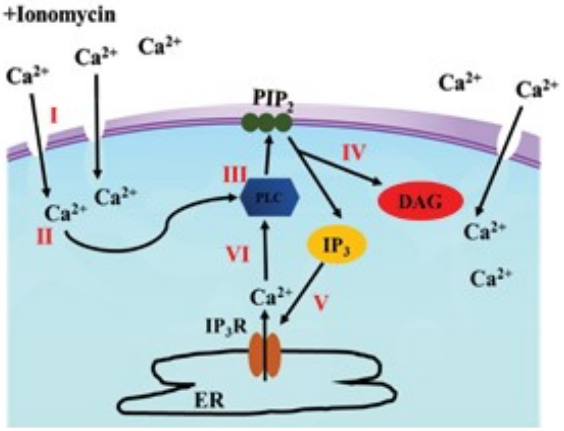
+Ionomycin
Ca2+
PIP2
I
II
III
IV
V
VI
PLC
DAG
IP3
IP3R
ER

(B)

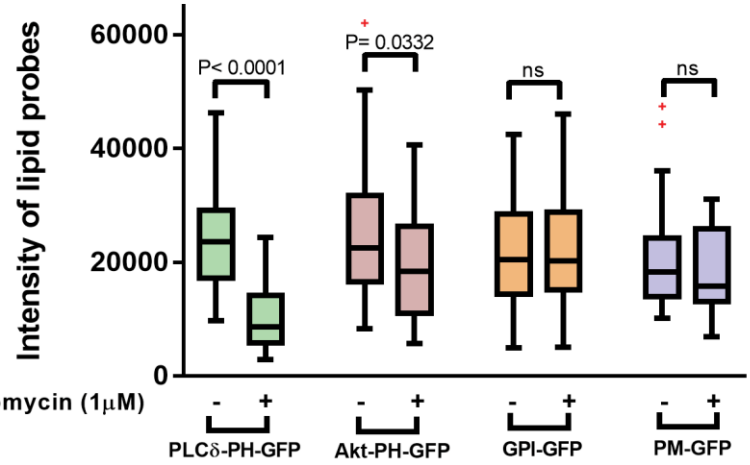
Intensity of lipid probes
60000
40000
20000
0
P< 0.0001
P= 0.0332
ns
ns
Ionomycin (1μM)
- +
PLCδ-PH-GFP
Akt-PH-GFP
GPI-GFP
PM-GFP

(C)

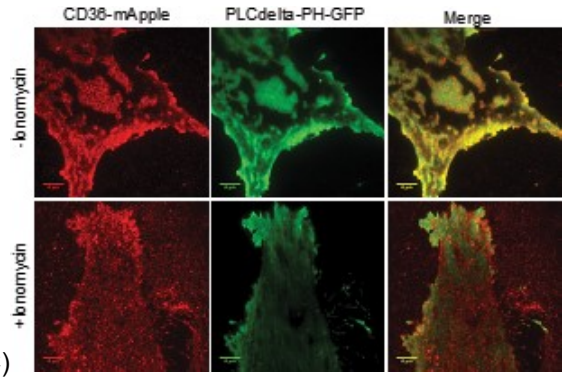
CD36-mApple
PLCdelta-PH-GFP
Merge
-Ionomycin
+Ionomycin

(D)

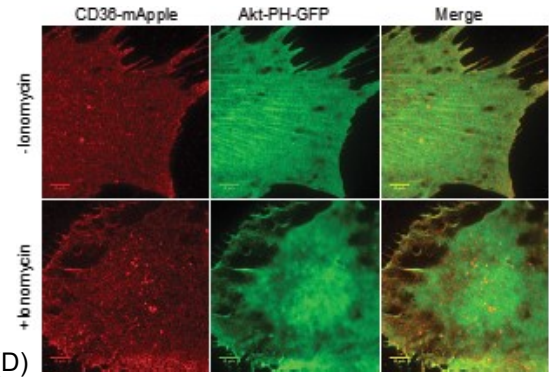
CD36-mApple
Akt-PH-GFP
Merge
-Ionomycin
+Ionomycin

(E)

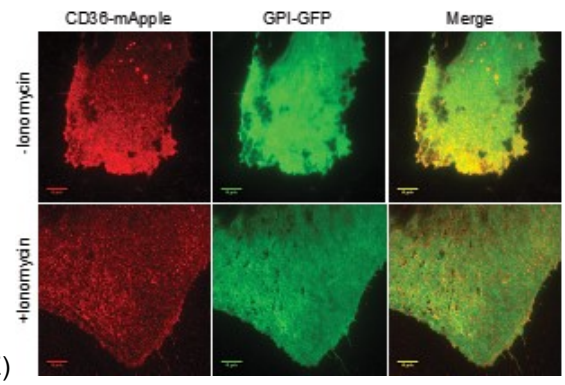
CD36-mApple
GPI-GFP
Merge
-Ionomycin
+Ionomycin

(F)

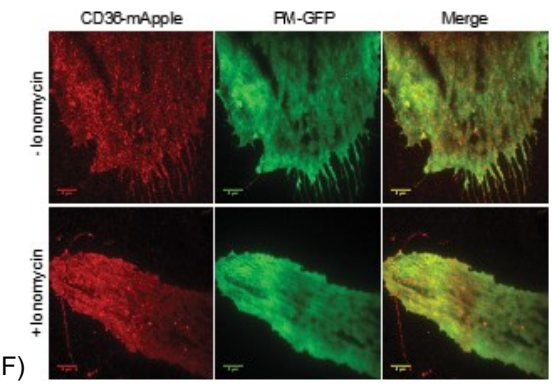
CD36-mApple
PM-GFP
Merge
-Ionomycin
+Ionomycin

Figure 3.5 – Intensity of PI(4,5)P2, PI (3,4,5)P3, GPI and PM after treatment with 1 µM ionomycin in HMEC-CD36-mApple cells.
(A) Diagram of ionomycin and Ca^{2+} activation and depletion of PI(4,5)P2 (B) Intensity of lipid probes with and without ionomycin (C, D, E and F) TIRF-M images of different lipid probes (PLCdelta-PH-GFP, Akt-PH-GFP, GPI-GFP and PM-GFP) with and without ionomycin. 40 data points from 3 independent experiments were analyzed for images. Boxplots and statistical analysis was performed as described in Chapter 2 - 6.

2.5. Effect of PI(4,5)P2 depletion on Fyn activation

We tested the effects of PIP2 depletion from the membrane on Fyn activation by following the levels phosphorylation at Tyr 420. HMEC cells stably expressing CD36-myc were treated with ionomycin according to the protocol in Chapter 2 - 2.4. Upon TSP-1 stimulation, Fyn activation increased, however, similarly to the LY294002 treatment, this increase was inhibited after ionomycin treatment further confirming our findings that eliminating PIP2 from the membrane and reducing PIP3 production decreased the TSP-1 mediated Fyn activation in endothelial cells. In the blots, we used tubulin as a loading control to measure the activation of Fyn instead of using total Fyn, this was due to our previous data demonstrating that activation of Fyn using either tubulin or total Fyn as control did not have any significant impacts on Fyn activation upon normalization of the data.

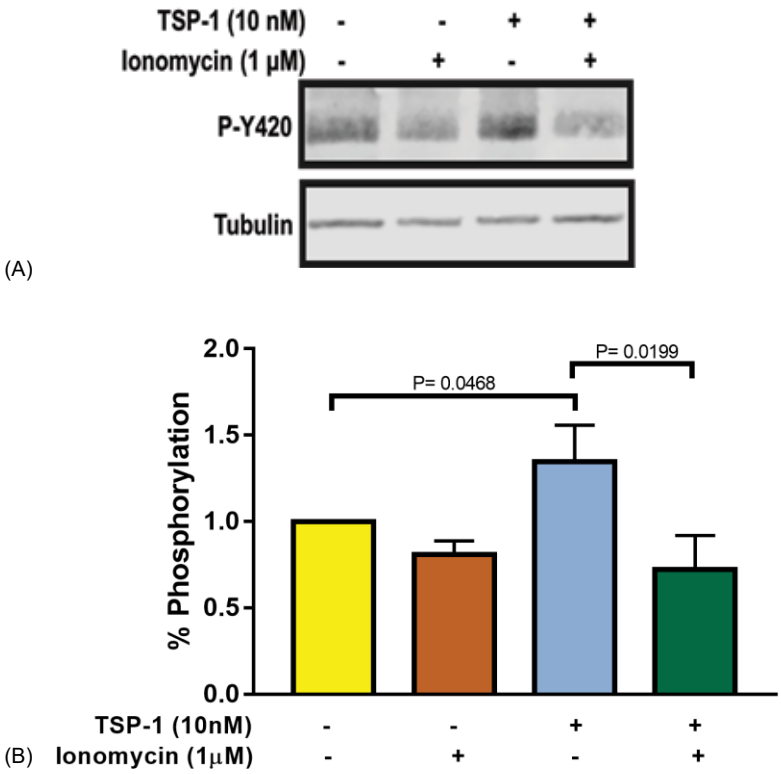

Figure 3.6 – Western blot analysis of Fyn activation.
(A) Activation of Fyn on HMEC-CD36-Myc cells treated with TSP-1 and depleted PI(4,5)P2 from the membrane using ionomycin. (B) Normalized Fyn activation to total Fyn. Data taken from 3 independent experiments for western blots. Bar graphs and statistical analysis was performed as described in Chapter 2 - 6.

2.6. Effect of PI (4,5)P2 depletion on CD36 nanocluster formation

To establish the role PI(4,5)P2 in CD36 nanocluster formation in endothelial cells, we employed the method of depleting PI(4,5)P2 from the plasma membrane via the action of PLC enzyme. Treatment with ionomycin increases the intracellular Ca^{2+} which activates PLC. PLC hydrolyze PI(4,5)P2 into diacylglycerol (DAG) and inositol triphosphate (IP3). By using this mechanism, we studied the effects of PI(4,5)P2 CD36 nanocluster formation on endothelial cells. The cluster properties are shown below.

(A)

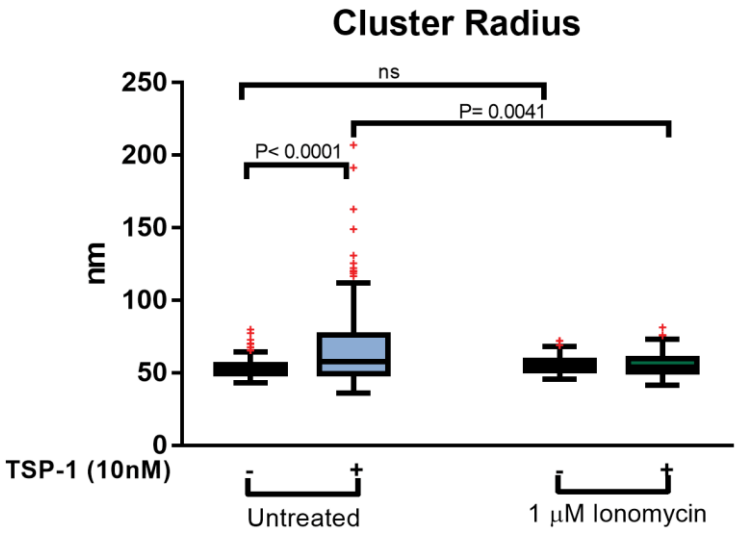
Cluster Radius
ns
P= 0.0041
P< 0.0001
250
200
150
100
50
0
nm
TSP-1 (10nM)
-
+
-
+
Untreated
1 μM Ionomycin

(B)

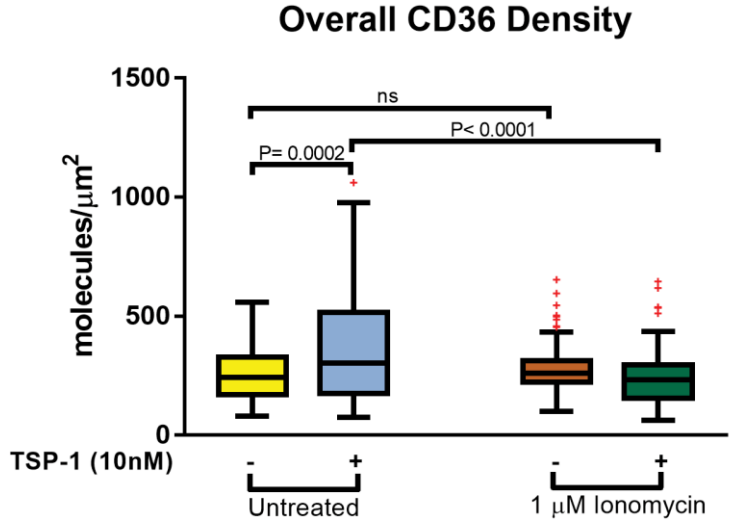
Overall CD36 Density
ns
P< 0.0001
P= 0.0002
1500
1000
500
0
molecules/μm2
TSP-1 (10nM)
-
+
-
+
Untreated
1 μM Ionomycin

(C)

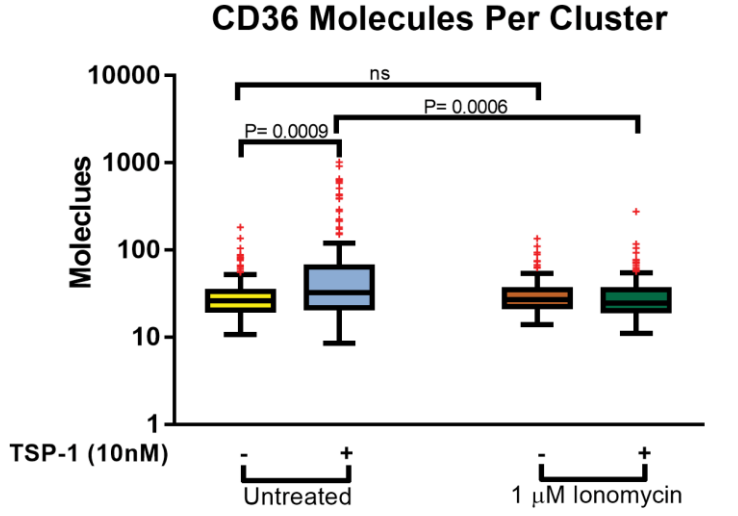
CD36 Molecules Per Cluster
ns
P= 0.0006
P= 0.0009
10000
1000
100
10
1
Moleclues
TSP-1 (10nM)
-
+
-
+
Untreated
1 μM Ionomycin

Figure 3.7– Properties of CD36 nanoclusters after stimulation with 10 nM TSP-1 and treatment with 1 µM Ionomycin.
(A) CD36 nanoclusters radii in nm (B) Density of CD36 nanoclusters in molecules/µm2 (C) CD36 molecules per cluster. 155 data points from 3 independent experiments were analyzed for all conditions for images. Boxplots and statistical analysis was performed as described in Chapter 2 - 6.

Our analysis revealed that treatment with ionomycin has decreased CD36 nanoclusters' radii, density and number of molecules per cluster in TSP-1 mediated clustering. This observation is comparable to the previous observation achieved by LY294002 treatment in inhibiting the production of PI3K.

This combined data with LY294002 and ionomycin indicate that inhibiting PI(3,4,5)P3 production by either using pharmacological inhibition of PI3K or depletion of PI(4,5)P2 from the plasma membrane have significant effects in both CD36 nanoclustering and downstream kinase Fyn activation although it is unclear why disrupting PIP2 have with ionomycin alone has shown no significant effects on CD36 nanoclusters size, radii and density. Essentially, the mechanism of this outcome remains unclear which led us perform additional experiments to clarity if decrease in Fyn activation caused by PI3K inhibition and PI(4,5)P2 depletion is the consequence of disruptions in CD36 nanocluster enhancements. To clarify this, we employed a technique that allows us to enhance the CD36 nanoclusters without TSP-1 to determine if CD36 nanoclusters enhancements (clustering) alone could activate Fyn.

2.7. Activation of Fyn upon stimulation with TSP-1 in TIME mEmerald-CD36 cells

We investigated the activity of Fyn after treatment with TSP-1 in TIME cells stably expressing CD36-mEmerald. TIME cells are human immortalized endothelial cells obtained from dermal microvascular endothelium of foreskin (ATCC® CRL-4025™). In this cell, we generated an inducible expression of CD36 tagged with mEmerald, which is a monomeric variant of green fluorescent protein (Shaner et al., 2013) using tetracycline inducible system which is explained in

Chapter 4 - 2.1. This system allows for the tight control of gene expression. Using immunofluorescence, we tested the levels of Fyn activation by using antibody targeted against phosphoSrc at tyrosine 418 and detected by Alexa Fluor 647 in TIME cells induced with or without doxycycline. This allows us to measure the intensity of Fyn fluorescence within CD36 clusters to determine Fyn activation. The quantification is done as discussed earlier in Chapter 2 - 5.1. This data suggests that Fyn activation is dependent on CD36 expression and there is a significant activation of Fyn upon stimulation with TSP-1.

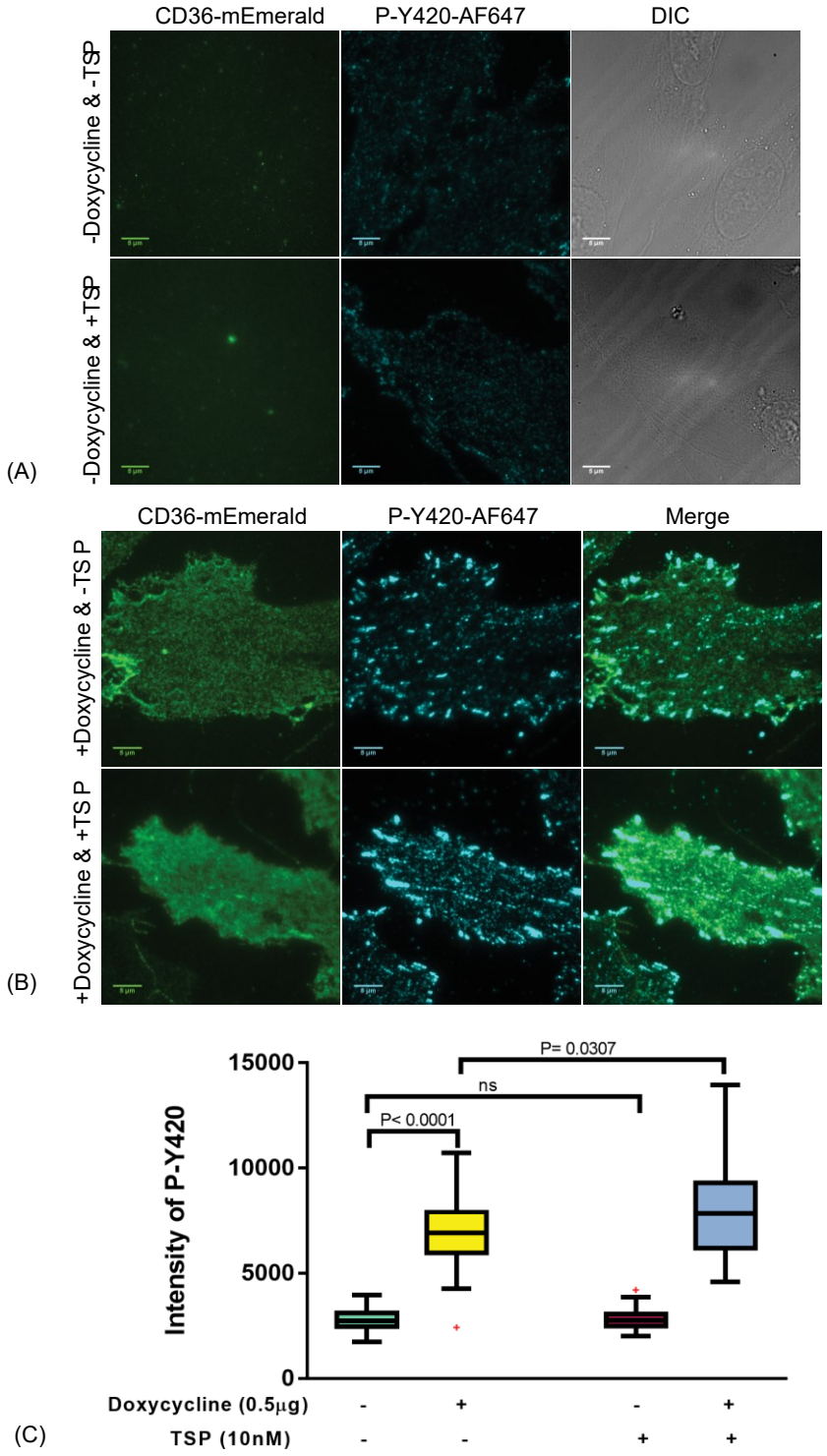

Figure 3.8 – Activation of Fyn in TIME-CD36-mEmerald.

(A) TIRF-M images of TIME cells induced with doxycycline for expression of CD36, stimulated with or without TSP-1 and tested for activation of Fyn using P-Y420 in Alexa Fluor 647. (B) TIRF-M images of TIME cells induced with doxycycline, stimulated with or without TSP-1 and test for Fyn activation (C) Normalized intensity for Fyn activation. 40 images were analyzed from 2

independent experiments. Boxplots and statistical analysis were performed according to Chapter 2 - 6.

2.8. Enhancements of CD36 nanocluster using Light-Activated Reversible Inhibition by Assembled Trap (LARIAT)

Optogenetic tools for controlling protein functions and modulating signaling pathways spatiotemporally in cells have become increasingly popular. We employed an optogenetic technique (LARIAT) (Amata et al., 2014) in this part of our project to selectively induce CD36 cluster formation in TIME cells expressing mEmerald-CD36. LARIAT utilizes blue light to reversibly sequesters target proteins into clusters. This is mediated by the actions of multimeric protein (MP) and a blue light-induced heterodimerization between a Cytochrome Interacting Basic helix-loop-helix protein (CIB1) and Cryptochrome 2 (CRY2). CIB1 and CRY2 are found in *Arabidopsis thaliana* and they interact with each other upon blue light induction and subsequently work together with other CIB1- related proteins in CYR2 dependent floral initiation (Kennedy et al., 2010; Taslimi et al., 2016). By using this heterodimerization system together with multimeric proteins and a single chain variable fragment (ScFv) targeting GFP, we induced CD36 cluster formation and studied the activation of Fyn upon formation of CD36 clusters. TIME cells stably expressing CD36-mEmerald were induced with doxycycline and synthetically triggered to produce CD36 (Figure 3.9A). Upon treatment with blue light, CRY2 heterodimerizes with a multimeric protein containing multiple CIB1 to recruit more CRY2 targeting CD36 which assembled into larger clusters (Figure 3.9C). We also used CIB1 without the multimeric protein as a control to observe the effects of blue-light induction. As we can see from (Figure 3.9D), the control without the MP did not show any evidence of cluster formation while the CIB1-MP exhibited cluster formation and co-localization with CD36-mEmerald upon UV induction.

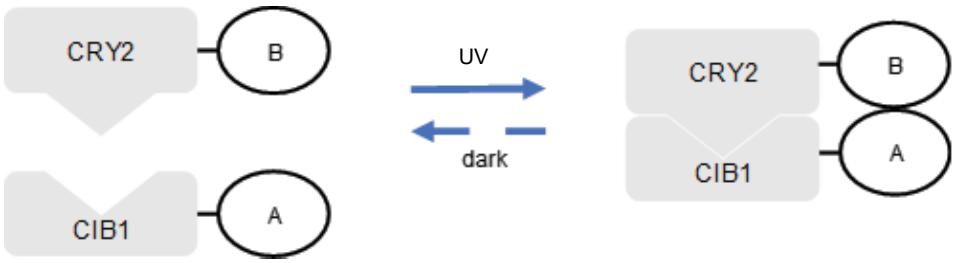
CRY2
B
CIB1
A
UV
dark
CRY2
B
CIB1
A

(A)

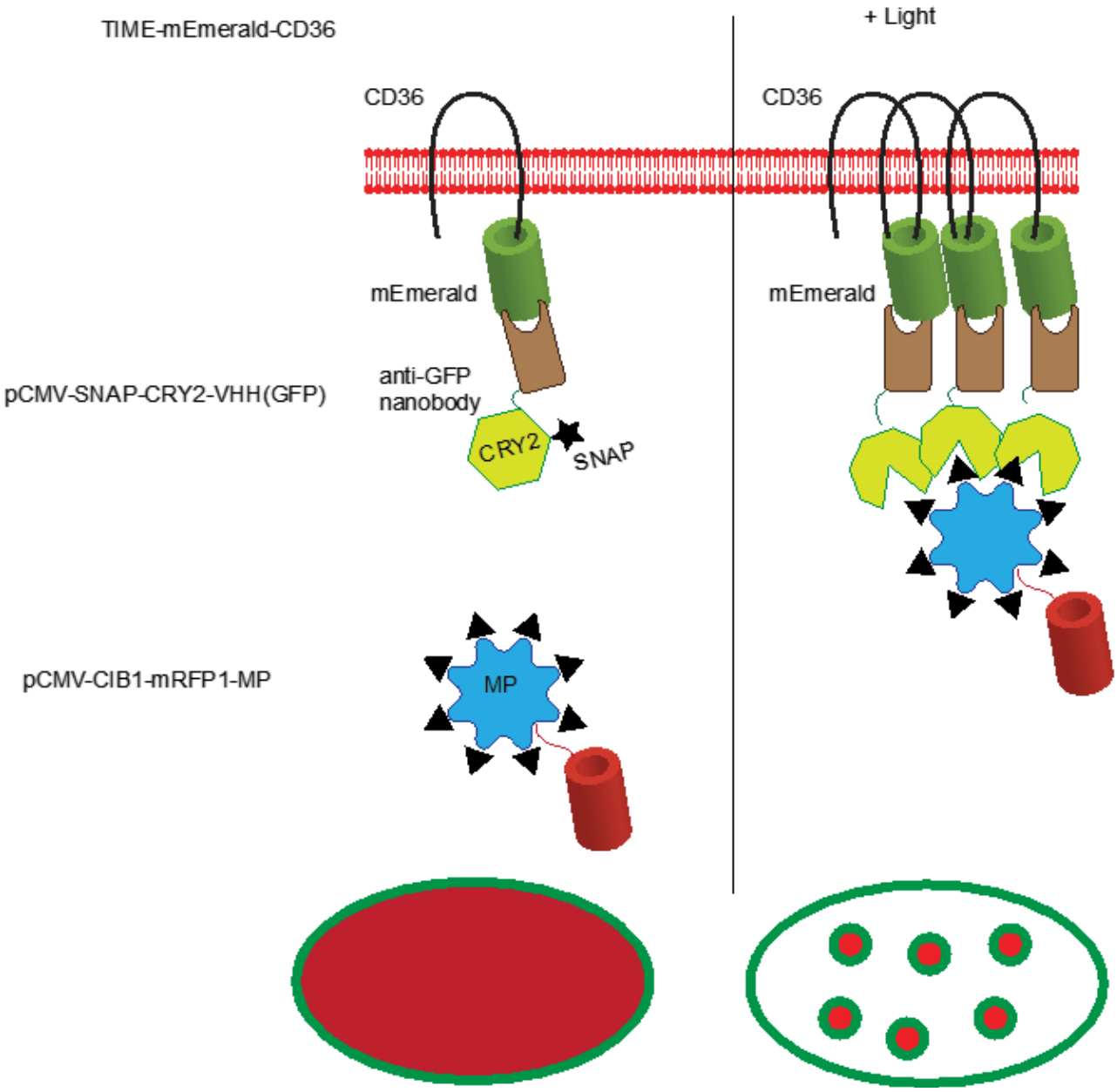
TIME-mEmerald-CD36
+ Light
CD36
CD36
mEmerald
mEmerald
pCMV-SNAP-CRY2-VHH(GFP)
anti-GFP
nanobody
CRY2
SNAP
pCMV-CIB1-mRFP1-MP
MP

(B)

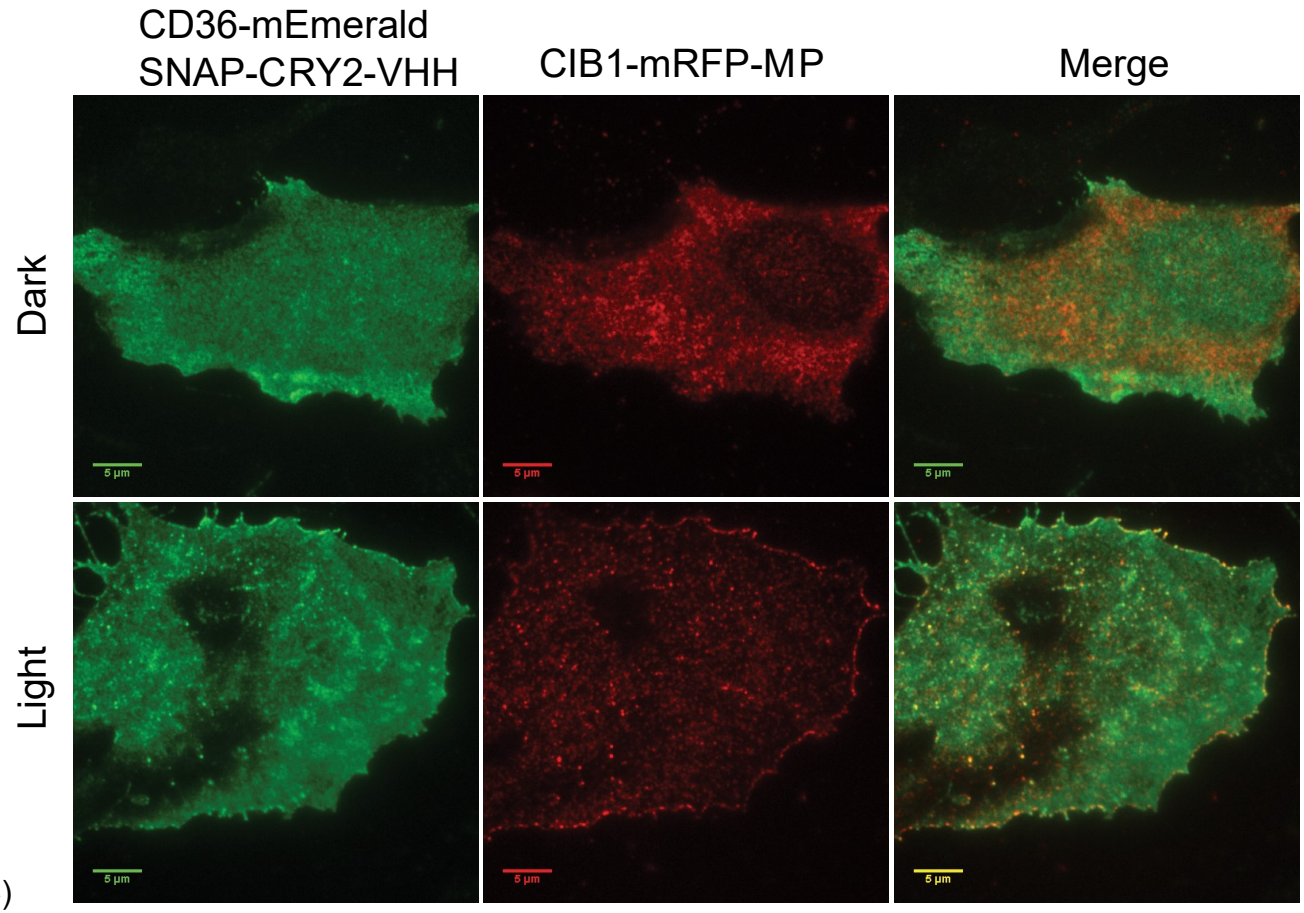
CD36-mEmerald
SNAP-CRY2-VHH
CIB1-mRFP-MP
Merge
Dark
Light
5 µm

(C)

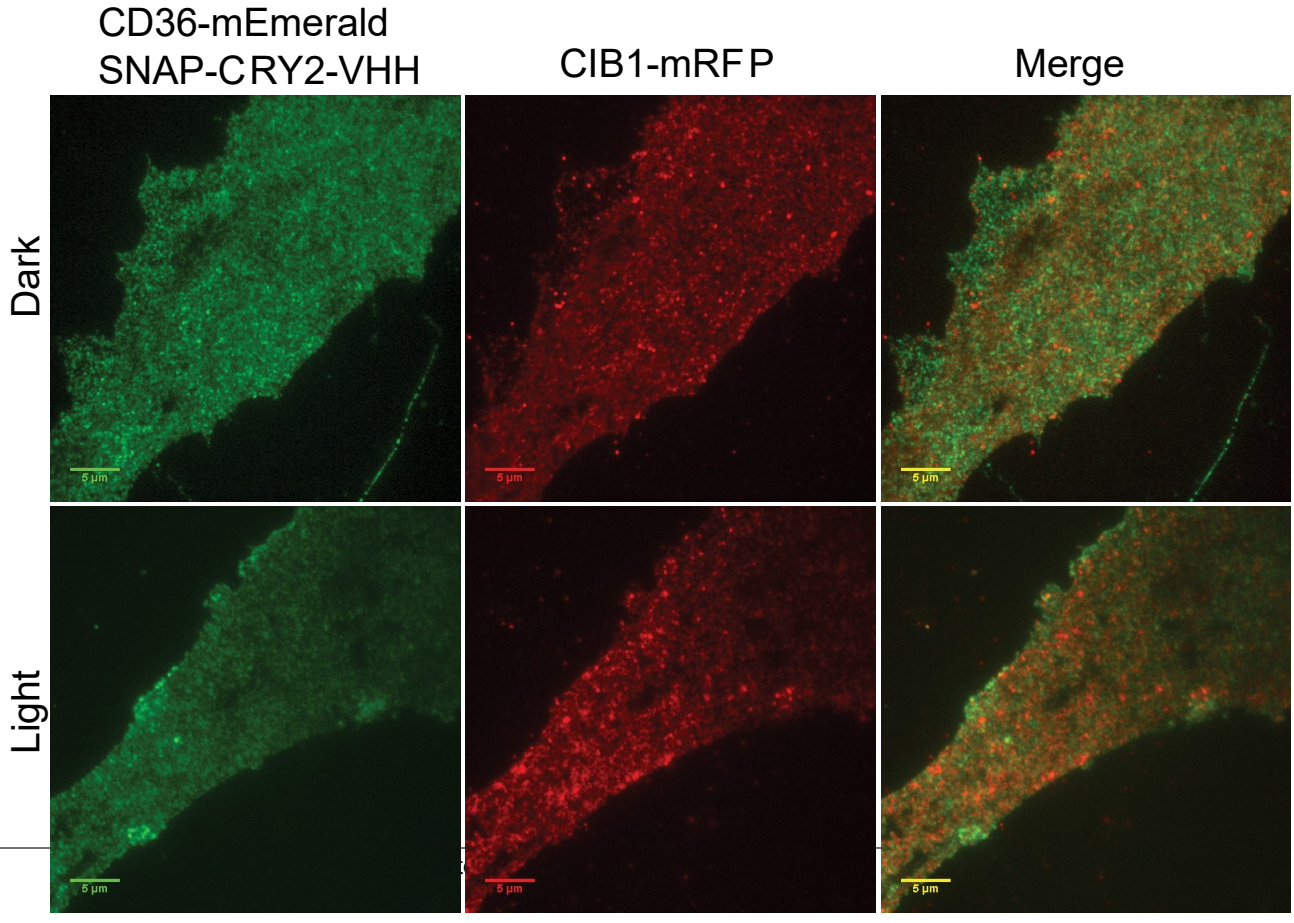
CD36-mEmerald
SNAP-CRY2-VHH
CIB1-mRFP
Merge
Dark
Light
5 µm

(D)

Figure 3.9 – Optogenetic approach for intracellular clustering of CD36.
(A) Schematic of CRY2 and CIB1 (B) Schematic of CRY2 and CIB1-MP heterodimerization system upon induction of UV. (C) TIRF-M images of TIME-CD36-mEmerald co-transfected with CRY2-SNAP and CIB1-MP with or without UV illumination. (D) TIRF-M images of TIME-CD36-mEmerald co-transfected with CRY2-SNAP and CIB1-mCherry (no MP) with or without UV illumination. 40 images were analyzed from 2 independent experiments.

2.9. PI(3,4,5)P3 is important for Fyn activation in endothelial cells

After using optogenetic approach to create CD36 clusters intracellularly, we studied the activation of Fyn using immunofluorescence and TIRF-M. As we can see from (Figure 3.10), CD36 gathered into clusters upon UV illumination. The activation of Fyn, detected by P-Y418-AF647 was measured within the clusters and it significantly increased when CD36 arranged into clusters. Next, we used the LY294002 treatment and investigated how it affects Fyn activation. Fyn activation produced by CD36 clustering was reduced when the cells were treated with LY294002 (Figure 3.10B & E). We also compared the levels of Fyn activation with the control (without MP) (Figure 3.10- D & F) and quantified the intensity of P-Y420 enriched within these clusters. We observed that the reduction in Fyn activation upon inhibiting PI3K was not evident in control (without MP) even after LY294002 treatment. Altogether, our results indicate that PI(3,4,5)P3 produced from PI3K is indeed important for the Fyn activation.

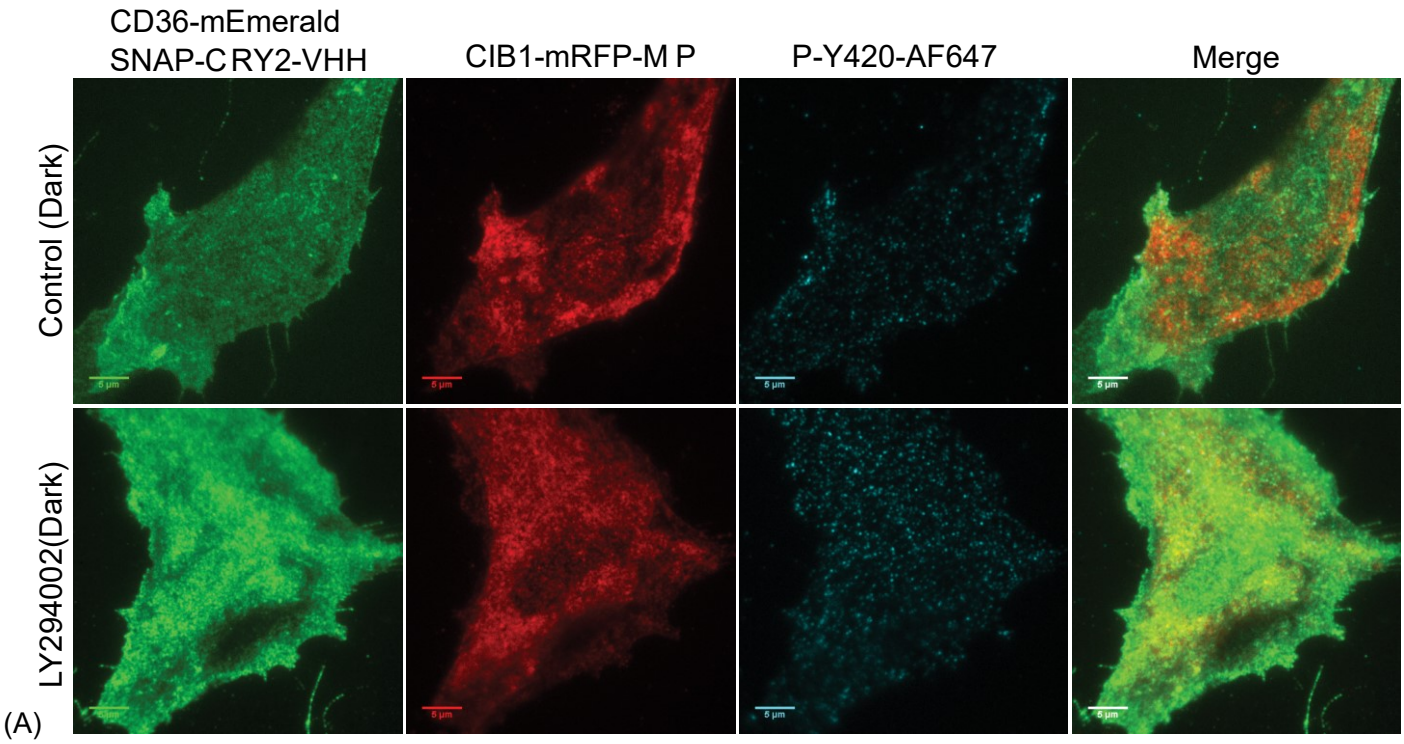
CD36-mEmerald
SNAP-CRY2-VHH
CIB1-mRFP-MP
P-Y420-AF647
Merge
Control (Dark)
LY294002(Dark)
(A)

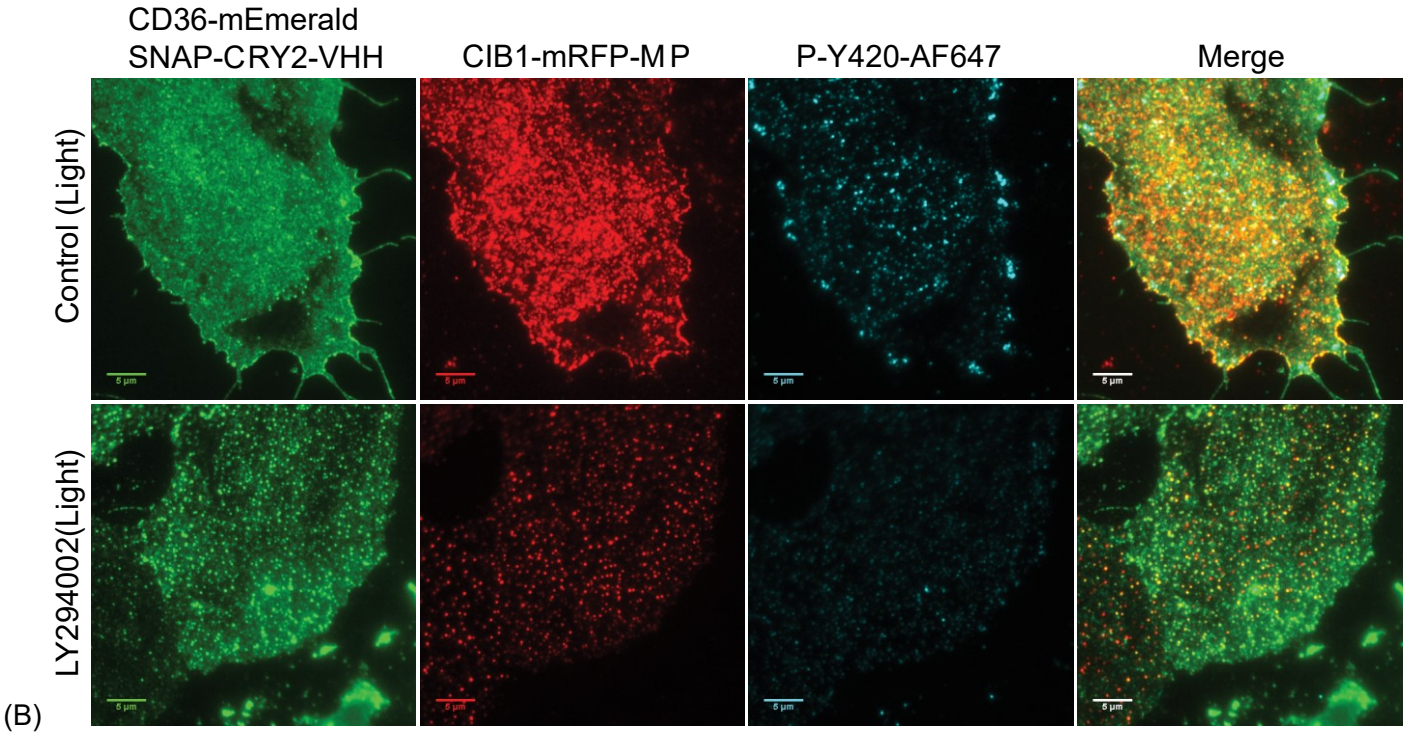
CD36-mEmerald
SNAP-CRY2-VHH
CIB1-mRFP-MP
P-Y420-AF647
Merge
Control (Light)
LY294002(Light)
(B)

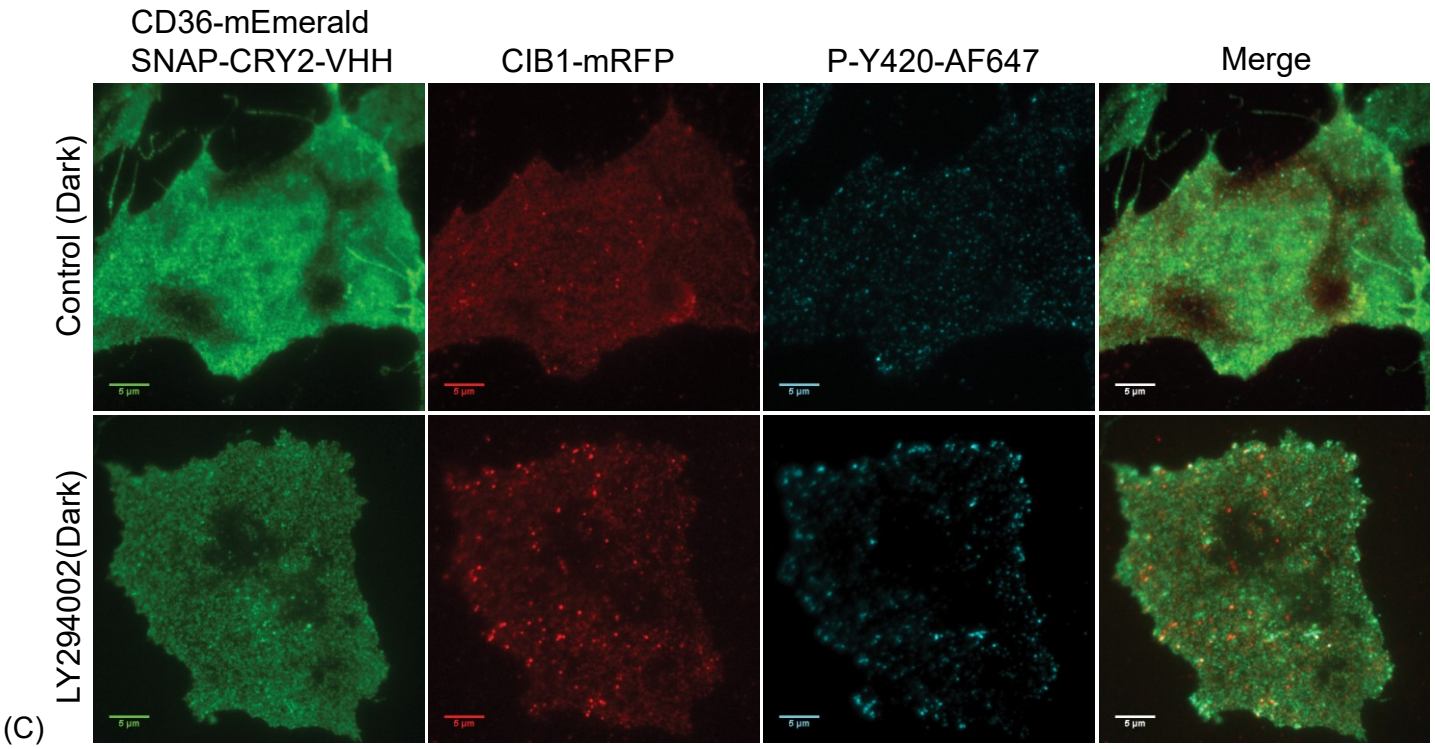
CD36-mEmerald
SNAP-CRY2-VHH
CIB1-mRFP
P-Y420-AF647
Merge
Control (Dark)
LY294002(Dark)
5 µm

(C)

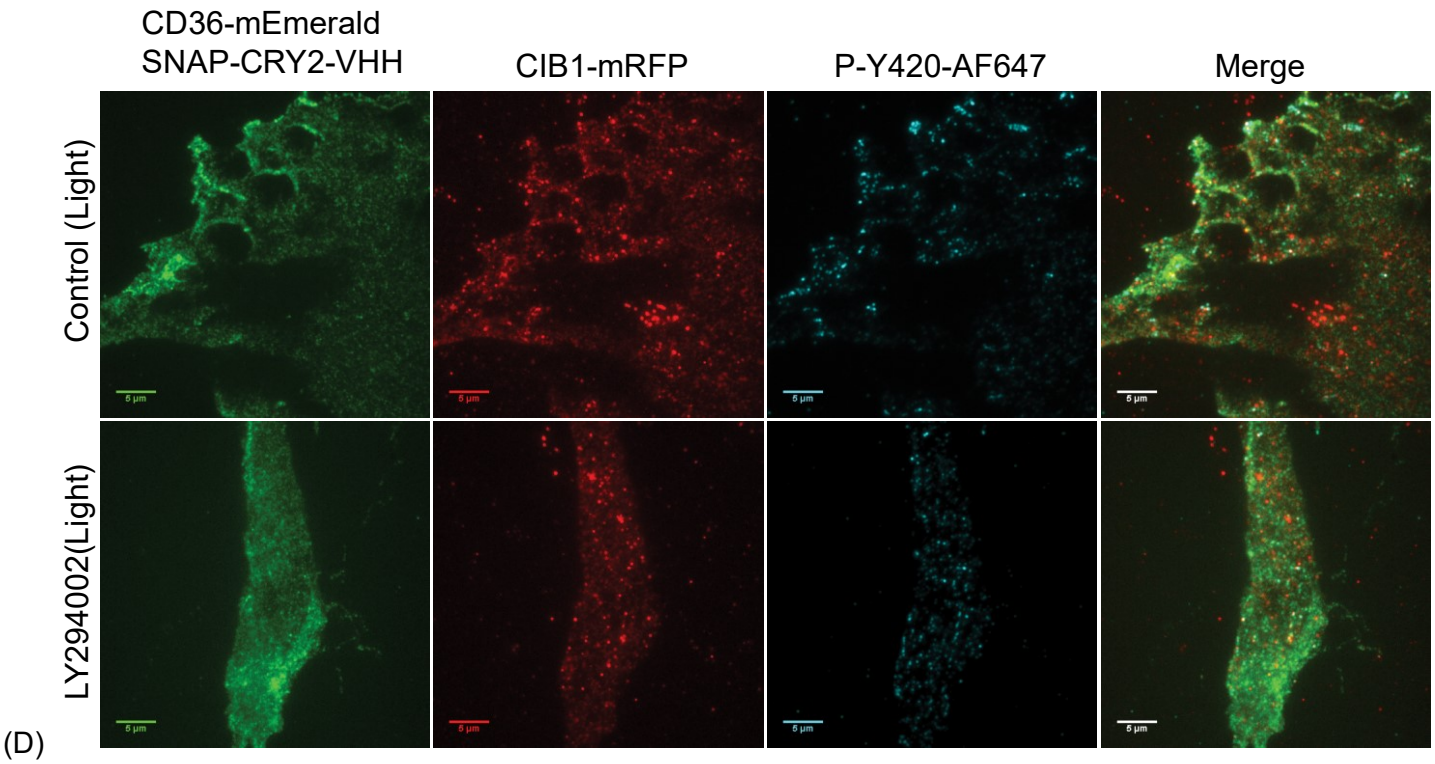
CD36-mEmerald
SNAP-CRY2-VHH
CIB1-mRFP
P-Y420-AF647
Merge
Control (Light)
LY294002(Light)
5 µm

(D)

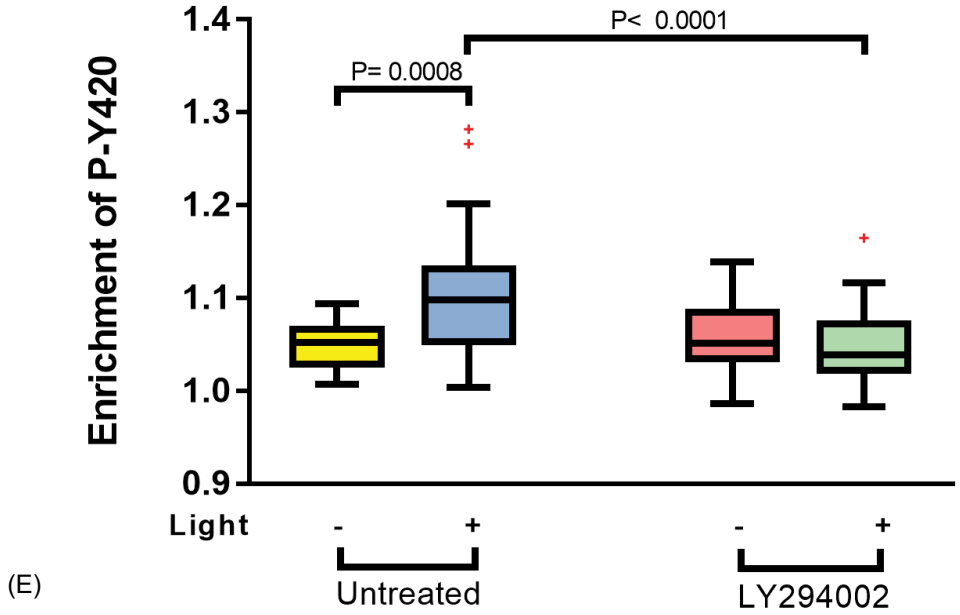

(E)

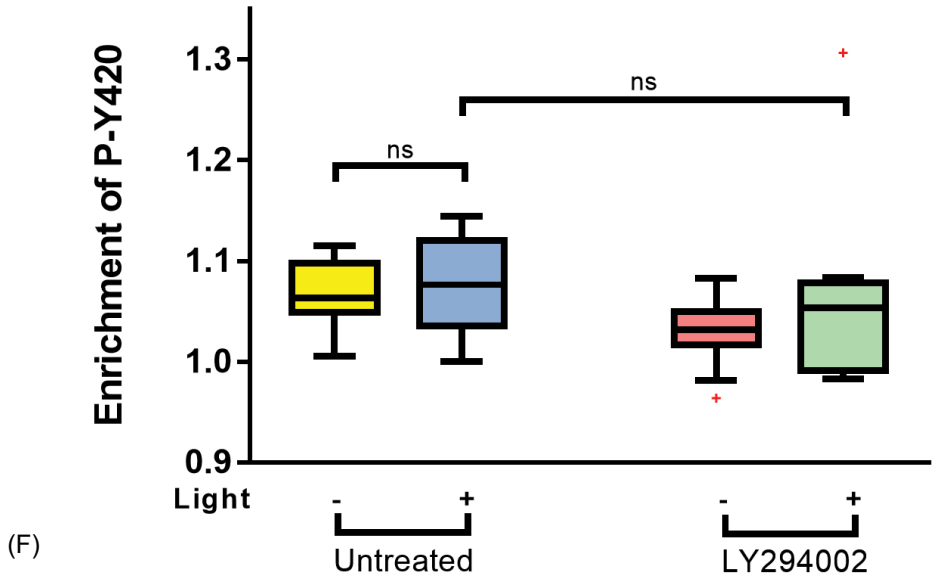

(F)

Figure 3.10 – Fyn activation in TIME-CD36-mEmerald exposed to UV illumination.
(A) TIRF-M images of Fyn activation detected by P-Y420-AF647 in TIME-CD36-mEmerald co-transfected with CRY2-SNAP and CIB1-MP treated with or without LY294002 and without exposure to UV illumination. (B) TIRF-M images of Fyn activation in TIME-CD36-mEmerald co-transfected with CRY2-SNAP and CIB1-MP treated with or without LY294002 and with exposure to UV illumination. (C) TIRF-M images of Fyn activation detected by P-Y420-AF647 in TIME-CD36-mEmerald co-transfected with CRY2-SNAP and CIB1-mCherry (no MP) treated with or without LY294002 and without exposure to UV illumination. (D) TIRF-M images of Fyn activation

detected by P-Y420-AF647 in TIME-CD36-mEmerald co-transfected with CRY2-SNAP and CIB1-mCherry (no MP) treated with or without LY294002 and with exposure to UV illumination. (E) Quantification of p-Y420 intensity in cells (MP) treated with or without LY294002 and with or without exposure to UV. (F) Quantification of p-Y420 intensity in cells (no MP) treated with or without LY294002 and with or without exposure to UV. 40 images were analyzed from 2 independent experiments. Boxplots and statistical analysis were performed according to Chapter 2 - 6.

3. Discussion

Our study suggests that CD36 nanoclusters are enriched with PI(4,5)P2 at basal state, however, TSP-1 stimulation not only induced nanoclusters enhancement and compaction but also engaged PI3K which phosphorylates PI(4,5)P2 to PI(3,4,5)P3. PIs have been involved in nearly all aspects of cell physiology. They initiate direct signaling effects by binding to cytosolic proteins or domains of membrane proteins. PI(4,5)P2 is implicated in many cellular mechanisms such as membrane trafficking, organization of membrane/cytoskeletal interface and cell signaling (Insall and Weiner, 2001).

Here we show that CD36 nanoclusters are enriched with specific inner leaflet lipids, especially PIP2 and PS. While investigating the nature of lipids present in the inner leaflet of CD36 enriched domains, we also investigated if the spatial organization of CD36 nanoclusters with PI(4,5)P2 perhaps occur at plasma membrane nanodomains enriched in glycosphingolipids and cholesterol (specialized domain) where PI(4,5)P2 is reported to be concentrated (Fujita et al., 2009), however, our findings suggest that at basal state, CD36 nanoclusters and PI(4,5)P2 organization is not compartmentalized in these specialized membrane domains. Perhaps, receptor activation with TSP-1 triggers clustering of CD36 molecules into these specialized domains. Moreover, during TSP-1 stimulation, the concomitant decrease of PIP2 with a PIP3 increase suggested the involvement of a PI3-Kinase. We carried out experiments to decipher the role of PIP3 and PI-3Kinase in the CD36-Fyn signal transduction pathway.

Although, the arrangement of CD36 nanoclusters on the surface of endothelial cell membrane is still being investigated, our analyses suggest that CD36 nanoclusters are enriched with PI(4,5)P2 on the inner leaflet of the plasma membrane and this arrangement is somewhat reliant on the membrane ultrastructure such as cortical F-actin and cholesterols in the plasma membrane nanodomains (Githaka et al., 2016). Similarly, Zhou and Hancock have shown that Ras (small GTPases) gather into transient nanoclusters on the plasma membrane, the formation, stability and dynamic of these nanoclusters being dependent on the nature of the inner leaflet lipid interacting with Ras and the specific lipids on the plasma membrane play an important role in mediating the formation, stability and dynamic of Ras nanoclusters. For instance, PS is found evenly among three types of Ras GTPases (K-RasGTP, H-RasGTP and H-RasGDP) nanoclusters whereas PA is more enriched in K-RasGTP than H-RasGTP nanodomains (Zhou et al., 2014). While PI(4,5)P2 is enriched specially in H-RasGDP nanoclusters, PI(3,4,5)P3 is present in all three nanoclusters (Zhou et al., 2014). Although, the activity of these lipids within Ras nanoclusters are still being explored, PS depletion studies have shown that plasma membrane PS is required for the structural stability of K-RasGTP nanoclusters but not H-RasGTP or H-RasGDP (Zhou et al., 2014; Zhou and Hancock, 2015). Hence, the concept of specific lipids predominantly phosphoinositides interplay in CD36 nanoclustering is highly conceivable.

The production of PI(3,4,5)P3 at the site of CD36 nanoclusters with TSP-1 stimulation was observed using PI(3,4,5)P3 bio-sensor. This lipid is present in low amounts in the plasma membrane of resting cells, but it can quickly and dramatically increase following growth factor stimulation. The regulatory role of PI(3,4,5)P3 has been implicated in the physiology of higher eukaryotes as it participates in a large variety of processes, including cell proliferation, migration, chemotaxis, phago and macro-pinocytosis, differentiation, survival and metabolic changes (Hinchliffe, 2001). PI(3,4,5)P3 recruits effectors that activate synergistic signaling pathways (Hinchliffe, 2001). One of the most recognized PI(3,4,5)P3 target proteins are GEFs and GAPs

for small GTPases whose functions involved in regulation of the actin cytoskeleton and the protein kinases PDK and AKT/PKB (Salamon and Backer, 2013). Although, the presence of PIP3 is detected in TSP-1 mediated CD36-Fyn signaling, it was unclear if the latter pathway (AKT/PKB) is activated since involvement of Akt implicates the cell proliferation pathway (somewhat counter intuitive as this pathway triggers apoptosis). To test this, we investigated the activation of Akt using immunoblotting and found that in fact, there was no activation of Akt in the TSP-1 mediated CD36-Fyn signaling (Figure 3.3A) which indicates that PIP3 production may result in the regulation of the actin cytoskeleton in endothelial cells. Numerous studies have reported PIP3 as a cellular mediator for cytoskeleton regulation by interacting with RacGTPases (Welch et al., 2003). This is demonstrated by increase in activity of Vav protein (Rac-GEF) after reported association with PI(3,4,5)P3 while association with PI(4,5)P2 decrease Vav activity(Crespo et al., 1997; Katso et al., 2006; Palmby et al., 2002). Binding of PIP3 to the PH domain of Vav whose activity is controlled by phosphorylation of Tyr174 releases the inhibitory action and exposed the Tyr174 residue for additional phosphorylation by Src-family kinases (Aghazadeh et al., 2000; Campa et al., 2015; Palmby et al., 2002).

The synthesis of PIP3 is usually carried out by class I PI3K which we sought to explore by using PI3K inhibitor (LY294002). The inhibition of PI3K decreased the levels of PIP3 produced at CD36 nanoclusters during the TSP-1 stimulation (Figure 3.2D) which suggested the role of PI3K in the TSP-1 mediated CD36-Fyn signaling. The inhibition of PI3K also diminished the activation of Fyn upon TSP-1 induction (Figure 3.2E&F) further accentuating the importance of PI3K in Fyn activation. The contribution of PI3K in this pathway may not be limited to the role of PIP3 production and to the notion of cytoskeleton regulation. For instance, SH2 domain of Fyn has been reported to interact with p85 subunit of PI3K (Cuevas et al., 2001; Park et al., 2016; Yadav and Denning, 2011) which would relieve the intermolecular constraints that inhibit Fyn activation (Miller et al., 2014). The implication of PI3K in Fyn activation is not particularly a novel finding

nevertheless, this proposed mechanism warrants further investigation in endothelial cells. While PI3K inhibitor suppressed the production of PIP3 in our experiments, we were uncertain if the association with PI3K leads to the production of PIP3. Several studies have reported that PI3K activity is uncoupled from the PIP3 production at the membrane (Gillham et al., 1999; Pike and Miller, 1998). Reasonably, it is critical to distinguish the PI3K activity with PIP3 synthesis using tools such as rapamycin heterodimerization and light inducible heterodimerization that allow selective manipulation of membrane lipids. Despite our unsuccessful attempts to manipulate PIs using these tools, we were able to employ the use of ionophore (ionomycin) in depleting the lipid substrate PIP2 from the membrane to study the effects on Fyn activation and nanocluster enhancements.

Our initial experiments showed that ionomycin treatment provided a rather severe condition for the cells, thus we optimized conditions for ionomycin treatment that allowed the survival of the cells (without loss of proteins) while raising the intracellular Ca^{2+} concentration and depleting PIP2 from the membrane. Our results (Figure 3.5B) demonstrated that PIP2 and PIP3 was significantly depleted and not the controls (GPI and PM probes) after the addition of ionomycin which was exhibited by dissociation of PIP2 and PIP3 biosensors from the membrane, hence, decreasing intensity in TIRF measurements. Though, the effects of depleting PIP2 and PIP3 by ionomycin delivered comparable results with LY294002 treatment in Fyn activation and CD36 nanoclusters enhancements, the limitations of this technique must be considered. One caveat is the mechanism of Ca^{2+} transport into the cells by ionomycin, which is carried out by forming a pore in the membrane thus creating impacts on membrane architecture and hence possibly leading to the disruption of CD36 nanoclusters and association with Fyn. Although, the ionomycin experiment is not an ideal way to provide a clear answer for the un-coupling of PIP3 from PI3K, it provided a clearer representation for the PIP2 and PIP3 involvements in CD36-Fyn signaling.

The effect of LY294002 and ionomycin in CD36 nanoclusters were evident with our clustering data (Figure 3.4 and Figure 3.7) further supplementing the importance of PIP3 production in the pathway. One challenge concerning the data was the effect on Fyn activity after the decrease in the CD36 nanoclusters enhancements. The question we asked then is “Is the decrease in Fyn activation by LY294002 and ionomycin treatment, a consequence of the decrease in CD36 nanocluster enhancements?”. To answer this question, we pursued a unique method of triggering clustering of CD36 intracellularly (CRY2-CIB1 experiment Chapter 2 - 2.5) in the presence of LY294002 to dissociate PI3K effects on Fyn activation and CD36 clustering. Hypothetically, if PI3K activity was exclusively important for CD36 nanocluster enhancements, inhibition of PI3K would have little or no impact on Fyn activity with this “artificial” CD36 clustering. After formation of CD36 clusters using LARIAT, our data demonstrated significant increase in Fyn activation, consistent with our previous findings that CD36 nanoclustering promotes Fyn activation. Interestingly, the application of LY294002 during artificially induced CD36 clusters has decreased Fyn activation, which suggested another role for PIP3, perhaps a direct connection for PI3K or PIP3 in Fyn activation.

Altogether, our study proposed a model in which CD36 nanoclusters associates with PIP2 at steady state and PIP3 at ligand induced state. During ligand stimulation and PI3K engagement, CD36 nanoclusters enhances which leads to activation of Fyn and this activation is abolished by inhibiting PI3K or depleting PIP2 from the membrane establishing the role of PI3K or its lipid product (PIP3) in Fyn activation. The mechanism of Fyn activation in CD36 nanoclusters signaling has not been clearly elucidated in this study, however, it is possible that engagement of PI3K at the membrane or perhaps its lipid product (PIP3) upon enhancements of CD36 nanoclusters has a direct effect in activating Fyn by recruiting additional molecules possibly protein phosphatases which dephosphorylate inhibitory tyrosine- 531 residue in Fyn SH2 domain and thus relieving the intermolecular constrains in Fyn SH2 domain to allow interaction with p85 subunit of PI3K.

4. References

Aghazadeh, B., Lowry, W.E., Huang, X., and Rosen, M.K. (2000). Structural basis for relief of autoinhibition of the Dbl homology domain of proto-oncogene Vav by tyrosine phosphorylation. Cell 102, 625-633.

Amata, I., Maffei, M., and Pons, M. (2014). Phosphorylation of unique domains of Src family kinases. Frontiers in Genetics *5,* 181.

Campa, C.C., Ciraolo, E., Ghigo, A., Germena, G., and Hirsch, E. (2015). Crossroads of PI3K and Rac pathways. Small GTPases *6,* 71-80.

Crespo, P., Schuebel, K.E., Ostrom, A.A., Gutkind, J.S., and Bustelo, X.R. (1997). Phosphotyrosine-dependent activation of Rac-1 GDP/GTP exchange by the vav proto-oncogene product. Nature *385,* 169.

Cuevas, B.D., Lu, Y., Mao, M., Zhang, J., LaPushin, R., Siminovitch, K., and Mills, G.B. (2001). Tyrosine phosphorylation of p85 relieves its inhibitory activity on phosphatidylinositol 3-kinase. J. Biol. Chem. *276,* 27455-27461.

Fujita, A., Cheng, J., Tauchi-Sato, K., Takenawa, T., and Fujimoto, T. (2009). A distinct pool of phosphatidylinositol 4, 5-bisphosphate in caveolae revealed by a nanoscale labeling technique. Proceedings of the National Academy of Sciences *106,* 9256-9261.

Gillham, H., Golding, M.C., Pepperkok, R., and Gullick, W.J. (1999). Intracellular movement of green fluorescent protein–tagged phosphatidylinositol 3-kinase in response to growth factor receptor signaling. J. Cell Biol. *146,* 869-880.

Githaka, J.M., Vega, A.R., Baird, M.A., Davidson, M.W., Jaqaman, K., and Touret, N. (2016). Ligand-induced growth and compaction of CD36 nanoclusters enriched in Fyn induces Fyn signaling. J. Cell. Sci. *129,* 4175-4189.

Hinchliffe, K.A. (2001). Cellular signalling: stressing the importance of PIP3. Current Biology *11,* R373.

Insall, R.H., and Weiner, O.D. (2001). PIP3, PIP2, and cell movement—similar messages, different meanings? Developmental Cell *1,* 743-747.

Jaqaman, K., Kuwata, H., Touret, N., Collins, R., Trimble, W.S., Danuser, G., and Grinstein, S. (2011). Cytoskeletal control of CD36 diffusion promotes its receptor and signaling function. Cell *146,* 593-606.

Katso, R.M., Pardo, O.E., Palamidessi, A., Franz, C.M., Marinov, M., De Laurentiis, A., Downward, J., Scita, G., Ridley, A.J., and Waterfield, M.D. (2006). Phosphoinositide 3-kinase C2β regulates cytoskeletal organization and cell migration via Rac-dependent mechanisms. Mol. Biol. Cell *17,* 3729-3744.

Kennedy, M.J., Hughes, R.M., Peteya, L.A., Schwartz, J.W., Ehlers, M.D., and Tucker, C.L. (2010). Rapid blue-light–mediated induction of protein interactions in living cells. Nature Methods *7,* 973.

Kosenko, A., and Hoshi, N. (2013). A change in configuration of the calmodulin-KCNQ channel complex underlies Ca2 -dependent modulation of KCNQ channel activity. PloS One *8,* e82290.

Lingwood, D., Kaiser, H., Levental, I., and Simons, K. (2009). No title. Lipid Rafts as Functional Heterogeneity in Cell Membranes

Miller, M.S., Schmidt-Kittler, O., Bolduc, D.M., Brower, E.T., Chaves-Moreira, D., Allaire, M., Kinzler, K.W., Jennings, I.G., Thompson, P.E., and Cole, P.A. (2014). Structural basis of nSH2 regulation and lipid binding in PI3Kα. Oncotarget *5,* 5198.

Palmby, T.R., Abe, K., and Der, C.J. (2002). Critical role of the pleckstrin homology and cysteine-rich domains in Vav signaling and transforming activity. J. Biol. Chem. *277,* 39350-39359.

Park, M., Sheng, R., Silkov, A., Jung, D., Wang, Z., Xin, Y., Kim, H., Thiagarajan-Rosenkranz, P., Song, S., and Yoon, Y. (2016). SH2 domains serve as lipid-binding modules for pTyr-signaling proteins. Mol. Cell *62,* 7-20.

Pike, L.J., and Miller, J.M. (1998). Cholesterol depletion delocalizes phosphatidylinositol bisphosphate and inhibits hormone-stimulated phosphatidylinositol turnover. J. Biol. Chem. *273,* 22298-22304.

Rastogi, B.K., and Nordøy, A. (1980). Lipid composition of cultured human endothelial cells. Thromb. Res. *18,* 629-641.

Salamon, R.S., and Backer, J.M. (2013). Phosphatidylinositol-3, 4, 5-trisphosphate: Tool of choice for class I PI 3-kinases. Bioessays *35,* 602-611.

Shaner, N.C., Lambert, G.G., Chammas, A., Ni, Y., Cranfill, P.J., Baird, M.A., Sell, B.R., Allen, J.R., Day, R.N., and Israelsson, M. (2013). A bright monomeric green fluorescent protein derived from Branchiostoma lanceolatum. Nature Methods *10,* 407.

Shevchenko, A., and Simons, K. (2010). Lipidomics: coming to grips with lipid diversity. Nature Reviews Molecular Cell Biology *11,* 593.

Taslimi, A., Zoltowski, B., Miranda, J.G., Pathak, G.P., Hughes, R.M., and Tucker, C.L. (2016). Optimized second-generation CRY2–CIB dimerizers and photoactivatable Cre recombinase. Nature Chemical Biology *12,* 425.

Van Meer, G., Voelker, D.R., and Feigenson, G.W. (2008). Membrane lipids: where they are and how they behave. Nature Reviews Molecular Cell Biology *9,* 112.

Vanhaesebroeck, B., Stephens, L., and Hawkins, P. (2012). PI3K signalling: the path to discovery and understanding. Nature Reviews Molecular Cell Biology *13,* 195.

Welch, H.C., Coadwell, W.J., Stephens, L.R., and Hawkins, P.T. (2003). Phosphoinositide 3-kinase-dependent activation of Rac. FEBS Lett. *546,* 93-97.

Yadav, V., and Denning, M.F. (2011). Fyn is induced by Ras/PI3K/Akt signaling and is required for enhanced invasion/migration. Mol. Carcinog. *50,* 346-352.

Zachowski, A. (1993). Phospholipids in animal eukaryotic membranes: transverse asymmetry and movement. Biochem. J. *294,* 1.

Zhou, Y., and Hancock, J.F. (2015). Ras nanoclusters: Versatile lipid-based signaling platforms. Biochimica Et Biophysica Acta (BBA)-Molecular Cell Research *1853,* 841-849.

Zhou, Y., Liang, H., Rodkey, T., Ariotti, N., Parton, R.G., and Hancock, J.F. (2014). Signal integration by lipid-mediated spatial cross talk between Ras nanoclusters. Mol. Cell. Biol. *34,* 862-876.

Chapter 4 - **Identification of potential adaptor proteins in CD36 nanoclusters and F-actin organization**

1. Introduction

The association of CD36 and Fyn with cortical F-actin has been observed in our previous study, however, the mechanism of this association is poorly understood. The cortical F-actin is associated with receptor endocytosis and exocytosis, cell motility, cytokinesis and cell polarity (Saarikangas et al., 2010). Rho family GTPases and Arf family GTPases are well known

regulators of the actin cytoskeleton dynamics and organization near the plasma membrane (Myers and Casanova, 2008). In this second part of the project, we aim to determine the connections between CD36 and F-actin and possible association with the plasma membrane. The role of actin cytoskeleton in regulating plasma membranes receptors have been explained in detail in Chapter 1 - 5.3 Cortical cytoskeleton organization on the plasma membrane. To understand more of this F-actin and CD36 association, we searched for evidence of CD36 binding to actin directly or indirectly, however, we have not been able to locate any evidence reporting this association as yet which led us to propose that the connection between CD36 and F-actin must be assisted by adaptor molecules that can modulate actin cytoskeleton and plasma membrane organization. The goal of this study was to identify proteins (adaptor molecules) possibly interacting with CD36 and enriched on F-actin rich area. We first selected to biotinylate proteins in the proximity of CD36 using BioID and fractionated these associated proteins bound to F-actin, followed by identifying these proteins using mass spectrometry.

BioID is the one of the unique systems to investigate the physiologically relevant protein interactions that occur in living cells. It uses promiscuous biotin ligase (BirA) isolated from *E.coli* to biotinylate proteins in proximity to the protein of interest (Roux et al., 2013). Some of the advantages of BioID over conventional methods such as Immunoprecipitation are that BioID is insensitive to protein solubility or aggregation and it allows the experimenter to identify weak and transient interactions that are usually lost with conventional techniques. This was implemented by making a fusion protein between CD36 and BirA* carrying a Flag epitope and stably expressing the construct first in HeLa cells and then in ECs. To control the level of expression of the construct, a tetracycline inducible system was used. Once the cells were induced with doxycycline, CD36-BirA-Flag expression was tested using western blotting. After the successful expression of CD36-BirA-Flag construct, the cells were incubated with exogenous biotin to allow for proximity dependent biotinylation and finally, the cell lysates were separated into F and G actin fractions.

Last, biotinylated proteins associated with the F and G actin were enriched with streptavidin coated agarose resin and submitted to mass spectrometry. Using this 2 steps separation protocol our objective was to identify proteins which are both in the proximity of CD36 and associated with F-actin. Our future directions will be to characterize their role in the TSP-1 – CD36 – Fyn signal transduction pathway.

CD36 was fused to BirA* and Flag tag and HeLa cells stably expressing this plasmid were selected as described in Chapter 2 - 1.2. Moreover, in order to avoid false positive and artefactual behavior due to protein overexpression, we used a tetracycline inducible promoter system to allow controlled expression of BirA*-CD36. Tetracycline inducible system utilizes inducible promoters to control eukaryotic gene expression (Gossen and Bujard, 1992). Here we used the Tet-on system, in which the tetracycline response element (TRE) and the tetracycline transactivator (rtTA) are the critical components (Figure 4.1). In the absence of tetracycline or one of its analog (such as doxcycycline used hereafter), the rtTA is not bound to the TRE, repressing the transcription of BirA*-CD36. In the presence of tetracycline (or its analog doxycycline), doxycycline binds to rtTA, triggering the transcription of the construct. We used this technique to induce the expression of CD36-BirA-Flag construct in a doxycycline concentration dependent manner (Gossen et al., 1995).

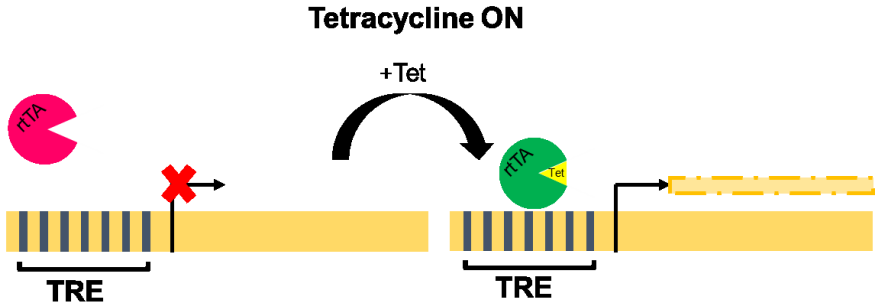

Figure 4.1 – Schematic of Tet On system.

Image adapted from Addgene, describing the Tet-on system. The presence of doxycycline allows the binding of the tetracycline transactivator to bind to the promoter's TRE sites and trigger gene the transcription of the gene of interest.

2. Results

2.1. Construction of HeLa-CD36-BirA-Flag using tetracycline inducible expression system

To control for the level of expression of CD36-BirA-Flag, the cells were treated with 1 µg/mL of doxycycline for 24 h. To induce BirA* biotinylation, cells were incubated with 100 µM biotin for 18 h. The cells were then lysed and immunoblotted using anti-Flag antibody and Streptavidin conjugated to IRDye 680 for detection of CD36-BirA-Flag.

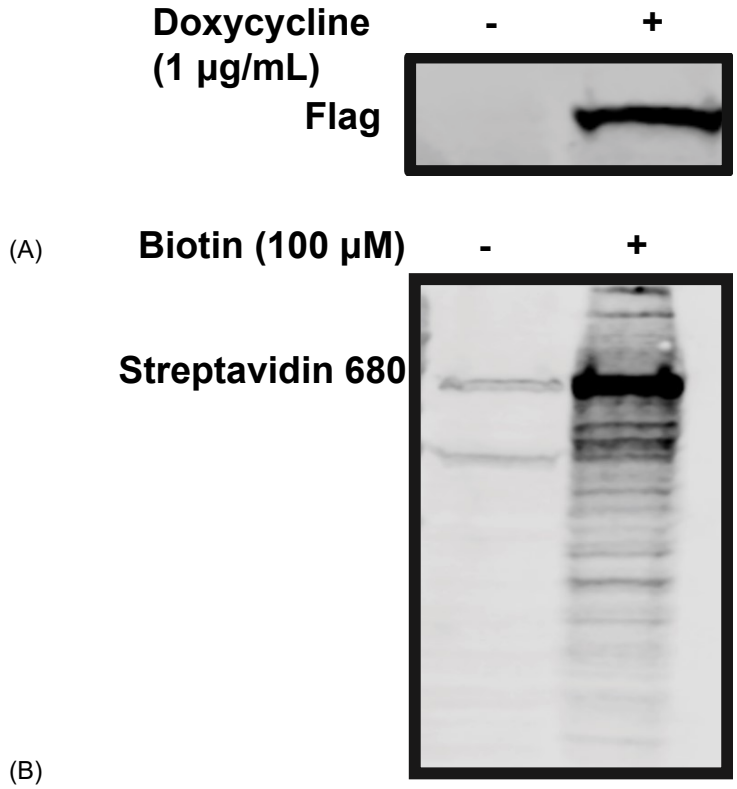

Figure 4.2 – Detection of CD36 in HeLa cells expressing CD36-BirA-Flag.
(A) Detection of CD36 after induction with 1 µg/mL of doxycycline for 24 h, detected using mouse anti Flag antibody. (B) Detection of biotinylated proteins after induction with doxycycline and treatment with 100 µM biotin for 18 h, detected using Streptavidin IRDye 680.

From the western blots, we observed that addition of 1 µg/mL of doxycycline for 24h allowed the expression of CD36-BirA-Flag compared to the control (without addition of Doxycycline). We were also able to see that once the cells were incubated with biotin (100 µM), biotinylation of proteins close to CD36 has occurred.

2.2. F- and G-actin separation

To identify adaptor proteins associated with CD36 and enriched on F-actin we first induced biotinylation of the proteins that are closely associated with CD36 as demonstrated in the previous section. Second, we developed a method to separate the monomeric (G- Actin) and filamentous (F- Actin) forms of actin in cell extracts. We successfully separated the G- and F-actin from cells using a specialized buffer which retained F-actin, solubilized G-actin and finally precipitating the F-actin using high speed ultracentrifugation. Furthermore, we performed a control experiment where we treated the cells with actin depolymerization agent (Latrunculin B) and F-actin stabilization agent (Jasplakinolide) to validate our method.

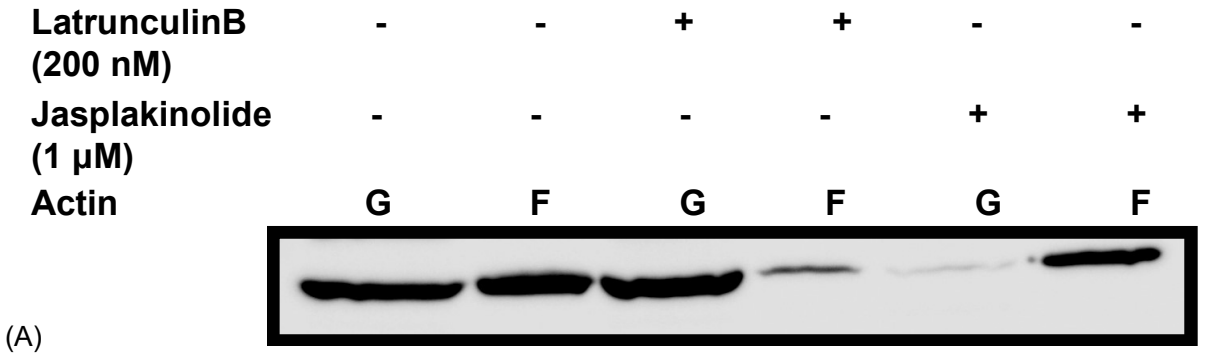

(A)

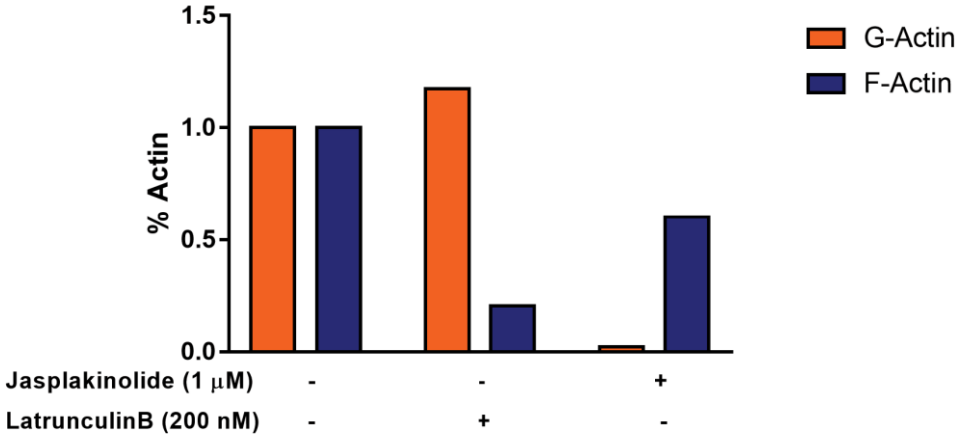

(B)

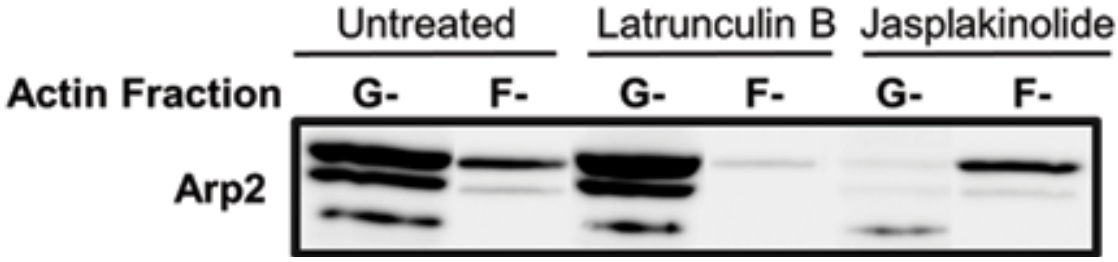

(C)

Figure 4.3 – Validation of F- and G- actin separation protocol using HeLa cells.
(A) Detection of actin after treatment with 200 nM Latrunculin B and 1µM Jasplakinolide, detected using rabbit anti actin. (B) Quantification of F and G actin present in the various fraction from A (C) Detection of Arp2 after treatment with 200 nM Latrunculin B and 1 µM Jasplakinolide detected using rabbit anti -Arp2.

As shown in the western blot above, there are approximately 50% G- and F-actin in the cells without any drug treatments. However, after the treatment with LatB, F-actin became depolymerized and the fraction of monomeric G-actin increases. A reverse effect is obtained using

treatment with Jasplakinolide in the western blots where the F-actin fraction is increased compared to G-actin. Additionally, we were able to detect the presence of Arp2 in our blot. Arp2 associates preferentially with F-actin and we were able to observe that in the presence of F-actin depolymerization agent (LatB), the presence of Arp2 was insignificant in F-actin fraction compared to G-actin fraction and reverse effect was seen in the presence of F-actin stabilization agent (Jasplakinolide) where a significant fraction of Arp2 was detected in F-actin fraction and not in G-actin fraction. From this data, we determined that we can successfully isolate G- and F-actin from cells.

2.3. Isolation of F and G actin from HeLa cells expressing CD36-BirA-Flag

F and G actin were isolated from HeLa cells stably expressing CD36-BirA-Flag. We treated the cells with 1 µg/mL doxycycline to induce expression of CD36-BirA-Flag. We then treated the cells with 100 µM biotin for 18 h and subjected the cell lysates to F- and G-actin separation. These G- and F-actin samples were separated, and biotinylated proteins were detected using streptavidin 680.

(A)

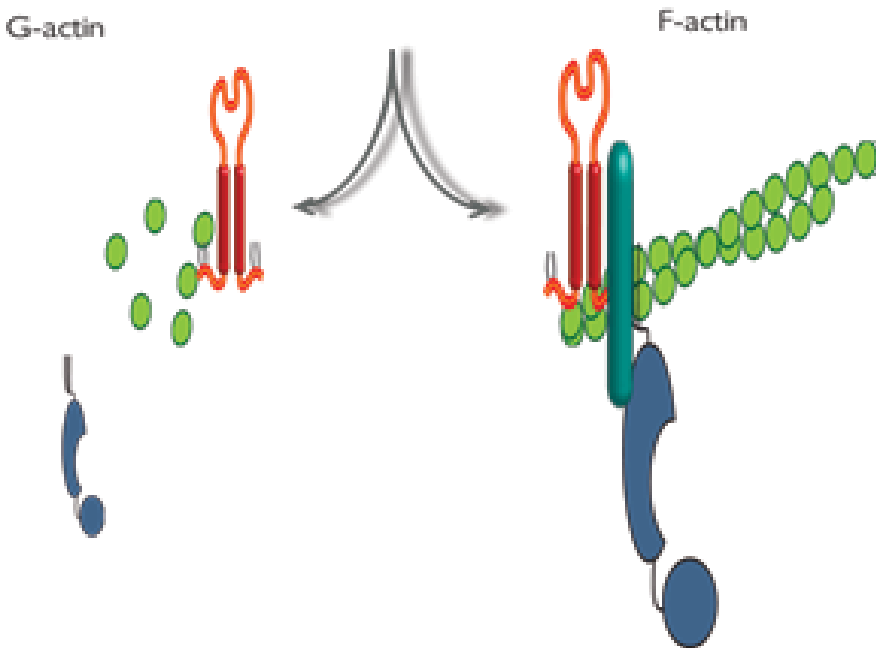

(B)

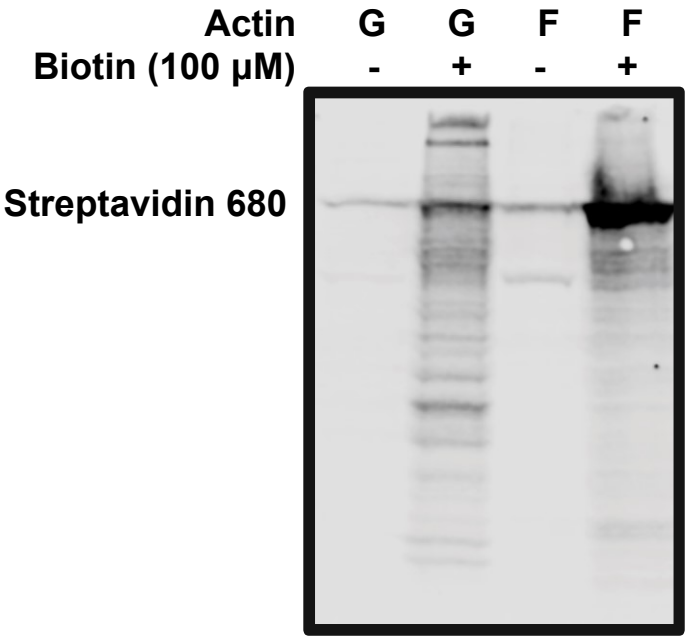

Figure 4.4 – Detection of biotinylated proteins in F- and G- actin fractions.
(A) Schematic of F and G actin separation (B) Detection of biotinylated proteins in F and G actin fractions in HeLa CD36-BirA-Flag.

As seen from the blot above, there were more biotinylated proteins in the G-actin fraction compared to F-actin fraction.

2.4. Identification of biotinylated proteins by Mass Spectrometry

To identify potential adaptor proteins using mass spectrometry, we proceeded to the purification of biotinylated proteins following F- and G- separation using streptavidin agarose resin. The procedure was carried out as described in Chapter 2 - 3.3. Before submitting the samples to mass spectrometry analysis, we first validated the separation of biotinylated proteins from the F- and G-actin fraction by western blot analysis using streptavidin-680 as shown below.

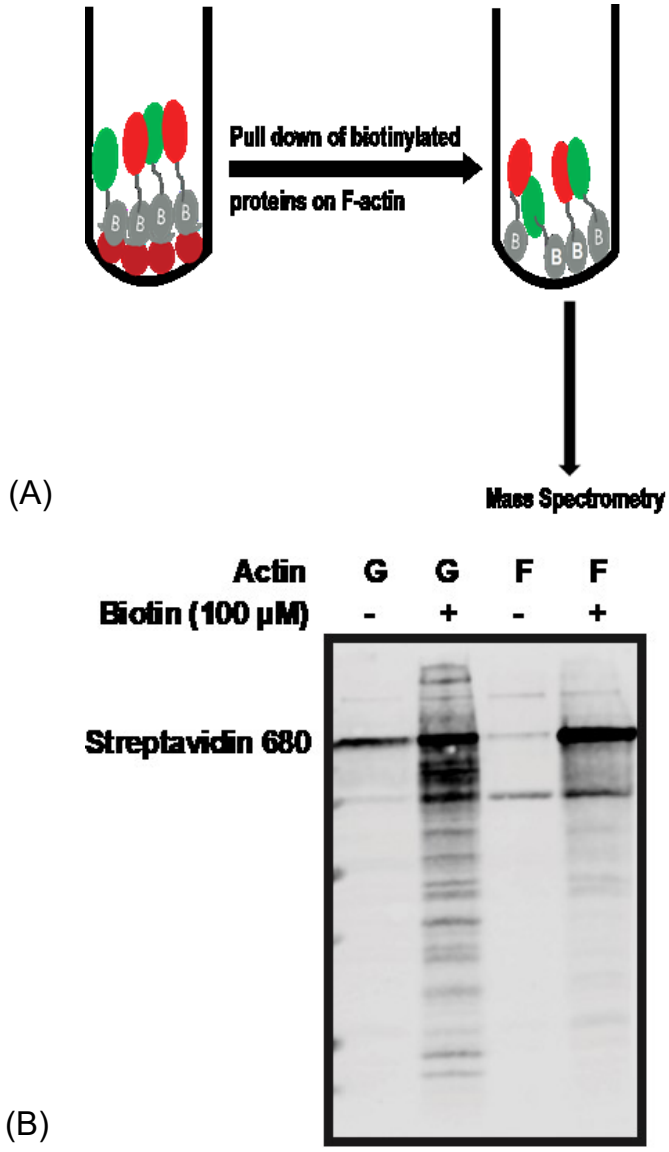

Figure 4.5 – Isolating biotinylated proteins from F and G- actin fractions.
(A) Schematic of protocol for the separation of biotinylated proteins from F- and G-actin fractions using streptavidin agarose resin. (B) Detection of biotinylated proteins on G- and F-actin fractions

enriched by streptavidin agarose resin.

We proceeded to the identification of the proteins present in the streptavidin pull-down in the F-actin fraction by mass spectrometry. Samples were processed by “on beads” digestion with trypsin in the Alberta Mass Spectrometry and Proteomics Facility and submitted for analysis. Results from the mass spectrometry analysis, identified 187 proteins from the 1st sample and 175 proteins in 2nd sample lysates containing CD36-BirA-Flag treated with biotin and segregated the F-actin fraction (see appendix for full list) (Table 2).

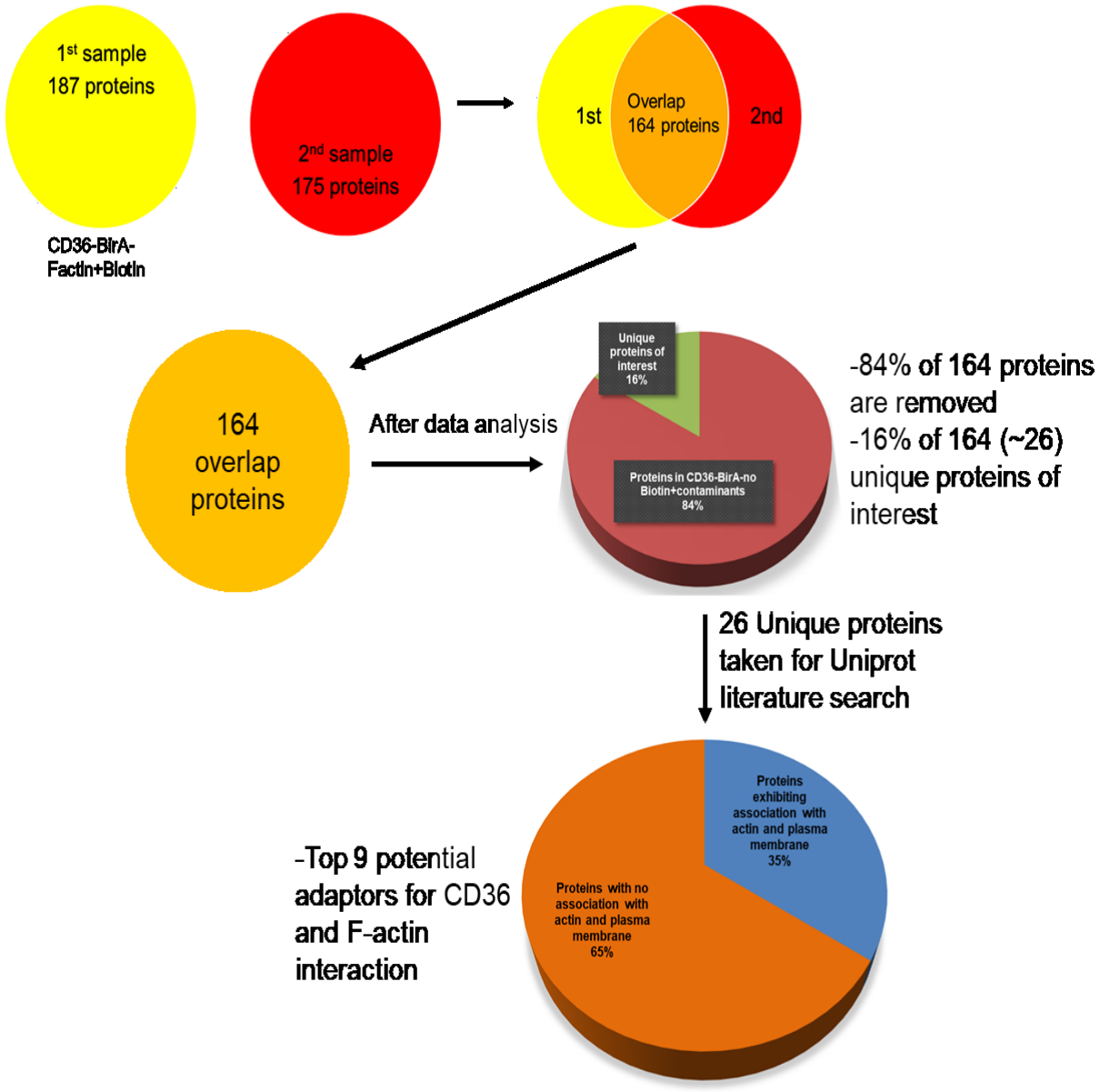

Figure 4.6 – Workflow of selecting potential candidates interacting with CD36 and F-actin.

The protein list was narrowed down to 164 after selecting proteins found in both duplicate experiments. Of these 164 proteins, the potential proteins were further narrowed down to 26 unique proteins after comparing to control samples (removing hits that were also found in the condition without biotin and BirA-Flag construct). These 26 proteins were further investigated using UniProt to explore if they were reported to have domains connecting to the plasma

membrane and/or the actin cytoskeleton. Finally, we narrowed down this list to 9 potential proteins.

Table 1 – Top 28 proteins narrowed down from mass spectrometry after comparing to the biotin treated and untreated samples.

	Description of Protein	Membrane Association	Actin Association	Comments
	Alpha-actinin-4	Yes	Yes- F actin crosslinking protein, anchor actin to various intracellular structure	Shown to interact with PDZ and LIM domain protein 1 (PDLIM1), brings actin to plasma membrane
	Ras GTPase-activating protein-binding protein 1	Yes-can be recruited to plasma membrane	Yes - focal adhesion	ATP binding, Ras protein signal transduction
	E3 ubiquitin-protein ligase UBR4	Yes	Yes - Clathrin, forms meshwork structures involved in membrane morphogenesis and cytoskeletal organization	Ubiquitin transferase activity, zinc ion binding
	PDZ and LIM domain protein 7	Yes- may be a scaffold for protein assembly	Yes-actin cytoskeleton organization	Zinc ion binding, scaffold protein, an adaptor for LIM binding domain
	Erythrocyte band 7 integral membrane protein	Yes-lipids rafts and cell membrane	Yes-colocalizes with cortical actin at small PM protrusions	Regulates ion channel activity and transmembrane ion transport
	Filamin-A	Yes- interacts with transmembrane receptor	Yes	Actin binding
	Plectin	Yes	Yes	Bind actin to plasma membrane in muscle

	Description of Protein	Membrane Association	Actin Association	Comments
	Ras GTPase-activating-like protein IQGAP1	Yes	Yes-scaffolding protein	Regulation of GTPases activity, Signal Transduction
	Talin-1	Yes	Yes-connection of major cytoskeletal structures to plasma membrane	LIM binding, platelet aggregation, expressed in HMEC cells (from previous mass spec run)
	LIM domain and actin-binding protein 1	Not sure	Yes- Actin filament bundle assembly, inhibits actin filament depolymerization	Zinc ion binding
	Inverted formin-2	Not sure	Yes-severs and accelerates actin polymerization	Interacts with LIM1, filamin, IQGAP
	Cytoplasmic dynein 1 light intermediate chain 1	No	Yes- microtubule cytoskeleton	Dynein to cargos and adaptor proteins
	Myosin-9	Not sure	Yes	Actin-binding, actin dependent ATP
	Clathrin heavy chain 1	Yes	No	Membrane organization, receptor-mediated endocytosis
	Sodium/potassium -transporting ATPase subunit alpha-1	Yes	No	Catalyzes ATP, sodium potassium exchange
	Transferrin receptor protein 1	Yes	Not sure	Glycoprotein binding, receptor mediated endocytosis, membrane organization

	Description of Protein	Membrane Association	Actin Association	Comments
	Glyceraldehyde-3-phosphate dehydrogenase	Yes-plasma membrane bound	Not sure	Oxidoreductase activity
	Matrin-3 (Fragment)	No - nuclear matrix protein	No	Nucleic acid binding, zinc ion binding
	Protein unc-45 homolog A	Not sure	No	Co-chaperon for HSP90
	Importin subunit alpha-3 (Fragment)	Not sure	No	Nuclear localization sequence binding
	Serine/threonine-protein phosphatase (Fragment)	Not sure	Not sure	Metal ion binding, phosphoprotein phosphatase activity
	Cullin-associated NEDD8-dissociated protein 1	Not sure	No	E3 ubiquitin ligase complexes
	Fatty acid synthase	No	No	Acyl carrier protein
	Myosin light polypeptide	Not sure	Not sure	Calcium ion binding
	E3 ubiquitin-protein ligase UBR5	Not sure	Not sure	Ubiquitin protein transferase activity
	AP-2 complex subunit beta	Maybe-clathrin adaptor complex	Not sure	vesicles mediated transport, intracellular protein transport

We established a procedure to identify protein in the vicinity of CD36 and connected to the F-actin cytoskeleton. Our preliminary work led us to pursue our investigations but with 2 major improvements. One is to establish this system in a native ECs environment. Therefore, we will carry out the same procedure in a novel model of ECs, named TIME cells. TIME cells are primary microvascular ECs, immortalized by maintenance of telomerase expression (hTERT) (Hayer et al., 2016; Lee et al., 2004). The advantage for using these cells over HMEC is that these cells allow maintenance of the primary ECs phenotype for much higher number of passages (Venetsanakos et al., 2002). Second, we have obtained from the group of Alice Ting (Stanford University, USA) a novel variant of BirA*, named miniTurbo, capable of biotinylation of proteins within minutes instead of hours. At the time of the preparation of this document, the verification and validation of the fusion between CD36 and miniTurbo are being performed.

3. Discussion

BioID or Proximity Dependent Biotin Identification has become an increasingly popular technique to elucidate protein-protein interaction network. BioID allows for the detection of potential interactions in their normal cellular context (Roux et al., 2012) and it circumvents the bait or prey solubility issues in techniques such as coimmunoprecipitation or pull-down assays (Roux et al., 2012). BioID can be used to detect both weak and transient interactions as biotinylation occurs before solubilization, hence, BioID is a suitable method to investigate the interacting partners of CD36 and cortical F-actin.

CD36 associates with F-actin and disruption of F-actin using Latrunculin B decrease the activation of Fyn in CD36 signaling (Githaka et al., 2016). The importance of F-actin in CD36-Fyn signaling led us to investigate the association of cortical F-actin with CD36 by screening for possible adaptor proteins using proximity dependent ligation assay, F- and G-actin fractionation, biotin pull-down and mass spectrometry protein identification.

The mass spectrometry search provided with a total of 212 proteins from duplicate experiments. In the sample containing biotin enriched with F-actin, there were approximately 187 proteins. From that we narrowed down the list to 164 proteins after selecting common proteins from duplicate experiments and eliminating the contaminants such as keratin as well as mitochondrial and nuclear proteins. The list was further narrowed to 26 unique proteins after comparison with control samples (without biotin). From these 26 proteins, we conducted a literature search and identified that 9 proteins have the potential to be our adaptor molecules between CD36 and F-actin. The top proteins in our list are alpha-actinin 4, Ras GTPase-activating protein-binding protein 1, E3 ubiquitin-protein ligase UBR4 (Table 1). These proteins have been revealed to associate with both plasma membrane and actin are alpha-actinin 4, Ras GTPase-activating protein-binding protein 1, E3 ubiquitin-protein ligase UBR4, PDZ and LIM domain protein 7, Erythrocyte band 7 integral membrane protein, Filamin-A, Plectin, Ras GTPase-activating-like protein IQGAP1 and Talin-1. For instance, alpha-actinin-4 has been shown to be regulated by PI(4,5)P2 (Sechi and Wehland, 2000), Ras GTPase-activating protein-binding protein 1 can be recruited to the plasma membrane in exponentially growing cells although the binding partners and mechanism have yet to be elucidated (Tourrière et al., 2003), studies have suggested that PDZ domain of PDZ and LIM domain protein 7 has the capability to associate with the plasma membrane (Fanning and Anderson, 1999) often involve in spatial clustering and anchoring of transmembrane receptors within specific subcellular domain which was demonstrated by coclustering of PDZ domain of PSD-95 and ligand of Shaker K+ on the cell surface (Kim et al., 1995), Erythrocyte band 7 integral membrane protein has been reported to colocalize with actin cytoskeleton at the plasma membrane protrusion (Snyers et al., 1997), Filamin A and Plectin-1 have been shown to associate with plasma membrane and/or transmembrane proteins (Adams et al., 2011; Koster et al., 2003) where Talin-1 has been annotated to bind to PS and PI (UniProt Consortium, 2014) and at last, IQGAP1 has been documented to bind to PI(3,4,5)P3 (Dixon et al., 2012).

We predict that these proteins listed in Table 1 may connect CD36 and F-actin either in direct or indirect manner. Proteins such as PDZ and LIM domain protein 1 and Ras GTPase activating like protein 1 (IQGAP) are known as scaffolding proteins interacting with proteins such as alpha-actinin -4 and activated Cdc42. These proteins may perhaps serve as an assembly scaffold for the organization of a multimolecular complex that would interface incoming signals to the reorganization of the actin cytoskeleton at the plasma membrane.

The first possible candidate, alpha-actinin 4 is an F-actin cross linking protein which is believed to anchor actin to the various intracellular structures (Saarikangas et al., 2010). Alpha-actinin 4 is a non-muscle alpha-actinin isoform which is concentrated in the cytoplasm and appears to be involved in binding actin to the membrane (Feng et al., 2016; Honda et al., 1998). In the case of CD36 and F-actin, alpha-actinin 4 could either directly mediate the association between CD36 and F-actin or it could provide indirect association by instead binding to other F-actin binding protein such as PDZ and LIM1 domain protein (PDLIM1) (Rual et al., 2005) and form a complex mediating the association of F-actin to CD36. Aside from binding to actin filaments, alpha-actinin connects to a variety of cytoskeletal and signaling molecule and cytoplasmic domains of transmembrane receptor and ion channels (Sjöblom et al., 2008). One of the features of alpha-actinin regulation is the role of phosphoinositides although the mechanism of this regulation remains unclear. Alpha-actinin 4 possess a calponin homology 2 domain which can bind to PI(4,5)P2 and PI(3,4,5)P3 and modulate its interaction with cortical F-actin and integrin receptors (Fraley et al., 2003; Fraley et al., 2005). PI(4,5)P2 promotes stability of alpha-actinin whereas PI(3,4,5)P3 reduces the stability of alpha-actinin (Full et al., 2007). It has been suggested that PI(4,5)P2 and PI(3,4,5)P3 regulate the structure and flexibly of alpha-actinin (Sprague et al., 2008).

Interestingly, we were also able to identify proteins which do not show clear association with both the plasma membrane and actin such as Fatty Acid Synthase. Fatty Acid Synthase (FAS) is

a multi-enzyme protein that catalyzes the fatty acid synthesis (Smith et al., 2003). The direct association of FAS and CD36 has not been reported, however, Febbraio et al.,1999 has shown that reducing FAS decreases the expression of CD36 in adipocytes. CD36 expression in adipocytes and involvement in uptake of oxidized low-density lipoprotein (oxLDL) may be contributing to the CD36 association with FAS (Febbraio et al., 1999). However, this interaction needs to be further verified before we can make positive conclusions about this association. Using BioID combined with mass spectrometry requires a stringent method to narrow down candidate proteins, hence as a control, we employed BirF construct which is not attached to CD36, however, still have the capacity to biotinylate proteins near BirF construct (in cytosol and on plasma membrane). The proteins obtained from BirF construct (proteins not surrounding CD36) were then used to eliminate proteins from our CD36-BirA-Flag construct, thus providing us with more reliable list of candidate proteins.

Finally, we expect to implement this screening method in endothelial cells (TIME cells) to obtain proteins that are specific for endothelial cells. Specificity of cells and tissues are one of the most important factors in studying protein-protein interaction. As CD36 is not endogenously expressed in HeLa cells, we suspect we may potentially be missing some important CD36 interacting proteins upon biotinylation. For instance, Fyn which is a known downstream kinase of CD36 is widely expressed in microvascular endothelial cells, however, it is not expressed in HeLa cells. Therefore, it is possible that the adaptor protein we are looking for is expressed in TIME cells and not in HeLa cells.

Additionally, we hope to use different versions of BioID (TurboID and mini Turbo) in TIME cells. TurboID and miniTurbo are 2 variants of BirA* developed by Dr. Alice Ting's lab at Stanford University and they apply the same biotinylation principle as BioID. The main difference between TurboID and mini Turbo is the length of these constructs and signal to background ratio (Branon et al., 2017). TurboID (35 kD) was constructed based off the full-length BioID enzyme which

makes it longer than mini Turbo (28 kD) and it has high background activity and it is not suitable for experiments with temporal sensitivity (Branon et al., 2017). Some of the advantages of these constructs over BioID is that they only require shorter biotinylation time (~10 min) and utilize less biotin. These techniques are more suited to better resolved temporally protein-protein interaction compared to conventional BioID (Branon et al., 2017). In collaboration with Dr. Alice Ting's lab, we have generated constructs, CD36-TurboID-Flag and CD36-miniTurbo-Flag, in our lentiviral and tetracycline inducible system and we will be soon starting to generate a stable cell line in dermal microvascular endothelial cells (TIME cells). By using this system, we would be able to screen proteins that are recruited upon TSP-1 stimulation of CD36 and compare to the un-ligated state. This evaluation would provide us with proteins that are transiently recruited during TSP-1 stimulation and a much clearer picture of CD36 signaling in endothelial cells upon TSP-1 stimulation. We hope to identify novel interactors of CD36 and F-actin during both with or without TSP-1 stimulation using this approach.

4. References

Adams, M., Simms, R.J., Abdelhamed, Z., Dawe, H.R., Szymanska, K., Logan, C.V., Wheway, G., Pitt, E., Gull, K., and Knowles, M.A. (2011). A meckelin–filamin A interaction mediates ciliogenesis. Hum. Mol. Genet. *21,* 1272-1286.

Branon, T.C., Bosch, J.A., Sanchez, A.D., Udeshi, N.D., Svinkina, T., Carr, S.A., Feldman, J.L., Perrimon, N., and Ting, A.Y. (2017). Directed evolution of TurboID for efficient proximity labeling in living cells and organisms. bioRxiv 196980.

Dixon, M.J., Gray, A., Schenning, M., Agacan, M., Tempel, W., Tong, Y., Nedyalkova, L., Park, H., Leslie, N.R., and Van Aalten, D.M. (2012). IQGAP proteins reveal an atypical phosphoinositide (aPI) binding domain with a pseudo C2 domain fold. J. Biol. Chem. *287,* 22483-22496.

Fanning, A.S., and Anderson, J.M. (1999). PDZ domains: fundamental building blocks in the organization of protein complexes at the plasma membrane. J. Clin. Invest. *103,* 767-772.

Febbraio, M., Abumrad, N.A., Hajjar, D.P., Sharma, K., Cheng, W., Pearce, S.F.A., and Silverstein, R.L. (1999). A null mutation in murine CD36 reveals an important role in fatty acid and lipoprotein metabolism. J. Biol. Chem. *274,* 19055-19062.

Feng, D., Steinke, J.M., Krishnan, R., Birrane, G., and Pollak, M.R. (2016). Functional Validation of an Alpha-Actinin-4 Mutation as a Potential Cause of an Aggressive Presentation of Adolescent Focal Segmental Glomerulosclerosis: Implications for Genetic Testing. PloS One *11,* e0167467.

Fraley, T.S., Pereira, C.B., Tran, T.C., Singleton, C., and Greenwood, J.A. (2005). Phosphoinositide binding regulates α-actinin dynamics mechanism for modulating cytoskeletal remodeling. J. Biol. Chem. *280,* 15479-15482.

Fraley, T.S., Tran, T.C., Corgan, A.M., Nash, C.A., Hao, J., Critchley, D.R., and Greenwood, J.A. (2003). Phosphoinositide binding inhibits α-actinin bundling activity. J. Biol. Chem. *278,* 24039-24045.

Full, S.J., Deinzer, M.L., Ho, P.S., and Greenwood, J.A. (2007). Phosphoinositide binding regulates α-actinin CH2 domain structure: Analysis by hydrogen/deuterium exchange mass spectrometry. Protein Science *16,* 2597-2604.

Githaka, J.M., Vega, A.R., Baird, M.A., Davidson, M.W., Jaqaman, K., and Touret, N. (2016). Ligand-induced growth and compaction of CD36 nanoclusters enriched in Fyn induces Fyn signaling. J. Cell. Sci. *129,* 4175-4189.

Gossen, M., and Bujard, H. (1992). Tight control of gene expression in mammalian cells by tetracycline-responsive promoters. Proceedings of the National Academy of Sciences *89,* 5547-5551.

Gossen, M., Freundlieb, S., Bender, G., Muller, G., Hillen, W., and Bujard, H. (1995). Transcriptional activation by tetracyclines in mammalian cells. Science *268,* 1766-1769.

Hayer, A., Shao, L., Chung, M., Joubert, L., Yang, H.W., Tsai, F., Bisaria, A., Betzig, E., and Meyer, T. (2016). Engulfed cadherin fingers are polarized junctional structures between collectively migrating endothelial cells. Nat. Cell Biol. *18,* 1311.

Honda, K., Yamada, T., Endo, R., Ino, Y., Gotoh, M., Tsuda, H., Yamada, Y., Chiba, H., and Hirohashi, S. (1998). Actinin-4, a novel actin-bundling protein associated with cell motility and cancer invasion. J. Cell Biol. *140,* 1383-1393.

Kim, E., Niethammer, M., Rothschild, A., Jan, Y.N., and Sheng, M. (1995). Clustering of Shaker-type K channels by interaction with a family of membrane-associated guanylate kinases. Nature *378,* 85.

Koster, J., Geerts, D., Favre, B., Borradori, L., and Sonnenberg, A. (2003). Analysis of the interactions between BP180, BP230, plectin and the integrin α6β4 important for hemidesmosome assembly. J. Cell. Sci. *116,* 387-399.

Lee, K.M., Choi, K.H., and Ouellette, M.M. (2004). Use of exogenous hTERT to immortalize primary human cells. Cytotechnology *45,* 33-38.

Myers, K.R., and Casanova, J.E. (2008). Regulation of actin cytoskeleton dynamics by Arf-family GTPases. Trends Cell Biol. *18,* 184-192.

Roux, K.J., Kim, D.I., Burke, B., and May, D.G. (2013). BioID: a screen for protein-protein interactions. Current Protocols in Protein Science 19.23. 15.

Roux, K.J., Kim, D.I., Raida, M., and Burke, B. (2012). A promiscuous biotin ligase fusion protein identifies proximal and interacting proteins in mammalian cells. J. Cell Biol. *196,* 801-810.

Rual, J., Venkatesan, K., Hao, T., Hirozane-Kishikawa, T., Dricot, A., Li, N., Berriz, G.F., Gibbons, F.D., Dreze, M., and Ayivi-Guedehoussou, N. (2005). Towards a proteome-scale map of the human protein–protein interaction network. Nature *437,* 1173.

Saarikangas, J., Zhao, H., and Lappalainen, P. (2010). Regulation of the actin cytoskeleton-plasma membrane interplay by phosphoinositides. Physiol. Rev. *90,* 259-289.

Sechi, A.S., and Wehland, J. (2000). The actin cytoskeleton and plasma membrane connection: PtdIns (4, 5) P (2) influences cytoskeletal protein activity at the plasma membrane. J. Cell. Sci. *113,* 3685-3695.

Sjöblom, B., Salmazo, A., and Djinović-Carugo, K. (2008). α-Actinin structure and regulation. Cellular and Molecular Life Sciences *65,* 2688.

Smith, S., Witkowski, A., and Joshi, A.K. (2003). Structural and functional organization of the animal fatty acid synthase. Prog. Lipid Res. *42,* 289-317.

Snyers, L., Thines-Sempoux, D., and Prohaska, R. (1997). Colocalization of stomatin (band 7.2 b) and actin microfilaments in UAC epithelial cells. Eur. J. Cell Biol. *73,* 281-285.

Sprague, C.R., Fraley, T.S., Jang, H.S., Lal, S., and Greenwood, J.A. (2008). Phosphoinositide binding to the substrate regulates susceptibility to proteolysis by calpain. J. Biol. Chem. *283,* 9217-9223.

Tourrière, H., Chebli, K., Zekri, L., Courselaud, B., Blanchard, J.M., Bertrand, E., and Tazi, J. (2003). The RasGAP-associated endoribonuclease G3BP assembles stress granules. J. Cell Biol. *160,* 823-831.

UniProt Consortium. (2014). UniProt: a hub for protein information. Nucleic Acids Res. *43,* D212.

Venetsanakos, E., Mirza, A., Fanton, C., Romanov, S.R., Tlsty, T., and McMahon, M. (2002). Induction of tubulogenesis in telomerase-immortalized human microvascular endothelial cells by glioblastoma cells. Exp. Cell Res. *273,* 21-33.

Chapter 5 - **Conclusion and Future Directions**

1. Role of PI(4,5)P2 and PI(3,4,5)P3 in CD36 organization and activation of Fyn

Investigating the association of lipid nanodomains in TSP-1 mediated CD36-Fyn signaling began with the identification of inner leaflet lipids of the plasma membrane enriched in CD36 nanoclusters. We identified that phosphoinositides, PS, PI(4,5)P2 and PI(3,4,5)P3 in the inner leaflet of the plasma membrane are associated with CD36 nanoclusters. CD36 nanoclusters are enriched with PI(4,5)P2 at a steady state and the enrichment shift to domains containing PIP3 upon TSP-1 stimulation. Additionally, we saw no changes in the enrichment of PS upon TSP-1 stimulation. The concomitant decrease of PIP2 and increase of PIP3 following TSP-1 stimulation led us propose a role for PI3-Kinase in this conversion. Therefore, we investigated the role of PI3K (a kinase responsible for phosphorylation of PIP2 to PIP3).

We studied the role of PI3K in Fyn activation as well as in CD36 nanoclusters enhancements using PI3K inhibitor (LY294002). Our data demonstrated that PIP3 production by PI3K is important for CD36 nanoclusters enhancement upon initiation with TSP-1 and for downstream Fyn activation in endothelial cells. However, it was difficult to distinguish if the decrease in Fyn activation is caused by the inhibition of CD36 nanocluster enhancement. Therefore, we designed a technique (based on LARIAT, see section Chapter 3 - 2.8, page 70) that allowed us to artificially cluster CD36 and studied the effects of PI3K inhibitor on Fyn activation. By using this system, we were able to activate Fyn in CD36 clusters that are artificially induced. Furthermore, this activation was blocked by the PI3Kinase inhibitor. Our data demonstrated that PI3K is important for Fyn activation even after artificial enhancement of CD36 clusters, suggesting that the phosphoinositide (PIP3) is responsible of Fyn activation downstream of cluster enhancement. While, the mechanism of this finding is not fully understood (how is PIP3 responsible for Fyn activation?), we can confirm that inner leaflet lipids PIP2 and PIP3 serve as crucial mediators in CD36 nanoclusters organization on the plasma membrane and downstream Fyn signaling (Figure 5.1). Our findings have provided the groundwork for understanding plasma membrane organization and signal transduction of membrane receptors that lack signaling capacity such as CD36.

Though, the mechanism of Fyn activation was not well established in this study, we propose two mechanisms that could be result in the activation of Fyn in CD36 nanoclusters for future study. We hypothesized that activation of Fyn in CD36 clusters could be taking place in two possible mechanisms. 1) After recruitment of PI3K to CD36 nanoclusters upon TSP-1 stimulation, p85 subunit of PI3K3 engaged with SH2 domain of Fyn which could relief the intermolecular inhibition and thus in turns leads to Fyn activation. Activated Fyn then not only phosphorylates downstream targets p38MAPK and p130Cas involved in anti-angiogenic pathway but also activates Vav protein which was recruited by production of PIP3. Vav protein binding to PIP3 becomes activated

which expose additional phosphorylation site at Tyr 174 by Src Family Kinase Member such as Fyn and leads to cytoskeletal re-arrangement in mechanism 1 (Figure 5.2). 2) The production of PIP3 at the membrane upon TSP-1 activation could affect the lipids organization within CD36 nanoclusters possibly partitioning CD36 clusters into specialized membrane domains (enriched in cholesterol). This would allow for interaction with other molecules such as protein phosphatases, particularly, RPTPα which has been reported to localize in specialized membrane domain and dephosphorylate the inhibitory phosphorylation at Tyr 531 and activating Fyn in Mechanism 2 (Figure 5.3) and allow for interaction with p85 subunit of PI3K.

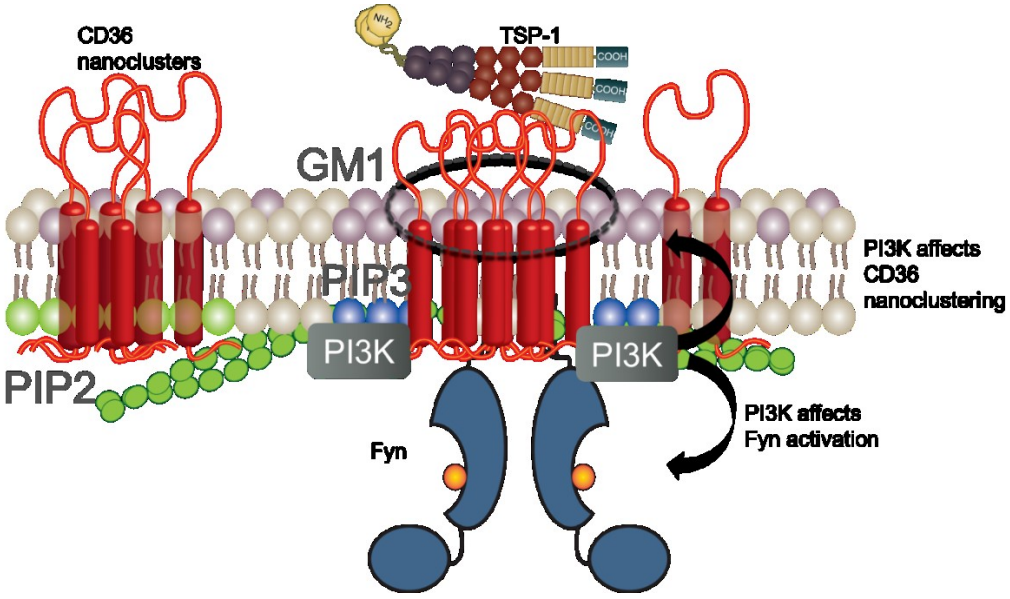

Figure 5.1 – Proposed model demonstrating the role of PI3K in CD36 nanocluster enhancements and Fyn activation on the plasma membrane.
At basal state, CD36 nanoclusters are enriched with PI(4,5)P2 in the inner leaflet and GM1 on the outer leaflet of the plasma membrane. This organization also occurs at the sites enriched with cortical F-actin. Upon TSP-1 stimulation, CD36 nanoclusters size and density significantly increases and engage with PI3K at the inner leaflet to phosphorylate PI(4,5)P2 to PI(3,4,5)P3. Production of PI(3,4,5)P3 by PI3K allows CD36 nanocluster enhancements and activation of downstream kinase Fyn.

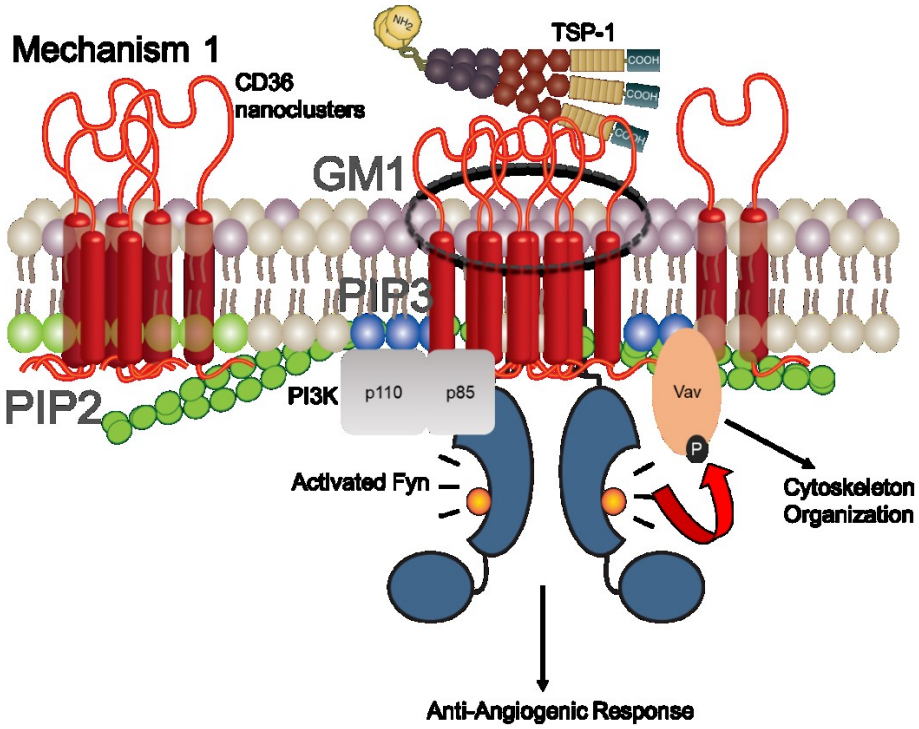

Figure 5.2 – Proposed mechanism 1 proposing Fyn activation within CD36 nanoclusters achieved by interaction of Fyn SH2 domain with p85 subunit of PI3K.

This model proposes that the mechanism of Fyn activation within CD36 nanoclusters upon TSP-1 stimulation occurs when p85 subunit of PI3K associates with SH2 domain of Fyn and hence activating Fyn by relieving the intermolecular constraints. Simultaneously, production of PI(3,4,5)P3 at the plasma membrane recruits Vav protein (RacGTPase) and re-arranges intermolecular interaction of Vav and becomes active by unloading GDP and loading GTP and trigger Rac signaling pathway for cytoskeleton organization. The rearrangement of intermolecular interaction of Vav by binding to PI(3,4,5)P3 exposes additional phosphorylation site at Tyr 174 which can then be phosphorylated by Fyn.

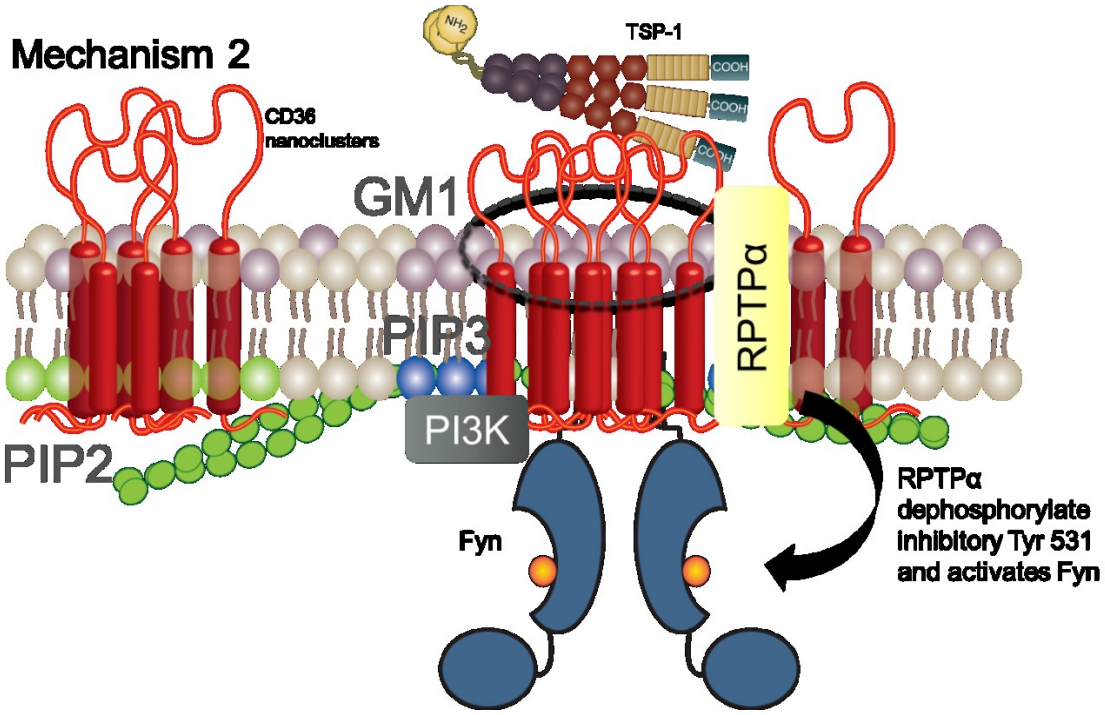

Figure 5.3 – Proposed mechanism 2 proposing activation of Fyn within CD36 nanocluster achieved by association with RPTPα.

This model proposes that upon TSP-1 stimulation, engagement of PI3K and production of PI(3,4,5)P3 at the membrane alter membrane organization of CD36 nanoclusters and enhancement, possibly, recruiting molecules or positioning CD36 nanoclusters into specialized microdomains enriched with cholesterol. This allows for interaction of CD-36-Fyn with transmembrane receptor tyrosine phosphatases that are present in the domains such as RPTPα or other tyrosine phosphatases get recruited to the site of clustering and dephosphorylate Tyr 531 (inhibitory) in Fyn which lead to phosphorylation at Tyr420 and hence activating Fyn.

1.1. Future Directions

We hope to test these possible mechanisms of Fyn activation by first demonstrating the PIP3 production in artificially induced CD36 clusters and the effects of inhibiting PI3K. We will then conduct experiments showing p85 subunits of PI3K interacts with SH2 domain of Fyn and hence activating Fyn and show recruitment of Vav protein to PIP3. Furthermore, we will test if Fyn can phosphorylate Vav protein at Tyr 174. For mechanism 2, we will test if the RPTPα can dephosphorylate inhibitory Tyr at 531. We also hope to further investigate the plasma membrane

organization of CD36 nanoclusters using selective depletion of PIP2 and synthesis of PIP3 at the membrane by light induced heterodimerization system.

2. Identification of potential adaptor proteins in CD36 nanoclusters and F-actin organization

To identify proteins that associate with CD36 and F-actin, we employed BioID proximity labeling method in HeLa cells expressing CD36 and used mass spectrometry for characterization. We have been able to identify 9 potential proteins specifically alpha-actinin-4, Ras GTPase-activating protein-binding protein 1, E3 ubiquitin-protein ligase UBR4 and many more (Table 1) in HeLa cells stably expressing CD36-BirA-Flag. We proposed that these proteins associate with CD36 and F-actin via direct and indirect interactions and we hope to validate these proteins after implementing similar system in endothelial cells which is highlighted in future directions.

2.1. Future Directions

To characterize proteins that are cell-specific, we hope to create a stable cell line in TIME cells (Dermal Microvascular Endothelium) expressing different versions of BioID (TurboID and mini Turbo) which are suited for temporally resolved experiments than conventional BioID. After construction of these cell lines, we would subject the samples to TSP-1 activation and crosslinking to identify proteins that are transiently associated with CD36 as well as F-actin. These isolated proteins will be then identified using mass spectrometry. This study will provide more information to understand the role of cortical F-actin cytoskeleton in CD36 organization on the membrane.

Bibliography

Abumrad, N.A., El-Maghrabi, M.R., Amri, E.Z., Lopez, E., and Grimaldi, P.A. (1993). Cloning of a rat adipocyte membrane protein implicated in binding or transport of long-chain fatty acids that is induced during preadipocyte differentiation. Homology with human CD36. J. Biol. Chem. *268,* 17665-17668.

Alberts, B., Johnson, A., Lewis, J., Raff, M., Roberts, K., and Walter, P. (2002). Molecular Biology of the Cell, (Garland Science, New York, 2008). Google Scholar 652.

Amata, I., Maffei, M., and Pons, M. (2014). Phosphorylation of unique domains of Src family kinases. Frontiers in Genetics *5,* 181.

Asch, A.S., Liu, I., Briccetti, F.M., Barnwell, J.W., Kwakye-Berko, F., Dokun, A., Goldberger, J., and Pernambuco, M. (1993). Analysis of CD36 binding domains: ligand specificity controlled by dephosphorylation of an ectodomain. Science *262,* 1436-1440.

Baenziger, N.L., Brodie, G.N., and Majerus, P.W. (1971). A thrombin-sensitive protein of human platelet membranes. Proceedings of the National Academy of Sciences *68,* 240-243.

Bohdanowicz, M., and Grinstein, S. (2013). Role of phospholipids in endocytosis, phagocytosis, and macropinocytosis. Physiol. Rev. *93,* 69-106.

Bruce, A., Johnson, A., Lewis, J., Raff, M., Roberts, K., and Walter, P. (2007). Molecular Biology of the Cell 5th edn (New York: Garland Science).

Chu, L., and Silverstein, R.L. (2012). CD36 ectodomain phosphorylation blocks thrombospondin-1 binding: structure-function relationships and regulation by protein kinase C. Arterioscler. Thromb. Vasc. Biol. *32,* 760-767.

Coronas, S., Ramel, D., Pendaries, C., Gaits-Iacovoni, F., Tronchere, H., and Payrastre, B. Paper presented at Biochemical Society Symposia.

Czech, M.P. (2003). Dynamics of phosphoinositides in membrane retrieval and insertion. Annu. Rev. Physiol. *65,* 791-815.

D'Angelo, G., Vicinanza, M., Di Campli, A., and De Matteis, M.A. (2008). The multiple roles of PtdIns (4) P–not just the precursor of PtdIns (4, 5) P2. J. Cell. Sci. *121,* 1955-1963.

Dawson, D.W., Pearce, S.F.A., Zhong, R., Silverstein, R.L., Frazier, W.A., and Bouck, N.P. (1997). CD36 mediates the in vitro inhibitory effects of thrombospondin-1 on endothelial cells. J. Cell Biol. *138,* 707-717.

Di Paolo, G., and De Camilli, P. (2006). Phosphoinositides in cell regulation and membrane dynamics. Nature *443,* 651.

Doughman, R.L., Firestone, A.J., and Anderson, R.A. (2003). Phosphatidylinositol phosphate kinases put PI4, 5P 2 in its place. J. Membr. Biol. *194,* 77-89.

Dove, S.K., Dong, K., Kobayashi, T., Williams, F.K., and Michell, R.H. (2009). Phosphatidylinositol 3, 5-bisphosphate and Fab1p/PIKfyve underPPIn endo-lysosome function. Biochem. J. *419,* 1-13.

Esemuede, N., Lee, T., Pierre-Paul, D., Sumpio, B.E., and Gahtan, V. (2004). The role of thrombospondin-1 in human disease1. J. Surg. Res. *122,* 135-142.

Falkenburger, B.H., Jensen, J.B., Dickson, E.J., Suh, B., and Hille, B. (2010). Symposium Review: Phosphoinositides: lipid regulators of membrane proteins. J. Physiol. (Lond.) *588,* 3179-3185.

Febbraio, M., Hajjar, D.P., and Silverstein, R.L. (2001). CD36: a class B scavenger receptor involved in angiogenesis, atherosclerosis, inflammation, and lipid metabolism. J. Clin. Invest. *108,* 785-791.

Freeman, S.A., Vega, A., Riedl, M., Collins, R.F., Ostrowski, P.P., Woods, E.C., Bertozzi, C.R., Tammi, M.I., Lidke, D.S., and Johnson, P. (2018). Transmembrane Pickets Connect Cyto-and Pericellular Skeletons Forming Barriers to Receptor Engagement. Cell *172,* 317. e10.

Geli, M.I., and Riezman, H. (1998). Endocytic internalization in yeast and animal cells: similar and different. J. Cell. Sci. *111,* 1031-1037.

Githaka, J.M., Vega, A.R., Baird, M.A., Davidson, M.W., Jaqaman, K., and Touret, N. (2016). Ligand-induced growth and compaction of CD36 nanoclusters enriched in Fyn induces Fyn signaling. J. Cell. Sci. *129,* 4175-4189.

Goodridge, H.S., Underhill, D.M., and Touret, N. (2012). Mechanisms of Fc Receptor and Dectin-1 Activation for Phagocytosis. Traffic *13,* 1062-1071.

Gruarin, P., Sitia, R., and Alessio, M. (1997). Formation of one or more intrachain disulphide bonds is required for the intracellular processing and transport of CD36. Biochem. J. *328,* 635.

Gruarin, P., Thorne, R.F., Dorahy, D.J., Burns, G.F., Sitia, R., and Alessio, M. (2000). CD36 is a ditopic glycoprotein with the N-terminal domain implicated in intracellular transport. Biochem. Biophys. Res. Commun. *275,* 446-454.

Gunning, P.W., Ghoshdastider, U., Whitaker, S., Popp, D., and Robinson, R.C. (2015). The evolution of compositionally and functionally distinct actin filaments. J. Cell. Sci. *128,* 2009-2019.

Hagelberg, C., and Allan, D. (1990). Restricted diffusion of integral membrane proteins and polyphosphoinositides leads to their depletion in microvesicles released from human erythrocytes. Biochem. J. *271,* 831.

Hilpelä, P., Vartiainen, M.K., and Lappalainen, P. (2004). Regulation of the actin cytoskeleton by PI (4, 5) P 2 and PI (3, 4, 5) P 3. In Phosphoinositides in Subcellular Targeting and Enzyme Activation, Springer) pp. 117-163.

Hisatsune, C., Kuroda, Y., Nakamura, K., Inoue, T., Nakamura, T., Michikawa, T., Mizutani, A., and Mikoshiba, K. (2004). Regulation of TRPC6 channel activity by tyrosine phosphorylation. J. Biol. Chem. *279,* 18887-18894.

Ho, C.Y., Alghamdi, T.A., and Botelho, R.J. (2012). Phosphatidylinositol-3, 5-Bisphosphate: No Longer the Poor PIP2. Traffic *13,* 1-8.

Ho, M., Hoang, H.L., Lee, K.M., Liu, N., MacRae, T., Montes, L., Flatt, C.L., Yipp, B.G., Berger, B.J., and Looareesuwan, S. (2005). Ectophosphorylation of CD36 regulates cytoadherence of Plasmodium falciparum to microvascular endothelium under flow conditions. Infect. Immun. *73,* 8179-8187.

Hoosdally, S.J., Andress, E.J., Wooding, C., Martin, C.A., and Linton, K.J. (2009). The human scavenger receptor CD36 glycosylation status and its role in trafficking and function. J. Biol. Chem. *284,* 16277-16288.

Huntington, N.D., and Tarlinton, D.M. (2004). CD45: direct and indirect government of immune regulation. Immunol. Lett. *94,* 167-174.

Ikonomov, O.C., Sbrissa, D., and Shisheva, A. (2001). Mammalian cell morphology and endocytic membrane homeostasis require enzymatically active phosphoinositide 5-kinase PIKfyve. J. Biol. Chem. *276,* 26141-26147.

Jaffe, A.B., and Hall, A. (2005). Rho GTPases: biochemistry and biology. Annu.Rev.Cell Dev.Biol. *21,* 247-269.

Jaqaman, K., Kuwata, H., Touret, N., Collins, R., Trimble, W.S., Danuser, G., and Grinstein, S. (2011). Cytoskeletal control of CD36 diffusion promotes its receptor and signaling function. Cell *146,* 593-606.

Jaqaman, K., Loerke, D., Mettlen, M., Kuwata, H., Grinstein, S., Schmid, S.L., and Danuser, G. (2008). Robust single-particle tracking in live-cell time-lapse sequences. Nature Methods *5,* 695.

Jimenez, B., Volpert, O.V., Crawford, S.E., Febbraio, M., Silverstein, R.L., and Bouck, N. (2000). Signals leading to apoptosis-dependent inhibition of neovascularization by thrombospondin-1. Nat. Med. *6,* 41.

Jimenez, B., Volpert, O.V., Reiher, F., Chang, L., Munoz, A., Karin, M., and Bouck, N. (2001). c-Jun N-terminal kinase activation is required for the inhibition of neovascularization by thrombospondin-1. Oncogene *20,* 3443.

Kalay, Z., Fujiwara, T.K., Otaka, A., and Kusumi, A. (2014). Lateral diffusion in a discrete fluid membrane with immobile particles. Physical Review E *89,* 022724.

Karathanassis, D., Stahelin, R.V., Bravo, J., Perisic, O., Pacold, C.M., Cho, W., and Williams, R.L. (2002). Binding of the PX domain of p47phox to phosphatidylinositol 3, 4-bisphosphate and phosphatidic acid is masked by an intramolecular interaction. Embo J. *21,* 5057-5068.

Klenotic, P.A., Page, R.C., Li, W., Amick, J., Misra, S., and Silverstein, R.L. (2013). Molecular Basis of Antiangiogenic Thrombospondin-1 Type 1 Repeat Domain Interactions With CD36Significance. Arterioscler. Thromb. Vasc. Biol. *33,* 1655-1662.

Klenotic, P.A., Page, R.C., Misra, S., and Silverstein, R.L. (2011). Expression, purification and structural characterization of functionally replete thrombospondin-1 type 1 repeats in a bacterial expression system. Protein Expr. Purif. *80,* 253-259.

Koldsø, H., and Sansom, M.S. (2015). Organization and dynamics of receptor proteins in a plasma membrane. J. Am. Chem. Soc. *137,* 14694-14704.

Kusumi, A., Fujiwara, T.K., Chadda, R., Xie, M., Tsunoyama, T.A., Kalay, Z., Kasai, R.S., and Suzuki, K.G. (2012). Dynamic organizing principles of the plasma membrane that regulate signal transduction: commemorating the fortieth anniversary of Singer and Nicolson's fluid-mosaic model. Annu. Rev. Cell Dev. Biol. *28,* 215-250.

Kusumi, A., Nakada, C., Ritchie, K., Murase, K., Suzuki, K., Murakoshi, H., Kasai, R.S., Kondo, J., and Fujiwara, T. (2005). Paradigm shift of the plasma membrane concept from the two-dimensional continuum fluid to the partitioned fluid: high-speed single-molecule tracking of membrane molecules. Annu.Rev.Biophys.Biomol.Struct. *34,* 351-378.

Kusumi, A., and Sako, Y. (1996). Cell surface organization by the membrane skeleton. Curr. Opin. Cell Biol. *8,* 566-574.

Kusumi, A., Sako, Y., and Yamamoto, M. (1993). Confined lateral diffusion of membrane receptors as studied by single particle tracking (nanovid microscopy). Effects of calcium-induced differentiation in cultured epithelial cells. Biophys. J. *65,* 2021-2040.

Lawler, P.R., and Lawler, J. (2012). Molecular basis for the regulation of angiogenesis by thrombospondin-1 and-2. Cold Spring Harbor Perspectives in Medicine *2,* a006627.

Lee, A.G., Birdsall, N., Metcalfe, J.C., Toon, P.A., and Warren, G.B. (1974). Clusters in lipid bilayers and the interpretation of thermal effects in biological membranes. Biochemistry (N. Y.) *13,* 3699-3705.

Lemmon, M.A. (2008). Membrane recognition by phospholipid-binding domains. Nature Reviews Molecular Cell Biology *9,* 99.

Lindmo, K., and Stenmark, H. (2006). Regulation of membrane traffic by phosphoinositide 3-kinases. J. Cell. Sci. *119,* 605-614.

Liu, P., Cheng, H., Roberts, T.M., and Zhao, J.J. (2009). Targeting the phosphoinositide 3-kinase pathway in cancer. Nature Reviews Drug Discovery *8,* 627.

Lodish, H., Berk, A., Zipursky, S.L., Matsudaira, P., Baltimore, D., and Darnell, J. (2000a). The actin cytoskeleton.

Lodish, H., Berk, A., Zipursky, S.L., Matsudaira, P., Baltimore, D., and Darnell, J. (2000b). Biomembranes: Structural organization and basic functions.

Marcora, E., Carlisle, H.J., and Kennedy, M.B. (2008). The Role of the Postsynaptic Density and the Spine Cytoskeleton in Synaptic Plasticity.

Markovic, S.N., Suman, V.J., Rao, R.A., Ingle, J.N., Kaur, J.S., Erickson, L.A., Pitot, H.C., Croghan, G.A., McWilliams, R.R., and Merchan, J. (2007). A phase II study of ABT-510 (thrombospondin-1 analog) for the treatment of metastatic melanoma. American Journal of Clinical Oncology *30,* 303-309.

McLaughlin, S., Wang, J., Gambhir, A., and Murray, D. (2002). PIP2 and proteins: interactions, organization, and information flow. Annu. Rev. Biophys. Biomol. Struct. *31,* 151-175.

Murphy-Ullrich, J.E., and Poczatek, M. (2000). Activation of latent TGF-β by thrombospondin-1: mechanisms and physiology. Cytokine Growth Factor Rev. *11,* 59-69.

Navazo, M.D.P., Daviet, L., Ninio, E., and McGregor, J.L. (1996). Identification on human CD36 of a domain (155-183) implicated in binding oxidized low-density lipoproteins (Ox-LDL). Arterioscler. Thromb. Vasc. Biol. *16,* 1033-1039.

Neculai, D., Schwake, M., Ravichandran, M., Zunke, F., Collins, R.F., Peters, J., Neculai, M., Plumb, J., Loppnau, P., and Pizarro, J.C. (2013). Structure of LIMP-2 provides functional insights with implications for SR-BI and CD36. Nature *504,* 172.

Nicolson, G.L. (2014). The Fluid—Mosaic Model of Membrane Structure: Still relevant to understanding the structure, function and dynamics of biological membranes after more than 40years. Biochimica Et Biophysica Acta (BBA)-Biomembranes *1838,* 1451-1466.

Niggli, V. (2005). Regulation of protein activities by phosphoinositide phosphates. Annu.Rev.Cell Dev.Biol. *21,* 57-79.

Nishida, N., Yano, H., Nishida, T., Kamura, T., and Kojiro, M. (2006). Angiogenesis in cancer. Vascular Health and Risk Management *2,* 213.

Noutsi, P., Gratton, E., and Chaieb, S. (2016). Assessment of Membrane Fluidity Fluctuations during Cellular Development Reveals Time and Cell Type Specificity. PloS One *11,* e0158313.

Okada, M. (2012). Regulation of the SRC family kinases by Csk. International Journal of Biological Sciences *8,* 1385.

Owen, D.M., Rentero, C., Rossy, J., Magenau, A., Williamson, D., Rodriguez, M., and Gaus, K. (2010). PALM imaging and cluster analysis of protein heterogeneity at the cell surface. Journal of Biophotonics *3,* 446-454.

Park, Y.M. (2014). CD36, a scavenger receptor implicated in atherosclerosis. Exp. Mol. Med. *46,* e99.

Park, Y.M., Febbraio, M., and Silverstein, R.L. (2009). CD36 modulates migration of mouse and human macrophages in response to oxidized LDL and may contribute to macrophage trapping in the arterial intima. J. Clin. Invest. *119,* 136-145.

Pearce, S.F.A., Wu, J., and Silverstein, R.L. (1995). Recombinant GST/CD36 Fusion Proteins Define a Thrombospondin Binding Domain EVIDENCE FOR A SINGLE CALCIUM-DEPENDENT BINDING SITE ON CD36. J. Biol. Chem. *270,* 2981-2986.

Posadas, E.M., Al-Ahmadie, H., Robinson, V.L., Jagadeeswaran, R., Otto, K., Kasza, K.E., Tretiakov, M., Siddiqui, J., Pienta, K.J., and Stadler, W.M. (2009). FYN is overexpressed in human prostate cancer. BJU Int. *103,* 171-177.

Rege, T.A., Stewart, J., Dranka, B., Benveniste, E.N., Silverstein, R.L., and Gladson, C.L. (2009). Thrombospondin-1-induced apoptosis of brain microvascular endothelial cells can be mediated by TNF-R1. J. Cell. Physiol. *218,* 94-103.

Ren, B., Yee, K.O., Lawler, J., and Khosravi-Far, R. (2006). Regulation of tumor angiogenesis by thrombospondin-1. Biochimica Et Biophysica Acta (BBA)-Reviews on Cancer *1765,* 178-188.

Ritchie, K., Shan, X., Kondo, J., Iwasawa, K., Fujiwara, T., and Kusumi, A. (2005). Detection of non-Brownian diffusion in the cell membrane in single molecule tracking. Biophys. J. *88,* 2266-2277.

Roskoski, R. (2005). Src kinase regulation by phosphorylation and dephosphorylation. Biochem. Biophys. Res. Commun. *331,* 1-14.

Russell, S., Duquette, M., Liu, J., Drapkin, R., Lawler, J., and Petrik, J. (2015). Combined therapy with thrombospondin-1 type I repeats (3TSR) and chemotherapy induces regression and significantly improves survival in a preclinical model of advanced stage epithelial ovarian cancer. The FASEB Journal *29,* 576-588.

Saarikangas, J., Zhao, H., and Lappalainen, P. (2010). Regulation of the actin cytoskeleton-plasma membrane interplay by phosphoinositides. Physiol. Rev. *90,* 259-289.

Saha, S., Lee, I., Polley, A., Groves, J.T., Rao, M., and Mayor, S. (2015). Diffusion of GPI-anchored proteins is influenced by the activity of dynamic cortical actin. Mol. Biol. Cell *26,* 4033-4045.

Sala-Valdés, M., Ursa, A, Charrin, S., Rubinstein, E., Hemler, M.E., Sánchez-Madrid, F., and Yáñez-Mó, M. (2006). EWI-2 and EWI-F link the tetraspanin web to the actin cytoskeleton through their direct association with ezrin-radixin-moesin proteins. J. Biol. Chem. *281,* 19665-19675.

Sasaki, S., Yui, N., and Noda, Y. (2014). Actin directly interacts with different membrane channel proteins and influences channel activities: AQP2 as a model. Biochimica Et Biophysica Acta (BBA)-Biomembranes *1838,* 514-520.

Sasaki, T., Takasuga, S., Sasaki, J., Kofuji, S., Eguchi, S., Yamazaki, M., and Suzuki, A. (2009). Mammalian phosphoinositide kinases and phosphatases. Prog. Lipid Res. *48,* 307-343.

Sato, I., Obata, Y., Kasahara, K., Nakayama, Y., Fukumoto, Y., Yamasaki, T., Yokoyama, K.K., Saito, T., and Yamaguchi, N. (2009). Differential trafficking of Src, Lyn, Yes and Fyn is specified by the state of palmitoylation in the SH4 domain. J. Cell. Sci. *122,* 965-975.

Sechi, A.S., and Wehland, J. (2000). The actin cytoskeleton and plasma membrane connection: PtdIns (4, 5) P (2) influences cytoskeletal protein activity at the plasma membrane. J. Cell. Sci. *113,* 3685-3695.

Sen, B., and Johnson, F.M. (2011). Regulation of SRC family kinases in human cancers. Journal of Signal Transduction *2011,*

Silverstein, R.L., and Febbraio, M. (2009). CD36, a scavenger receptor involved in immunity, metabolism, angiogenesis, and behavior. Sci.Signal. *2,* re3.

Simantov, R., and Silverstein, R.L. (2003). CD36: a critical anti-angiogenic receptor. Front. Biosci. *8,* 874.

Simons, K., and Gerl, M.J. (2010). Revitalizing membrane rafts: new tools and insights. Nature Reviews Molecular Cell Biology *11,* nrm2977.

Simons, K., and Sampaio, J.L. (2011). Membrane organization and lipid rafts. Cold Spring Harbor Perspectives in Biology *3,* a004697.

Singer, S.J., and Nicolson, G.L. (1972). The fluid mosaic model of the structure of cell membranes. Science *175,* 720-731.

Sydor, A.M., Czymmek, K.J., Puchner, E.M., and Mennella, V. (2015). Super-resolution microscopy: from single molecules to supramolecular assemblies. Trends Cell Biol. *25,* 730-748.

Tan, K., Duquette, M., Liu, J., Dong, Y., Zhang, R., Joachimiak, A., Lawler, J., and Wang, J. (2002). Crystal structure of the TSP-1 type 1 repeats: a novel layered fold and its biological implication. J. Cell Biol. *159,* 373-382.

Tan, K., and Lawler, J. (2009). The interaction of Thrombospondins with extracellular matrix proteins. Journal of Cell Communication and Signaling *3,* 177-187.

Tao, N., Wagner, S.J., and Lublin, D.M. (1996). CD36 is palmitoylated on both N-and C-terminal cytoplasmic tails. J. Biol. Chem. *271,* 22315-22320.

Tolsma, S.S., Volpert, O.V., Good, D.J., Frazier, W.A., Polverini, P.J., and Bouck, N. (1993). Peptides derived from two separate domains of the matrix protein thrombospondin-1 have anti-angiogenic activity. J. Cell Biol. *122,* 497-511.

Vacaresse, N., Møller, B., Danielsen, E.M., Okada, M., and Sap, J. (2008). Activation of c-Src and Fyn kinases by protein-tyrosine phosphatase RPTPα is substrate-specific and compatible with lipid raft localization. J. Biol. Chem. *283,* 35815-35824.

Van Meer, G., Voelker, D.R., and Feigenson, G.W. (2008). Membrane lipids: where they are and how they behave. Nature Reviews Molecular Cell Biology *9,* 112.

Vanhaesebroeck, B., Stephens, L., and Hawkins, P. (2012). PI3K signalling: the path to discovery and understanding. Nature Reviews Molecular Cell Biology *13,* 195.

Volpert, O.V., Zaichuk, T., Zhou, W., Reiher, F., Ferguson, T.A., Stuart, P.M., Amin, M., and Bouck, N.P. (2002). Inducer-stimulated Fas targets activated endothelium for destruction by anti-angiogenic thrombospondin-1 and pigment epithelium–derived factor. Nat. Med. *8,* 349.

Welch, H.C., Coadwell, W.J., Stephens, L.R., and Hawkins, P.T. (2003). Phosphoinositide 3-kinase-dependent activation of Rac. FEBS Lett. *546,* 93-97.

Wilkinson, B., Koenigsknecht-Talboo, J., Grommes, C., Lee, C.D., and Landreth, G. (2006). Fibrillar β-amyloid-stimulated intracellular signaling cascades require Vav for induction

of respiratory burst and phagocytosis in monocytes and microglia. J. Biol. Chem. *281,* 20842-20850.

Wolf, R.M., Wilkes, J.J., Chao, M.V., and Resh, M.D. (2001). Tyrosine phosphorylation of p190 RhoGAP by Fyn regulates oligodendrocyte differentiation. Developmental Neurobiology *49,* 62-78.

Wunderlich, F., Ronai, A., Speth, V., Seelig, J., and Blume, A. (1975). Thermotropic lipid clustering in Tetrahymena membranes. Biochemistry (N. Y.) *14,* 3730-3735.

Yamaguchi, H., Shiraishi, M., Fukami, K., Tanabe, A., Ikeda-Matsuo, Y., Naito, Y., and Sasaki, Y. (2009). MARCKS regulates lamellipodia formation induced by IGF-I via association with PIP2 and β-actin at membrane microdomains. J. Cell. Physiol. *220,* 748-755.

Yamamoto, M., Hilgemann, D.H., Feng, S., Bito, H., Ishihara, H., Shibasaki, Y., and Yin, H.L. (2001). Phosphatidylinositol 4, 5-bisphosphate induces actin stress-fiber formation and inhibits membrane ruffling in CV1 cells. J. Cell Biol. *152,* 867-876.

Yang, T., Massa, S.M., and Longo, F.M. (2006). LAR protein tyrosine phosphatase receptor associates with TrkB and modulates neurotrophic signaling pathways. Developmental Neurobiology *66,* 1420-1436.

Zachowski, A. (1993). Phospholipids in animal eukaryotic membranes: transverse asymmetry and movement. Biochem. J. *294,* 1.

Zeng, Y., Tao, N., Chung, K., Heuser, J.E., and Lublin, D.M. (2003). Endocytosis of oxidized low density lipoprotein through scavenger receptor CD36 utilizes a lipid raft pathway that does not require caveolin-1. J. Biol. Chem. *278,* 45931-45936.

Zheng, X., Resnick, R.J., and Shalloway, D. (2000). A phosphotyrosine displacement mechanism for activation of Src by PTPα. Embo J. *19,* 964-978.

Githaka, J.M., Vega, A.R., Baird, M.A., Davidson, M.W., Jaqaman, K., and Touret, N. (2016). Ligand-induced growth and compaction of CD36 nanoclusters enriched in Fyn induces Fyn signaling. J. Cell. Sci. 129, 4175-4189.

Jaqaman, K., Loerke, D., Mettlen, M., Kuwata, H., Grinstein, S., Schmid, S.L., and Danuser, G. (2008). Robust single-particle tracking in live-cell time-lapse sequences. Nature Methods 5, 695.

Owen, D.M., Rentero, C., Rossy, J., Magenau, A., Williamson, D., Rodriguez, M., and Gaus, K. (2010). PALM imaging and cluster analysis of protein heterogeneity at the cell surface. Journal of Biophotonics 3, 446-454.

Williamson, D.P., and Shmoys, D.B. (2011). The design of approximation algorithms Cambridge university press).

Aghazadeh, B., Lowry, W.E., Huang, X., and Rosen, M.K. (2000). Structural basis for relief of autoinhibition of the Dbl homology domain of proto-oncogene Vav by tyrosine phosphorylation. Cell 102, 625-633.

Amata, I., Maffei, M., and Pons, M. (2014). Phosphorylation of unique domains of Src family kinases. Frontiers in Genetics *5,* 181.

Campa, C.C., Ciraolo, E., Ghigo, A., Germena, G., and Hirsch, E. (2015). Crossroads of PI3K and Rac pathways. Small GTPases *6,* 71-80.

Crespo, P., Schuebel, K.E., Ostrom, A.A., Gutkind, J.S., and Bustelo, X.R. (1997). Phosphotyrosine-dependent activation of Rac-1 GDP/GTP exchange by the vav proto-oncogene product. Nature *385,* 169.

Cuevas, B.D., Lu, Y., Mao, M., Zhang, J., LaPushin, R., Siminovitch, K., and Mills, G.B. (2001). Tyrosine phosphorylation of p85 relieves its inhibitory activity on phosphatidylinositol 3-kinase. J. Biol. Chem. *276,* 27455-27461.

Fujita, A., Cheng, J., Tauchi-Sato, K., Takenawa, T., and Fujimoto, T. (2009). A distinct pool of phosphatidylinositol 4, 5-bisphosphate in caveolae revealed by a nanoscale labeling technique. Proceedings of the National Academy of Sciences *106,* 9256-9261.

Gillham, H., Golding, M.C., Pepperkok, R., and Gullick, W.J. (1999). Intracellular movement of green fluorescent protein–tagged phosphatidylinositol 3-kinase in response to growth factor receptor signaling. J. Cell Biol. *146,* 869-880.

Githaka, J.M., Vega, A.R., Baird, M.A., Davidson, M.W., Jaqaman, K., and Touret, N. (2016). Ligand-induced growth and compaction of CD36 nanoclusters enriched in Fyn induces Fyn signaling. J. Cell. Sci. *129,* 4175-4189.

Hinchliffe, K.A. (2001). Cellular signalling: stressing the importance of PIP3. Current Biology *11,* R373.

Insall, R.H., and Weiner, O.D. (2001). PIP3, PIP2, and cell movement—similar messages, different meanings? Developmental Cell *1,* 743-747.

Jaqaman, K., Kuwata, H., Touret, N., Collins, R., Trimble, W.S., Danuser, G., and Grinstein, S. (2011). Cytoskeletal control of CD36 diffusion promotes its receptor and signaling function. Cell *146,* 593-606.

Katso, R.M., Pardo, O.E., Palamidessi, A., Franz, C.M., Marinov, M., De Laurentiis, A., Downward, J., Scita, G., Ridley, A.J., and Waterfield, M.D. (2006). Phosphoinositide 3-kinase C2β regulates cytoskeletal organization and cell migration via Rac-dependent mechanisms. Mol. Biol. Cell *17,* 3729-3744.

Kennedy, M.J., Hughes, R.M., Peteya, L.A., Schwartz, J.W., Ehlers, M.D., and Tucker, C.L. (2010). Rapid blue-light–mediated induction of protein interactions in living cells. Nature Methods *7,* 973.

Kosenko, A., and Hoshi, N. (2013). A change in configuration of the calmodulin-KCNQ channel complex underlies Ca2 -dependent modulation of KCNQ channel activity. PloS One *8,* e82290.

Lingwood, D., Kaiser, H., Levental, I., and Simons, K. (2009). No title. Lipid Rafts as Functional Heterogeneity in Cell Membranes

Miller, M.S., Schmidt-Kittler, O., Bolduc, D.M., Brower, E.T., Chaves-Moreira, D., Allaire, M., Kinzler, K.W., Jennings, I.G., Thompson, P.E., and Cole, P.A. (2014). Structural basis of nSH2 regulation and lipid binding in PI3Kα. Oncotarget *5,* 5198.

Palmby, T.R., Abe, K., and Der, C.J. (2002). Critical role of the pleckstrin homology and cysteine-rich domains in Vav signaling and transforming activity. J. Biol. Chem. *277,* 39350-39359.

Park, M., Sheng, R., Silkov, A., Jung, D., Wang, Z., Xin, Y., Kim, H., Thiagarajan-Rosenkranz, P., Song, S., and Yoon, Y. (2016). SH2 domains serve as lipid-binding modules for pTyr-signaling proteins. Mol. Cell *62,* 7-20.

Pike, L.J., and Miller, J.M. (1998). Cholesterol depletion delocalizes phosphatidylinositol bisphosphate and inhibits hormone-stimulated phosphatidylinositol turnover. J. Biol. Chem. *273,* 22298-22304.

Rastogi, B.K., and Nordøy, A. (1980). Lipid composition of cultured human endothelial cells. Thromb. Res. *18,* 629-641.

Salamon, R.S., and Backer, J.M. (2013). Phosphatidylinositol-3, 4, 5-trisphosphate: Tool of choice for class I PI 3-kinases. Bioessays *35,* 602-611.

Shaner, N.C., Lambert, G.G., Chammas, A., Ni, Y., Cranfill, P.J., Baird, M.A., Sell, B.R., Allen, J.R., Day, R.N., and Israelsson, M. (2013). A bright monomeric green fluorescent protein derived from Branchiostoma lanceolatum. Nature Methods *10,* 407.

Shevchenko, A., and Simons, K. (2010). Lipidomics: coming to grips with lipid diversity. Nature Reviews Molecular Cell Biology *11,* 593.

Taslimi, A., Zoltowski, B., Miranda, J.G., Pathak, G.P., Hughes, R.M., and Tucker, C.L. (2016). Optimized second-generation CRY2–CIB dimerizers and photoactivatable Cre recombinase. Nature Chemical Biology *12,* 425.

Van Meer, G., Voelker, D.R., and Feigenson, G.W. (2008). Membrane lipids: where they are and how they behave. Nature Reviews Molecular Cell Biology *9,* 112.

Vanhaesebroeck, B., Stephens, L., and Hawkins, P. (2012). PI3K signalling: the path to discovery and understanding. Nature Reviews Molecular Cell Biology *13,* 195.

Welch, H.C., Coadwell, W.J., Stephens, L.R., and Hawkins, P.T. (2003). Phosphoinositide 3-kinase-dependent activation of Rac. FEBS Lett. *546,* 93-97.

Yadav, V., and Denning, M.F. (2011). Fyn is induced by Ras/PI3K/Akt signaling and is required for enhanced invasion/migration. Mol. Carcinog. *50,* 346-352.

Zachowski, A. (1993). Phospholipids in animal eukaryotic membranes: transverse asymmetry and movement. Biochem. J. *294,* 1.

Zhou, Y., and Hancock, J.F. (2015). Ras nanoclusters: Versatile lipid-based signaling platforms. Biochimica Et Biophysica Acta (BBA)-Molecular Cell Research *1853,* 841-849.

Zhou, Y., Liang, H., Rodkey, T., Ariotti, N., Parton, R.G., and Hancock, J.F. (2014). Signal integration by lipid-mediated spatial cross talk between Ras nanoclusters. Mol. Cell. Biol. *34,* 862-876.

Adams, M., Simms, R.J., Abdelhamed, Z., Dawe, H.R., Szymanska, K., Logan, C.V., Wheway, G., Pitt, E., Gull, K., and Knowles, M.A. (2011). A meckelin–filamin A interaction mediates ciliogenesis. Hum. Mol. Genet. *21,* 1272-1286.

Branon, T.C., Bosch, J.A., Sanchez, A.D., Udeshi, N.D., Svinkina, T., Carr, S.A., Feldman, J.L., Perrimon, N., and Ting, A.Y. (2017). Directed evolution of TurboID for efficient proximity labeling in living cells and organisms. bioRxiv 196980.

Dixon, M.J., Gray, A., Schenning, M., Agacan, M., Tempel, W., Tong, Y., Nedyalkova, L., Park, H., Leslie, N.R., and Van Aalten, D.M. (2012). IQGAP proteins reveal an atypical phosphoinositide (aPI) binding domain with a pseudo C2 domain fold. J. Biol. Chem. *287,* 22483-22496.

Fanning, A.S., and Anderson, J.M. (1999). PDZ domains: fundamental building blocks in the organization of protein complexes at the plasma membrane. J. Clin. Invest. *103,* 767-772.

Febbraio, M., Abumrad, N.A., Hajjar, D.P., Sharma, K., Cheng, W., Pearce, S.F.A., and Silverstein, R.L. (1999). A null mutation in murine CD36 reveals an important role in fatty acid and lipoprotein metabolism. J. Biol. Chem. *274,* 19055-19062.

Feng, D., Steinke, J.M., Krishnan, R., Birrane, G., and Pollak, M.R. (2016). Functional Validation of an Alpha-Actinin-4 Mutation as a Potential Cause of an Aggressive Presentation of Adolescent Focal Segmental Glomerulosclerosis: Implications for Genetic Testing. PloS One *11,* e0167467.

Fraley, T.S., Pereira, C.B., Tran, T.C., Singleton, C., and Greenwood, J.A. (2005). Phosphoinositide binding regulates α-actinin dynamics mechanism for modulating cytoskeletal remodeling. J. Biol. Chem. *280,* 15479-15482.

Fraley, T.S., Tran, T.C., Corgan, A.M., Nash, C.A., Hao, J., Critchley, D.R., and Greenwood, J.A. (2003). Phosphoinositide binding inhibits α-actinin bundling activity. J. Biol. Chem. *278,* 24039-24045.

Full, S.J., Deinzer, M.L., Ho, P.S., and Greenwood, J.A. (2007). Phosphoinositide binding regulates α-actinin CH2 domain structure: Analysis by hydrogen/deuterium exchange mass spectrometry. Protein Science *16,* 2597-2604.

Githaka, J.M., Vega, A.R., Baird, M.A., Davidson, M.W., Jaqaman, K., and Touret, N. (2016). Ligand-induced growth and compaction of CD36 nanoclusters enriched in Fyn induces Fyn signaling. J. Cell. Sci. *129,* 4175-4189.

Gossen, M., and Bujard, H. (1992). Tight control of gene expression in mammalian cells by tetracycline-responsive promoters. Proceedings of the National Academy of Sciences *89,* 5547-5551.

Gossen, M., Freundlieb, S., Bender, G., Muller, G., Hillen, W., and Bujard, H. (1995). Transcriptional activation by tetracyclines in mammalian cells. Science *268,* 1766-1769.

Hayer, A., Shao, L., Chung, M., Joubert, L., Yang, H.W., Tsai, F., Bisaria, A., Betzig, E., and Meyer, T. (2016). Engulfed cadherin fingers are polarized junctional structures between collectively migrating endothelial cells. Nat. Cell Biol. *18,* 1311.

Honda, K., Yamada, T., Endo, R., Ino, Y., Gotoh, M., Tsuda, H., Yamada, Y., Chiba, H., and Hirohashi, S. (1998). Actinin-4, a novel actin-bundling protein associated with cell motility and cancer invasion. J. Cell Biol. *140,* 1383-1393.

Kim, E., Niethammer, M., Rothschild, A., Jan, Y.N., and Sheng, M. (1995). Clustering of Shaker-type K channels by interaction with a family of membrane-associated guanylate kinases. Nature *378,* 85.

Koster, J., Geerts, D., Favre, B., Borradori, L., and Sonnenberg, A. (2003). Analysis of the interactions between BP180, BP230, plectin and the integrin α6β4 important for hemidesmosome assembly. J. Cell. Sci. *116,* 387-399.

Lee, K.M., Choi, K.H., and Ouellette, M.M. (2004). Use of exogenous hTERT to immortalize primary human cells. Cytotechnology *45,* 33-38.

Myers, K.R., and Casanova, J.E. (2008). Regulation of actin cytoskeleton dynamics by Arf-family GTPases. Trends Cell Biol. *18,* 184-192.

Roux, K.J., Kim, D.I., Burke, B., and May, D.G. (2013). BioID: a screen for protein-protein interactions. Current Protocols in Protein Science 19.23. 15.

Roux, K.J., Kim, D.I., Raida, M., and Burke, B. (2012). A promiscuous biotin ligase fusion protein identifies proximal and interacting proteins in mammalian cells. J. Cell Biol. *196,* 801-810.

Rual, J., Venkatesan, K., Hao, T., Hirozane-Kishikawa, T., Dricot, A., Li, N., Berriz, G.F., Gibbons, F.D., Dreze, M., and Ayivi-Guedehoussou, N. (2005). Towards a proteome-scale map of the human protein–protein interaction network. Nature *437,* 1173.

Saarikangas, J., Zhao, H., and Lappalainen, P. (2010). Regulation of the actin cytoskeleton-plasma membrane interplay by phosphoinositides. Physiol. Rev. *90,* 259-289.

Sechi, A.S., and Wehland, J. (2000). The actin cytoskeleton and plasma membrane connection: PtdIns (4, 5) P (2) influences cytoskeletal protein activity at the plasma membrane. J. Cell. Sci. *113,* 3685-3695.

Sjöblom, B., Salmazo, A., and Djinović-Carugo, K. (2008). α-Actinin structure and regulation. Cellular and Molecular Life Sciences *65,* 2688.

Smith, S., Witkowski, A., and Joshi, A.K. (2003). Structural and functional organization of the animal fatty acid synthase. Prog. Lipid Res. *42,* 289-317.

Snyers, L., Thines-Sempoux, D., and Prohaska, R. (1997). Colocalization of stomatin (band 7.2 b) and actin microfilaments in UAC epithelial cells. Eur. J. Cell Biol. *73,* 281-285.

Sprague, C.R., Fraley, T.S., Jang, H.S., Lal, S., and Greenwood, J.A. (2008). Phosphoinositide binding to the substrate regulates susceptibility to proteolysis by calpain. J. Biol. Chem. *283,* 9217-9223.

Tourrière, H., Chebli, K., Zekri, L., Courselaud, B., Blanchard, J.M., Bertrand, E., and Tazi, J. (2003). The RasGAP-associated endoribonuclease G3BP assembles stress granules. J. Cell Biol. *160,* 823-831.

UniProt Consortium. (2014). UniProt: a hub for protein information. Nucleic Acids Res. *43,* D212.

Venetsanakos, E., Mirza, A., Fanton, C., Romanov, S.R., Tlsty, T., and McMahon, M. (2002). Induction of tubulogenesis in telomerase-immortalized human microvascular endothelial cells by glioblastoma cells. Exp. Cell Res. *273,* 21-33.

Appendix

Description	Average amount (size of the peak) over duplicate experiments
Tubulin alpha-1B chain OS=Homo sapiens GN=TUBA1B PE=1 SV=1 - [TBA1B_HUMAN]	1.54E+09
Tubulin alpha-1A chain OS=Homo sapiens GN=TUBA1A PE=1 SV=1 - [TBA1A_HUMAN]	1.54E+09
Tubulin alpha-1C chain OS=Homo sapiens GN=TUBA1C PE=1 SV=1 - [TBA1C_HUMAN]	1.54E+09
Actin, cytoplasmic 1 OS=Homo sapiens GN=ACTB PE=1 SV=1 - [ACTB_HUMAN]	1.49E+09
Tubulin beta chain OS=Homo sapiens GN=TUBB PE=1 SV=2 - [TBB5_HUMAN]	1.35E+09
Tubulin beta-4B chain OS=Homo sapiens GN=TUBB4B PE=1 SV=1 - [TBB4B_HUMAN]	1.32E+09
Tubulin beta-2B chain OS=Homo sapiens GN=TUBB2B PE=1 SV=1 - [TBB2B_HUMAN]	1.32E+09

Description	Average amount (size of the peak) over duplicate experiments
Tubulin alpha-4A chain OS=Homo sapiens GN=TUBA4A PE=1 SV=1 - [TBA4A_HUMAN]	1.02E+09
Tubulin beta-4A chain OS=Homo sapiens GN=TUBB4A PE=1 SV=2 - [TBB4A_HUMAN]	9.69E+08
Actin, alpha cardiac muscle 1 OS=Homo sapiens GN=ACTC1 PE=1 SV=1 - [ACTC_HUMAN]	6.98E+08
Tubulin beta-6 chain OS=Homo sapiens GN=TUBB6 PE=1 SV=1 - [TBB6_HUMAN]	5.26E+08
Elongation factor 1-alpha 1 OS=Homo sapiens GN=EEF1A1 PE=1 SV=1 - [EF1A1_HUMAN]	5.06E+08
Heat shock protein beta-1 OS=Homo sapiens GN=HSPB1 PE=1 SV=2 - [HSPB1_HUMAN]	2.79E+08
Heat shock protein 75 kDa, mitochondrial OS=Homo sapiens GN=TRAP1 PE=1 SV=3 - [TRAP1_HUMAN]	2.40E+08
40S ribosomal protein S7 OS=Homo sapiens GN=RPS7 PE=1 SV=1 - [RS7_HUMAN]	1.61E+08
Heat shock protein HSP 90-beta OS=Homo sapiens GN=HSP90AB1 PE=1 SV=4 - [HS90B_HUMAN]	1.61E+08
60S ribosomal protein L14 OS=Homo sapiens GN=RPL14 PE=1 SV=1 - [E7EPB3_HUMAN]	1.55E+08
Heat shock protein HSP 90-alpha OS=Homo sapiens GN=HSP90AA1 PE=1 SV=5 - [HS90A_HUMAN]	1.47E+08
Myosin-9 OS=Homo sapiens GN=MYH9 PE=1 SV=4 - [MYH9_HUMAN]	1.38E+08
60S ribosomal protein L11 OS=Homo sapiens GN=RPL11 PE=1 SV=2 - [RL11_HUMAN]	1.34E+08
60S ribosomal protein L18 OS=Homo sapiens GN=RPL18 PE=1 SV=1 - [G3V203_HUMAN]	9.97E+07
40S ribosomal protein S16 OS=Homo sapiens GN=RPS16 PE=1 SV=1 - [M0R3H0_HUMAN]	9.69E+07

Description	Average amount (size of the peak) over duplicate experiments
T-complex protein 1 subunit gamma OS=Homo sapiens GN=CCT3 PE=1 SV=1 - [B4DUR8_HUMAN]	9.20E+07
40S ribosomal protein S3 OS=Homo sapiens GN=RPS3 PE=1 SV=2 - [RS3_HUMAN]	8.96E+07
60S ribosomal protein L7a (Fragment) OS=Homo sapiens GN=RPL7A PE=1 SV=1 - [Q5T8U3_HUMAN]	8.71E+07
Carbamoyl-phosphate synthase [ammonia], mitochondrial OS=Homo sapiens GN=CPS1 PE=1 SV=2 - [CPSM_HUMAN]	8.62E+07
60S ribosomal protein L38 OS=Homo sapiens GN=RPL38 PE=1 SV=1 - [J3KT73_HUMAN]	8.61E+07
Inosine-5'-monophosphate dehydrogenase 2 OS=Homo sapiens GN=IMPDH2 PE=1 SV=2 - [IMDH2_HUMAN]	8.60E+07
Histone H2A type 1-H OS=Homo sapiens GN=HIST1H2AH PE=1 SV=3 - [H2A1H_HUMAN]	8.34E+07
40S ribosomal protein S5 (Fragment) OS=Homo sapiens GN=RPS5 PE=1 SV=1 - [M0R0F0_HUMAN]	7.86E+07
Heat shock cognate 71 kDa protein OS=Homo sapiens GN=HSPA8 PE=1 SV=1 - [HSP7C_HUMAN]	7.68E+07
40S ribosomal protein S4, X isoform OS=Homo sapiens GN=RPS4X PE=1 SV=2 - [RS4X_HUMAN]	7.57E+07
T-complex protein 1 subunit delta OS=Homo sapiens GN=CCT4 PE=1 SV=4 - [TCPD_HUMAN]	7.39E+07
Heterogeneous nuclear ribonucleoprotein H OS=Homo sapiens GN=HNRNPH1 PE=1 SV=1 - [E9PCY7_HUMAN]	7.27E+07
Epiplakin OS=Homo sapiens GN=EPPK1 PE=1 SV=2 - [EPIPL_HUMAN]	7.16E+07
T-complex protein 1 subunit alpha OS=Homo sapiens GN=TCP1 PE=1 SV=1 - [TCPA_HUMAN]	6.99E+07
Cytoplasmic dynein 1 heavy chain 1 OS=Homo sapiens GN=DYNC1H1 PE=1 SV=5 - [DYHC1_HUMAN]	6.98E+07

Description	Average amount (size of the peak) over duplicate experiments
Keratin, type II cytoskeletal 1 OS=Homo sapiens GN=KRT1 PE=1 SV=6 - [K2C1_HUMAN]	6.90E+07
T-complex protein 1 subunit zeta OS=Homo sapiens GN=CCT6A PE=1 SV=3 - [TCPZ_HUMAN]	6.81E+07
60S acidic ribosomal protein P0 OS=Homo sapiens GN=RPLP0 PE=1 SV=1 - [F8VWS0_HUMAN]	6.67E+07
60S ribosomal protein L4 OS=Homo sapiens GN=RPL4 PE=1 SV=5 - [RL4_HUMAN]	6.60E+07
Clathrin heavy chain 1 OS=Homo sapiens GN=CLTC PE=1 SV=5 - [CLH1_HUMAN]	6.41E+07
40S ribosomal protein S25 OS=Homo sapiens GN=RPS25 PE=1 SV=1 - [RS25_HUMAN]	6.13E+07
T-complex protein 1 subunit beta OS=Homo sapiens GN=CCT2 PE=1 SV=1 - [F8VQ14_HUMAN]	6.08E+07
Calnexin OS=Homo sapiens GN=CANX PE=1 SV=2 - [CALX_HUMAN]	6.05E+07
Keratin, type II cytoskeletal 2 epidermal OS=Homo sapiens GN=KRT2 PE=1 SV=2 - [K22E_HUMAN]	6.04E+07
T-complex protein 1 subunit eta OS=Homo sapiens GN=CCT7 PE=1 SV=2 - [TCPH_HUMAN]	5.94E+07
40S ribosomal protein S8 OS=Homo sapiens GN=RPS8 PE=1 SV=1 - [Q5JR95_HUMAN]	5.88E+07
40S ribosomal protein S13 OS=Homo sapiens GN=RPS13 PE=1 SV=1 - [J3KMX5_HUMAN]	5.78E+07
60S ribosomal protein L12 OS=Homo sapiens GN=RPL12 PE=1 SV=1 - [RL12_HUMAN]	5.63E+07
Pyruvate kinase PKM OS=Homo sapiens GN=PKM PE=1 SV=4 - [KPYM_HUMAN]	5.51E+07
Elongation factor 2 OS=Homo sapiens GN=EEF2 PE=1 SV=4 - [EF2_HUMAN]	5.49E+07

Description	Average amount (size of the peak) over duplicate experiments
T-complex protein 1 subunit epsilon OS=Homo sapiens GN=CCT5 PE=1 SV=1 - [B7ZAR1_HUMAN]	5.36E+07
40S ribosomal protein S17 OS=Homo sapiens GN=RPS17 PE=1 SV=2 - [RS17_HUMAN]	5.33E+07
Sequestosome-1 OS=Homo sapiens GN=SQSTM1 PE=1 SV=1 - [SQSTM_HUMAN]	5.27E+07
60S ribosomal protein L13 OS=Homo sapiens GN=RPL13 PE=1 SV=4 - [RL13_HUMAN]	5.12E+07
Poly(rC)-binding protein 2 (Fragment) OS=Homo sapiens GN=PCBP2 PE=1 SV=1 - [F8VXH9_HUMAN]	4.73E+07
Probable ATP-dependent RNA helicase DDX5 OS=Homo sapiens GN=DDX5 PE=1 SV=1 - [J3KTA4_HUMAN]	4.50E+07
Keratin, type I cytoskeletal 9 OS=Homo sapiens GN=KRT9 PE=1 SV=3 - [K1C9_HUMAN]	4.42E+07
60S ribosomal protein L6 OS=Homo sapiens GN=RPL6 PE=1 SV=3 - [RL6_HUMAN]	4.40E+07
60S ribosomal protein L30 (Fragment) OS=Homo sapiens GN=RPL30 PE=1 SV=1 - [E5RI99_HUMAN]	4.37E+07
60S acidic ribosomal protein P1 OS=Homo sapiens GN=RPLP1 PE=1 SV=1 - [RLA1_HUMAN]	4.33E+07
78 kDa glucose-regulated protein OS=Homo sapiens GN=HSPA5 PE=1 SV=2 - [GRP78_HUMAN]	4.07E+07
26S protease regulatory subunit 6B OS=Homo sapiens GN=PSMC4 PE=1 SV=2 - [PRS6B_HUMAN]	4.05E+07
Importin subunit beta-1 OS=Homo sapiens GN=KPNB1 PE=1 SV=2 - [IMB1_HUMAN]	3.83E+07
60S acidic ribosomal protein P2 OS=Homo sapiens GN=RPLP2 PE=1 SV=1 - [RLA2_HUMAN]	3.81E+07
60S ribosomal protein L7 OS=Homo sapiens GN=RPL7 PE=1 SV=1 - [A8MUD9_HUMAN]	3.73E+07

Description	Average amount (size of the peak) over duplicate experiments
ATP-dependent RNA helicase DDX3X OS=Homo sapiens GN=DDX3X PE=1 SV=1 - [A0A0D9SFB3_HUMAN]	3.53E+07
60S ribosomal protein L10 (Fragment) OS=Homo sapiens GN=RPL10 PE=1 SV=7 - [X1WI28_HUMAN]	3.51E+07
T-complex protein 1 subunit theta OS=Homo sapiens GN=CCT8 PE=1 SV=4 - [TCPQ_HUMAN]	3.49E+07
Myosin regulatory light chain 12A OS=Homo sapiens GN=MYL12A PE=1 SV=2 - [ML12A_HUMAN]	3.40E+07
Transcription intermediary factor 1-beta OS=Homo sapiens GN=TRIM28 PE=1 SV=5 - [TIF1B_HUMAN]	3.40E+07
Fatty acid synthase OS=Homo sapiens GN=FASN PE=1 SV=1 - [A0A0U1RQF0_HUMAN]	3.33E+07
Exportin-1 OS=Homo sapiens GN=XPO1 PE=1 SV=1 - [XPO1_HUMAN]	3.31E+07
Ribosomal protein L15 (Fragment) OS=Homo sapiens GN=RPL15 PE=1 SV=1 - [E7EQV9_HUMAN]	3.30E+07
Exportin-2 OS=Homo sapiens GN=CSE1L PE=1 SV=3 - [XPO2_HUMAN]	3.27E+07
60S ribosomal protein L3 OS=Homo sapiens GN=RPL3 PE=1 SV=1 - [G5E9G0_HUMAN]	3.22E+07
Ras GTPase-activating protein-binding protein 1 OS=Homo sapiens GN=G3BP1 PE=1 SV=1 - [G3BP1_HUMAN]	3.13E+07
Bifunctional glutamate/proline--tRNA ligase OS=Homo sapiens GN=EPRS PE=1 SV=5 - [SYEP_HUMAN]	3.12E+07
Heterogeneous nuclear ribonucleoprotein K OS=Homo sapiens GN=HNRNPK PE=1 SV=1 - [HNRPK_HUMAN]	3.10E+07
ATP synthase subunit alpha, mitochondrial OS=Homo sapiens GN=ATP5A1 PE=1 SV=1 - [ATPA_HUMAN]	3.10E+07
Polyadenylate-binding protein OS=Homo sapiens GN=PABPC1 PE=1 SV=1 - [A0A087WTT1_HUMAN]	3.09E+07

Description	Average amount (size of the peak) over duplicate experiments
Polyadenylate-binding protein OS=Homo sapiens GN=PABPC4 PE=1 SV=1 - [B1ANR0_HUMAN]	3.09E+07
40S ribosomal protein S14 OS=Homo sapiens GN=RPS14 PE=1 SV=3 - [RS14_HUMAN]	3.06E+07
26S protease regulatory subunit 6A OS=Homo sapiens GN=PSMC3 PE=1 SV=1 - [R4GNH3_HUMAN]	3.03E+07
Transferrin receptor protein 1 OS=Homo sapiens GN=TFRC PE=1 SV=2 - [TFR1_HUMAN]	2.93E+07
26S protease regulatory subunit 8 OS=Homo sapiens GN=PSMC5 PE=1 SV=1 - [PRS8_HUMAN]	2.86E+07
Arginine--tRNA ligase, cytoplasmic OS=Homo sapiens GN=RARS PE=1 SV=2 - [SYRC_HUMAN]	2.80E+07
DnaJ homolog subfamily A member 1 OS=Homo sapiens GN=DNAJA1 PE=1 SV=2 - [DNJA1_HUMAN]	2.79E+07
26S protease regulatory subunit 4 OS=Homo sapiens GN=PSMC1 PE=1 SV=1 - [PRS4_HUMAN]	2.79E+07
Importin subunit alpha-1 OS=Homo sapiens GN=KPNA2 PE=1 SV=1 - [IMA1_HUMAN]	2.76E+07
Filamin-A OS=Homo sapiens GN=FLNA PE=1 SV=1 - [Q5HY54_HUMAN]	2.61E+07
60S ribosomal protein L17 (Fragment) OS=Homo sapiens GN=RPL17 PE=3 SV=1 - [A0A087WXM6_HUMAN]	2.60E+07
Coatomer subunit gamma-1 OS=Homo sapiens GN=COPG1 PE=1 SV=1 - [COPG1_HUMAN]	2.60E+07
40S ribosomal protein S15 OS=Homo sapiens GN=RPS15 PE=1 SV=2 - [RS15_HUMAN]	2.60E+07
Coatomer subunit alpha OS=Homo sapiens GN=COPA PE=1 SV=2 - [COPA_HUMAN]	2.50E+07
Heat shock 70 kDa protein 1A OS=Homo sapiens GN=HSPA1A PE=1 SV=1 - [HS71A_HUMAN]	2.49E+07

Description	Average amount (size of the peak) over duplicate experiments
60S ribosomal protein L21 OS=Homo sapiens GN=RPL21 PE=1 SV=2 - [RL21_HUMAN]	2.42E+07
Cytoplasmic dynein 1 light intermediate chain 1 OS=Homo sapiens GN=DYNC1LI1 PE=1 SV=3 - [DC1L1_HUMAN]	2.29E+07
Isoleucine--tRNA ligase, cytoplasmic OS=Homo sapiens GN=IARS PE=1 SV=1 - [J3KR24_HUMAN]	2.24E+07
Eukaryotic translation initiation factor 3 subunit F OS=Homo sapiens GN=EIF3F PE=1 SV=1 - [EIF3F_HUMAN]	2.23E+07
ATP-dependent RNA helicase A OS=Homo sapiens GN=DHX9 PE=1 SV=4 - [DHX9_HUMAN]	2.21E+07
Myosin light polypeptide 6 OS=Homo sapiens GN=MYL6 PE=1 SV=1 - [F8VZU9_HUMAN]	2.20E+07
X-ray repair cross-complementing protein 6 OS=Homo sapiens GN=XRCC6 PE=1 SV=1 - [B1AHC9_HUMAN]	2.16E+07
D-3-phosphoglycerate dehydrogenase OS=Homo sapiens GN=PHGDH PE=1 SV=4 - [SERA_HUMAN]	2.16E+07
X-ray repair cross-complementing protein 5 OS=Homo sapiens GN=XRCC5 PE=1 SV=3 - [XRCC5_HUMAN]	2.05E+07
eIF-2-alpha kinase activator GCN1 OS=Homo sapiens GN=GCN1 PE=1 SV=6 - [GCN1_HUMAN]	2.01E+07
E3 ubiquitin-protein ligase UBR4 OS=Homo sapiens GN=UBR4 PE=1 SV=1 - [UBR4_HUMAN]	1.91E+07
Cytoplasmic dynein 1 light intermediate chain 2 OS=Homo sapiens GN=DYNC1LI2 PE=1 SV=1 - [DC1L2_HUMAN]	1.87E+07
Coatomer subunit beta OS=Homo sapiens GN=COPB1 PE=1 SV=3 - [COPB_HUMAN]	1.84E+07
Neuroblast differentiation-associated protein AHNAK OS=Homo sapiens GN=AHNAK PE=1 SV=2 - [AHNK_HUMAN]	1.84E+07

Description	Average amount (size of the peak) over duplicate experiments
Leucine--tRNA ligase, cytoplasmic OS=Homo sapiens GN=LARS PE=1 SV=2 - [SYLC_HUMAN]	1.81E+07
Lamina-associated polypeptide 2, isoform alpha OS=Homo sapiens GN=TMPO PE=1 SV=2 - [LAP2A_HUMAN]	1.79E+07
Erythrocyte band 7 integral membrane protein OS=Homo sapiens GN=STOM PE=1 SV=3 - [STOM_HUMAN]	1.70E+07
Eukaryotic initiation factor 4A-I OS=Homo sapiens GN=EIF4A1 PE=1 SV=1 - [IF4A1_HUMAN]	1.69E+07
Importin-7 OS=Homo sapiens GN=IPO7 PE=1 SV=1 - [IPO7_HUMAN]	1.67E+07
Valine--tRNA ligase (Fragment) OS=Homo sapiens GN=VARS PE=1 SV=1 - [A0A140T936_HUMAN]	1.66E+07
Eukaryotic translation initiation factor 3 subunit E (Fragment) OS=Homo sapiens GN=EIF3E PE=1 SV=1 - [E5RHS5_HUMAN]	1.65E+07
Signal recognition particle 14 kDa protein OS=Homo sapiens GN=SRP14 PE=1 SV=2 - [SRP14_HUMAN]	1.62E+07
Keratin, type I cytoskeletal 10 OS=Homo sapiens GN=KRT10 PE=1 SV=6 - [K1C10_HUMAN]	1.62E+07
Matrin-3 (Fragment) OS=Homo sapiens GN=MATR3 PE=1 SV=1 - [D6R991_HUMAN]	1.61E+07
Splicing factor 3B subunit 1 OS=Homo sapiens GN=SF3B1 PE=1 SV=3 - [SF3B1_HUMAN]	1.55E+07
DNA-dependent protein kinase catalytic subunit OS=Homo sapiens GN=PRKDC PE=1 SV=3 - [PRKDC_HUMAN]	1.53E+07
Transcription activator BRG1 OS=Homo sapiens GN=SMARCA4 PE=1 SV=2 - [SMCA4_HUMAN]	1.47E+07
Sodium/potassium-transporting ATPase subunit alpha-1 OS=Homo sapiens GN=ATP1A1 PE=1 SV=1 - [AT1A1_HUMAN]	1.42E+07

Description	Average amount (size of the peak) over duplicate experiments
Non-POU domain-containing octamer-binding protein OS=Homo sapiens GN=NONO PE=1 SV=4 - [NONO_HUMAN]	1.42E+07
ATP-dependent 6-phosphofructokinase, platelet type OS=Homo sapiens GN=PFKP PE=1 SV=2 - [PFKAP_HUMAN]	1.40E+07
Cell cycle and apoptosis regulator protein 2 OS=Homo sapiens GN=CCAR2 PE=1 SV=2 - [CCAR2_HUMAN]	1.40E+07
60S ribosomal protein L23 OS=Homo sapiens GN=RPL23 PE=1 SV=1 - [J3KT29_HUMAN]	1.38E+07
Cell division cycle 2, G1 to S and G2 to M, isoform CRA_a OS=Homo sapiens GN=CDC2 PE=1 SV=1 - [A0A024QZP7_HUMAN]	1.38E+07
Structural maintenance of chromosomes protein 2 OS=Homo sapiens GN=SMC2 PE=1 SV=2 - [SMC2_HUMAN]	1.34E+07
Gem-associated protein 5 OS=Homo sapiens GN=GEMIN5 PE=1 SV=3 - [GEMI5_HUMAN]	1.33E+07
Structural maintenance of chromosomes protein 4 OS=Homo sapiens GN=SMC4 PE=1 SV=2 - [SMC4_HUMAN]	1.32E+07
Heterogeneous nuclear ribonucleoprotein U OS=Homo sapiens GN=HNRNPU PE=1 SV=6 - [HNRPU_HUMAN]	1.32E+07
Splicing factor, proline- and glutamine-rich OS=Homo sapiens GN=SFPQ PE=1 SV=2 - [SFPQ_HUMAN]	1.29E+07
Poly [ADP-ribose] polymerase 1 OS=Homo sapiens GN=PARP1 PE=1 SV=4 - [PARP1_HUMAN]	1.28E+07
Enhancer of mRNA-decapping protein 4 OS=Homo sapiens GN=EDC4 PE=1 SV=1 - [EDC4_HUMAN]	1.27E+07
Ribonucleoside-diphosphate reductase large subunit OS=Homo sapiens GN=RRM1 PE=1 SV=1 - [E9PL69_HUMAN]	1.26E+07
60 kDa heat shock protein, mitochondrial OS=Homo sapiens GN=HSPD1 PE=1 SV=2 - [CH60_HUMAN]	1.23E+07

Description	Average amount (size of the peak) over duplicate experiments
U5 small nuclear ribonucleoprotein 200 kDa helicase OS=Homo sapiens GN=SNRNP200 PE=1 SV=2 - [U520_HUMAN]	1.22E+07
Serine/threonine-protein phosphatase (Fragment) OS=Homo sapiens GN=PPP1CB PE=1 SV=1 - [E7ETD8_HUMAN]	1.20E+07
Condensin complex subunit 1 OS=Homo sapiens GN=NCAPD2 PE=1 SV=3 - [CND1_HUMAN]	1.12E+07
PDZ and LIM domain protein 7 OS=Homo sapiens GN=PDLIM7 PE=1 SV=1 - [PDLI7_HUMAN]	1.06E+07
Plectin OS=Homo sapiens GN=PLEC PE=1 SV=3 - [PLEC_HUMAN]	1.06E+07
4F2 cell-surface antigen heavy chain OS=Homo sapiens GN=SLC3A2 PE=1 SV=1 - [F5GZS6_HUMAN]	1.02E+07
Methionine--tRNA ligase, cytoplasmic OS=Homo sapiens GN=MARS PE=1 SV=2 - [SYMC_HUMAN]	1.01E+07
Glutamine--tRNA ligase OS=Homo sapiens GN=QARS PE=1 SV=1 - [SYQ_HUMAN]	9.77E+06
E3 ubiquitin-protein ligase KCMF1 OS=Homo sapiens GN=KCMF1 PE=1 SV=2 - [KCMF1_HUMAN]	9.43E+06
Importin-9 OS=Homo sapiens GN=IPO9 PE=1 SV=3 - [IPO9_HUMAN]	9.01E+06
Pre-mRNA-processing-splicing factor 8 OS=Homo sapiens GN=PRPF8 PE=1 SV=2 - [PRP8_HUMAN]	8.99E+06
Sarcoplasmic/endoplasmic reticulum calcium ATPase 2 OS=Homo sapiens GN=ATP2A2 PE=1 SV=1 - [AT2A2_HUMAN]	8.98E+06
Eukaryotic translation initiation factor 4 gamma 1 OS=Homo sapiens GN=EIF4G1 PE=1 SV=1 - [E7EX73_HUMAN]	8.89E+06
Guanine nucleotide-binding protein G(i) subunit alpha-2 OS=Homo sapiens GN=GNAI2 PE=1 SV=3 - [GNAI2_HUMAN]	8.72E+06

Description	Average amount (size of the peak) over duplicate experiments
ATP synthase subunit beta, mitochondrial (Fragment) OS=Homo sapiens GN=ATP5B PE=1 SV=2 - [F8W0P7_HUMAN]	8.18E+06
Protein unc-45 homolog A OS=Homo sapiens GN=UNC45A PE=1 SV=1 - [UN45A_HUMAN]	8.11E+06
Importin subunit alpha-3 (Fragment) OS=Homo sapiens GN=KPNA4 PE=1 SV=1 - [H7C4F6_HUMAN]	7.63E+06
Coatomer subunit epsilon OS=Homo sapiens GN=COPE PE=1 SV=3 - [COPE_HUMAN]	7.36E+06
Cullin-associated NEDD8-dissociated protein 1 OS=Homo sapiens GN=CAND1 PE=1 SV=2 - [CAND1_HUMAN]	7.34E+06
E3 ubiquitin-protein ligase UBR5 OS=Homo sapiens GN=UBR5 PE=1 SV=1 - [E7EMW7_HUMAN]	7.32E+06
Alpha-actinin-4 OS=Homo sapiens GN=ACTN4 PE=1 SV=2 - [ACTN4_HUMAN]	6.69E+06
Lysine--tRNA ligase OS=Homo sapiens GN=KARS PE=1 SV=3 - [SYK_HUMAN]	6.46E+06
DNA replication licensing factor MCM3 OS=Homo sapiens GN=MCM3 PE=1 SV=3 - [MCM3_HUMAN]	5.68E+06
Aspartate--tRNA ligase, cytoplasmic OS=Homo sapiens GN=DARS PE=1 SV=2 - [SYDC_HUMAN]	5.39E+06
Mitochondrial import receptor subunit TOM70 OS=Homo sapiens GN=TOMM70 PE=1 SV=1 - [TOM70_HUMAN]	3.50E+06

Table 2 – Results from Mass Spectrometry Analysis of CD36-BirA-Flag treated with biotin and enriched in F-actin.
The amount present is calculated by averaging two samples. Highlighted in yellow are hits selected because of protein association with either plasma membrane or F-actin.